ENHANCEMENT OF INNATE IMMUNITY TO CONTROL VIRAL INFECTIONS IN LIVESTOCK SPECIES

A Dissertation

by

LISBETH RAMIREZ CARVAJAL

Submitted to the Office of Graduate and Professional Studies of
Texas A&M University
in partial fulfillment of the requirements for the degree of

DOCTOR OF PHILOSOPHY

Chair of Committee,	Charles R. Long
Committee Members,	Teresa de los Santos
	Luis L. Rodriguez
	Waithaka Mwangi
Head of Department,	John N. Stallone

August 2014

Major Subject: Biomedical Sciences

ABSTRACT

During viral infection, host cell elicits the innate immune response by sensing pathogen associated molecular patterns (PAMPs) and triggering pathways that usually converge in the activation of interferon (IFN) and interferon stimulated genes (ISGs). Foot-and-mouth disease virus (FMDV) and vesicular stomatitis virus (VSV) are distinct economically important viruses that cause clinically indistinguishable vesicular lesions in livestock; yet, both viruses are highly susceptible to IFN.

IFN regulatory factor 7 (IRF-7) is the main regulator of type I IFNs. Elongation initiation factor 4E binding proteins (4eBPs) and 2'-5'-oligoadenylate synthetase like-1 (OASL-1) are translational regulators of IRF-7 in mice. To possibly enhance the antiviral response, the present work investigated the regulatory mechanism of IRF-7-mediated IFN response in livestock species. First, 4eBPs transcripts were decreased by small interfering RNAs (siRNA) in bovine and porcine cells (~60-90 % relative reduction), but no effect on antiviral state was observed. However, porcine cells fully depleted of 4eBP-1 by CRISPR/Cas9 gene editing induced higher levels of IFN, ISGs transcripts, and lower VSV yields (~2 log10), demonstrating that antiviral response is enhanced after 4eBP-1 elimination.

Interestingly, an inhibitory effect over translation exerted by the 5’ untranslated region (5’UTR) of porcine IRF-7 (5’UTR poIRF-7) was independent of 4eBP-1 depletion or hyperactivation. Our RNA folding models of 5’UTR poIRF-7 failed to explain these effects. Additionally, knockdown or over-expression of porcine OASL had

minor effects over VSV replication or ISGs induction in swine cells. Thus, regulation of the antiviral state might involve 4eBP-1 and IRF-7 5'UTR but not OASL in porcine cells.

Lastly, a constitutively active fusion of poIRF-7 and poIRF-3 proteins [poIRF7/3(5D)] potently induced IFNα, β, and ω but not type III IFN, causing a significant and steady reduction in FMDV and VSV titers (~6 log10) and enhancement of IFNβ antiviral effects. Mice inoculated with a replication-defective adenovirus (Ad5) expressing poIRF7/3(5D) displayed high antiviral activity in sera, induction of IFNα/β, and no viremia upon FMDV challenge. These results highlight for the first time the antiviral potential of Ad5-poIRF7/3(5D) *in vitro* and *in vivo* against FMDV. Results described here may improve biotechnology tools to defend our agriculture animal resources against viral diseases.

DEDICATION

To my family

ACKNOWLEDGEMENTS

Thanks to God for this work and the strength to persevere throughout all these years.

I thank my graduate committee, Teresa de los Santos, Luis Rodriguez, Waithaka Mwangi and my graduate advisor Charles Long for their trust, support, and guidance. Particularly, I deeply thank Teresa for her friendship, assistance, and critical comments throughout this research. I extend my gratitude to all my labmates, friends and colleagues. I also thank Michael Golding, Neetu Singh, Roger Smith, Fayna Diaz-San Segundo, and James Zhu for their comments on the experimental design, for providing reagents, or for their help with laboratory techniques. I thank the faculty and staff of the Department of Veterinary Physiology and Pharmacology at the College of Veterinary Medicine and Biomedical Sciences and my collaborators at Plum Animal Disease Center (PIADC).

I especially thank my husband, Elías, for his patience, love, contagious enthusiasm, and unfailing company during this journey that has lasted several years. I also thank my mother, Ligia Carvajal-Castro, and father, Franklin Ramírez-Vargas, for their encouragement and support.

Lastly, I acknowledge the funding sources including several grants from PIADC, the College of Veterinary Medicine graduate trainee research award, International Peace Scholarship and the Fulbright scholarship.

TABLE OF CONTENTS

Page

Page

LIST OF FIGURES

Page

Page

LIST OF TABLES

Page

CHAPTER I

INTRODUCTION

Food security to the world's growing human population requires expansion in agricultural production and efficient control of agriculture production systems. Pork and beef represent excellent food resource and important growing industries worldwide as evidenced by ~10 million tons increase in global pork production from 2009- 2014 according to the livestock and poultry, world markets and trade report.

Globally, livestock industry is threatened by introduction or recurrence of viral diseases. Thus, veterinary viral diseases have great medical and economic significance. For instance, the impact of viral diseases on foreign trade is very important because of animal health restrictions based on endemic diseases.

Foot-and-mouth disease virus (FMDV) and vesicular stomatitis virus (VSV) are two distinct RNA viruses that cause clinically indistinguishable vesicular diseases in livestock. FMD is a major trade barrier for animal products as well as a potential agricultural threat in disease-free countries. In contrast, VSV is a potentially zoonotic virus that recurrently affects livestock in Central and South America and is occasionally reported in southern USA. During the course of viral infection, FMDV and VSV genomes encode distinct sets of proteins that allow them to take control over host cell machinery and processes, evade immune responses, and spread to susceptible cells. In this chapter, we will review important aspects of pathogenesis, genome organization, viral proteins and epidemiology of both viruses. Better understanding of FMDV and

VSV pathogenesis and their virulence factors will allow developing antiviral strategies that mitigate the adverse effects of these diseases on animal health and on global economy.

Foot-and-mouth disease

FMDV is among highly contagious viral diseases that affect cloven-hoofed animals worldwide. It also affects wildlife including members of *Suidae*, *Bovidae*, *Cervidae*, *Camelidae*, or *Giraffidae* families and the pathogenicity ranges from asymptomatic to fatal (1).

FMD natural infection normally initiates though aerosolized virus that reaches the respiratory route (2). Inefficiently, the infection can also arise via abrasions on the mucous membranes or skin (2). Virus is excreted into the milk, semen, urine, and feces. Infected species also aerosolize large amounts of virus, which can infect other animals (2). FMDV infection results in rapid replication, spread, and shedding of large amounts of virus, resulting in high morbidity (2).

FMD pathogenesis is quite similar in cattle and in small ruminants (3). During pre-viremic state, FMDV is found in the dorsal soft palate, pharynx, and retropharyngeal lymph node. Primary replication of FMDV is detected in esophageal-pharyngeal tissue within approximately 2–6 h of intranasal viral deposition. FMDV infection initiates at the follicle-associated epithelia at mucosa-associated lymphoid tissue of the nasopharynx but cause minimal inflammation and non-vesicular lesions in these regions (4). FMD becomes evident within the lungs and less apparent in the pharyngeal tissues as viremia is detected (4).

Pigs are also commonly studied species for FMD pathogenesis (3). Pigs generate great quantities of aerosolized virus (3), which transform them into large sources of infectious material with high potential to spread the virus.

During the establishment of FMDV viremia, the upper or lower respiratory tract but not lymphoid organs, may function as entrance to the systemic circulation (5). Even when infected animals develop lesions at secondary sites of replication, viremia may be undetectable (4). Nevertheless, this finding might be associated with insufficient sampling or low detection sensitivity (4).

In bovine the onset of viremia occurs at the peak of FMDV detection from esophageal-pharyngeal samples, 72 hours post-infection (hpi). This period typically coincides with the clinical phase of disease or earlier. Viremia is reported from 1 to 2 days before pyrexia is detected (4). Even in the absence of viremia, vesicles can occur in the oral cavity (including the tongue, gums, and hard palate), lip, muzzle, snout, feet, teats, and prepuce (4). Viremia causes widespread distribution of FMDV to various tissues and organs even across the blood-brain barrier, including epithelia and visceral organs. Vesicles can disrupt and allow viral shedding with potential contact transmission (4).

During FMDV viremic period, the palatine tonsils and lungs may be locations of extensive replication. FMDV replication in the lungs of cattle considerably contributes to maintenance of high-titer viremia but lesions might be found in other secondary tissues. Also bovine haired skin contains high FMDV titer in absence of clinical signs (5). There is not clear evidence of the replication or transport of FMDV in peripheral

blood mononuclear cells in cattle and lymphopenia or immunosuppression might not be a consequence of FMDV infection (4). In contrast, swine transient lymphopenia is detected early after infection probably as a consequence of viral infection of T cells (4).

Pigs infected with FMDV become viremic at 24-48 hpi and develop vesicles at 48-72 hpi. High-titer viremia may be maintained by FMDV replication in various peripheral tissues and the respiratory tract. During vesicle formation, it has been suggested that virus uses a cell-independent mechanism to transit from the intravascular space to the vesicular epithelium due to the lack of viral detection in vascular endothelial or dermal cells (3).

In bovine, rapid induction of specific antibodies characterizes the immune response against FMDV, leading to reduction of tissue viral loads and clearance of viremia (4). FMD post-viremia is characterized by resolution of clinical signs, short-term persistence of virus, antigen or viral RNA or persistent infection after 28 dpi (FMDV may be detected on oesophageal-pharyngeal samples) (3). FMDV has been isolated from several tissues of carrier animals including the pharynx, esophagus, soft palate, and tonsillar sinuses (4). Importantly, vaccinated animals exposed to live virus may become carriers (persistently infected) (6) and this phenomenon can result in trade restrictions of a normally FMD-free country when vaccination is adopted to control the disease.

Classically, pigs recover from FMD approximately 3–4 weeks post-infection (4). Persistent infections have not been described since infectious virus has not been isolated later than 28 dpi in pigs (4). The disease can cause myocarditis and death, especially in newborn animals, but most animals eventually recover from FMD (7).

FMDV genome organization

FMDV is a non-enveloped virus that belongs to the Picornaviridae family (2), (8), (9). It contains a single-stranded RNA (ssRNA) genome of positive polarity (10). FMDV is a prototype for studying the *Aphthovirus* genus. (2).

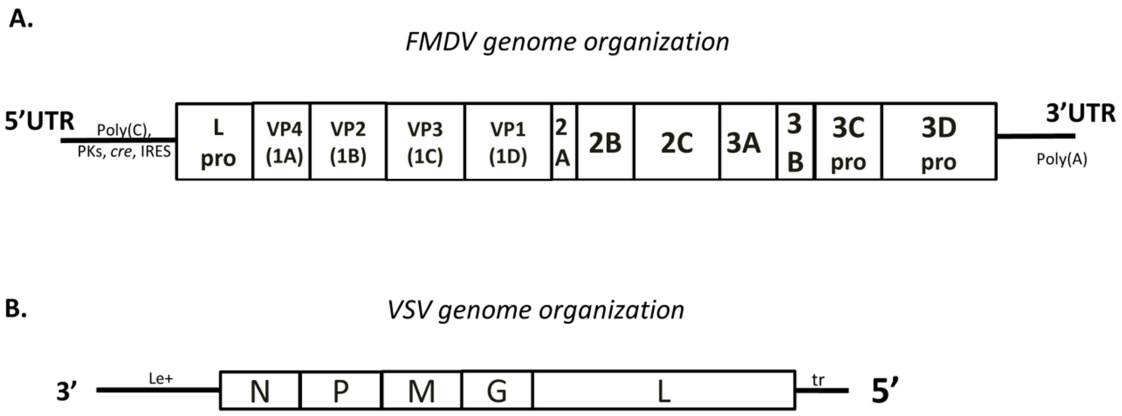

Figure. 1. Schematic diagrams of the FMDV and VSV genome organization. Boxes indicate regions encoding for viral proteins while lines indicate RNA structures. Viral proteins are described in the text.

FMDV genome is around 8.5 Kb and contains a short viral polypeptide VPg (3B) protein bound at the 5′ end and a poly(A) tract at the 3' end (2, 11). The genome contains a single long open reading frame (ORF) that encode a polyprotein which is processed by viral proteases into 4 structural proteins (VP1 through 4, also known as 1A, 1B, 1C, and 1D) and eight non-structural proteins (L, 2A, 2B, 2C, 3A, 3B, 3C and 3D) (2) (Fig 1A). Also, small amounts of a cleavage precursor of VP2 and VP4, (VP0 or 1AB) is found within the virion (2).The capsid has icosahedral morphology and it is composed of 60 copies of the structural proteins (2).

The 5′ untranslated region (UTR) is approximately 1300 bases in length (12). It contains an S-fragment (360 nt), a poly(C) tract, several pseudoknots, another hairpin loop structure known as cis-acting replication element (cre) (also known as the 3B-uridylylation site) (13), and the IRES (450 nt) which mediates the cap-independent translation of the viral RNA (2, 11).

FMDV IRES domains may be involved in RNA-RNA interactions necessary to preserve IRES structure and to interact with cellular factors (2). During FMDV infection, the C-terminal cleavage product of eIF4G binds to the IRES and also interacts with to proteins bound to the 40S ribosomal subunit (eIF4A and eIF3) (2). Thus, by cleaving eIF4G picornaviruses inhibit binding of capped mRNAs to the small ribosomal subunit but the cleaved eIF4G preserves its ability to recruit IRES-containing mRNAs to ribosome and viral translation proceeds normally (2).

The 3'UTR is 90-nt-long (2) and deletion or replacement is deleterious for viral replication (11). The 3′-end of the picornavirus genome contains a poly -A tract encoded in the viral genome (2). The poly-A tract might function to mediate viral genome circularization by binding to poly A binding protein (PABP) to connect the 5′-end of the genome (2).

FMDV viral proteins

Leader proteinase (Lpro)

The 5′-end of the FMDV ORF encodes the Lpro (12). There are two in-frame start codons that lead to the expression of 2 leader proteins, termed Lab and Lb (synthesized from the second AUG). Both products have been identified in infected cultured cells, but Lb is the main protein produce *in vivo* (14).

Lpro is a papain-like cysteine proteinase that cleaves itself from the nascent polyprotein at its C-terminal (15, 2, 14) and quickly induces the cleavage of the cellular translation factor eIF4G (16, 17). Lpro is shuts off host protein synthesis because intact eIF4G is required for translation of host capped mRNAs, while the remainder of the eIF4G complex is sufficient for IRES-dependent viral translation (14). Also, during FMDV infection, Lpro is localized to the nucleus of infected cells where it contributes to FMDV molecular pathogenesis (14). Lpro allows FMDV to block the IFN antiviral response by multiple strategies that will be briefly described in the next chapter.

A genetically engineered serotype A12 genome lacking of Lpro produces a viable virus designated leaderless virus (LLV) (18). Leaderless virus replicates at slightly slower rate than WT virus, and produces lower yields and smaller plaque size as compared to WT virus in cultured cells usually used to propagate FMDV (such as BHK-21 and IBRS-2) (18).

1A, 1B, 1C, and 1D

P1 region of the genome encoded the structural proteins and they are processed by 3Cpro. Each protomer contains one copy of each 4 proteins VP1 (1D), VP2 (1B), VP3 (1C), and VP4 (1A) (2, 14). Purified 1D or its proteolytically derived fragments elicit high levels of neutralizing antibodies. Also, an Arg-Gly-Asp (RGD) tripeptide sequence found in 1D is responsible for binding to the primary FMDV cellular receptors that belong to the integrin family (mainly αvβ3, αvβ6) (2). Heparan sulfate (HS) functions as an alternative receptor in cultured cells for some subtypes of FMDV as a result of tissue culture adaptation (19).

Importantly, the organization of the structural proteins within the virion influences virulence and ability to disseminate. The three-dimensional conformation determines the antigenic sites, mediates receptor binding, cell entry, and capsid stability (14). For instance, FMDV interacts more loosely with its receptor(s) than other picornaviruses because cell binding sites are more exposed (in contrast, other picornaviruses have receptor binding sites in a canyon on the viral surface) (2, 14).

2A/B/C

The P2 is processed into three mature polypeptides, namely 2A, 2B, and 2C. Cleavage at the 2A/2B site is independent of Lpro and 3Cpro (20). 2A is a very short peptide that remains associated with the P1 precursor by a ribosome skipping mechanism as 2A is neither a proteolytic element nor a substrate for cellular proteinases (20, 21). 2B and 2C proteins are related to virus-induced cytopathic effects (CPE) (2, 14). Both proteins are present at sites of genome replication in the outer surface of ER-

derived membranous vesicles (14). It is thought that these two proteins act together to block the transport from the endoplasmic reticulum to the Golgi complex (22). Thus, they affect the delivery of proteins to the cell surface or extracellular compartment, a mechanism that has been suggested to explain the down-regulation of superficial expression of major histocompatibility complex class I (MHC I) observed in epithelial cells infected with FMDV (22). A decrease in the MHC I limits viral antigens presentation and might delay the clearance of the infected cells (22, 9, 23).

FMDV 2C is the largest membrane-binding protein of viral RNA replication complex (22), it binds ssRNA and has ATPase and GTPase activity (24) but its precise role in virus replication has not been elucidated (24). The structure and size of 2C suggests that it interacts with host cellular factors during virus replication (25). 2C interacts with the host factor Beclin1 which is a regulator of the autophagy pathway. This interaction between FMDV 2C and Beclin1 is involved in the autophagy pathway, which was shown to be important for FMDV replication (25, 26).

3A/B

Protein 3B (also known as VPg) is attached to the 5′ end of the genome/anti-genome, and it primes picornavirus RNA synthesis (9, 14). There are three non-identical copies of 3B that are determinant of host range and virulence (27). The 3B peptides are uridylylated by 3Dpro (form VPgpU) and prime positive-strand RNA synthesis (13).

FMDV 3A protein is longer than in other picornaviruses (28) and forms homodimers (29). Both 3A and the stable intermediate 3AB are important viral RNA replication factors that are intimately associated with cellular membranes (28, 14).

FMDV 3A is important for virus replication, virulence, and host range (29). Changes in FMDV 3A are associated with species adaptation (27).

3C proteinase (3Cpro)

3Cpro performs most of the cleavages of the viral polyprotein (30) except the cleavage between P1 and P2 performed by 2A, the maturation cleavage of 1AB, and the autocatalytic cleavage of Lpro from P1 (2, 14, 30). 3Cpro also cleaves some host cell eIF4A (which is part of the cap-binding complex) (31) or eIF4G. EIF4G is cleaved at different sites as compared to Lpro and the cleavage occurs later in the viral cycle (31). 3Cpro or its precursor 3CD is involved in cleavage of nuclear protein H3 histone at its N-terminal which is consistent with inhibition of host transcription during FMDV infection (32), (9). FMDV 3Cpro induces Golgi fragmentation, loss of microtubule organization, and a block of secretory pathway (33).

3D polymerase (3Dpol)

The 3Dpol protein is the viral-encoded RNA dependent RNA polymerase (34) FMDV 3Dpol forms fibrous structures associated with membranes within infected cells (35). 3Dpol plays a central role in both transcription and viral genome replication (36). The enzyme executes these operations, together with other viral and probably host proteins, in the cytoplasm of host cells (34).The first step in RNA replication consists of the production of a minus-strand RNA molecule which is used as template to generate positive-strand progeny genomes (14) The 3D mediates the covalent binding of UMP on VPg, then uridylylated VPg primes viral RNA synthesis (36).

FMD epidemiology and control

FMDV is a highly antigenically variable virus comprising seven serotypes and multiple subtypes. Serotypes A, O, C, were first isolated in Europe and occur worldwide, while serotypes SAT 1-3 and Asia-1 have traditionally been restricted to Africa and Asia, respectively (14, 2, 9). FMD is enzootic in many regions of Africa and Asia, causing enormous economic and social impact to some of the poorest locations around the world (37). However, the current global epidemiological status of foot-and-mouth disease (FMD) varies widely between different countries and geographical regions and zones.

FMDV outbreaks have happened in almost every region of the world that contains livestock (2). The disease is enzootic in all continents except North America and Australia (2). There are zones recognized as free without vaccination for instance North (including Mexico, USA and Canada), Central America and Europe. Also there are zones where FMDV has been controlled by using vaccination such as regions in South America and some regions in Africa (37). Lastly, there are regions where the lack of epidemiological surveillance data renders a not recognized disease status. An updated map of FMD status worldwide can be found in OIE website.

In FMD-free countries, FMD is controlled by animal movement restriction, slaughter of in-contact susceptible animals, and in some instances, use of an inactivated vaccine followed by killing. Although in countries where the disease is enzootic, preventive vaccination is commonly used (2). FMD-free countries tend to avoid

vaccination due to the more restrictive trading policies imposed by the World Organization for Animal health (OIE) (2).

Inactivated vaccines, DNA vaccine, viral-vectored vaccines, and modified live vaccines have been developed in the past (several examples are cited by 37). The current inactivated whole virus vaccine is effective, but a number of limitations such as difficulty in distinguishing infected from vaccinated animals (DIVA), and requirement of an expensive high-containment facility for vaccine production has led investigators to develop alternative vaccine approaches (reviewed in (37, 38, 39). Although vaccination is largely utilized worldwide to protect against FMD in enzootic countries, current vaccines do not always prevent infection, but rather limit or block clinical signs and require at least 5-7 days to elicit a protective immune response which results in some animals becoming long-term carriers. Therefore, in case of a FMD outbreak in a disease-free country is necessary to limit disease spread and reduce slaughtered animals by inducing rapid protection prior to the induction of vaccine-induced adaptive immunity.

Existing FMD vaccines are not proper for global eradication for several reasons including: short-term protection and necessity of re-vaccination, lack of cross-protection against the multiple serotypes and subtypes, require a cold chain from production to delivery, have a short shelf life, or require biosafety level 3 facilities to expand live virus for vaccine production with a potential risk of viral escape and initiation of an outbreak in the region (37). Therefore an ideal vaccine would (i) be inexpensively produced, easy to administer, and accessible in regions where it is needed most, (ii) prevent infection shortly after vaccination, (iii) be effective across all serotypes and subtypes of FMDV

(iv) have the ability to quickly incorporate emerging viral strains, (v) provide life-long immunity, (vi) have prolonged shelf life and thermal stability (vii) have low biosafety requirements for its manufacturing (viii) allow discrimination between infected and vaccinated animals (DIVA), and (ix) have a short withdrawal period for food consumption (37). An alternative recombinant FMD vaccine was developed which uses a replication detective human Ad5 that delivers FMDV empty particles. This vaccine overcomes most of the limitations of the current commercially available vaccine and has been granted a conditional license for production in the USA (40).

Vesicular stomatitis virus

VSV belongs to Rhabdoviridae family, order Mononegavirales (41, 42) a diverse group of pathogens of humans, plants, animals, and/or insects (41, 42). VSV is a model for studying non-segmented negative-stranded RNA viruses (NSNR) (43) for several reasons such as (i) rapid disease course in several vertebrae host (ii) simple structure and genomic viral organization (42), (iii) high replication rate in different *in vitro* models and (iv) elevated mutation rate producing viral swarms (42, 44).

VSV is a strong candidate for oncolytic viral therapy because it can selectively infect and kill malignant cells. VSV ability as oncolytic virus has demonstrated success in preclinical studies against a variety of malignancies, including prostate, breast cancer, melanoma, colorectal cancer, liver cancer, glioblastoma, and other cancers (see citations within 45).

VSV affects a wide variety of livestock including cattle, pigs, equidae (horse, mule and donkey). But the host range includes camelids and wild rodents. The virus

even circulates in bats and tamarin monkeys in Brazil (46). VSV has zoonotic potential, causing symptoms such as conjuntitivis, headache, myalgia, fever, chills, nausea, pharyngitis, and lymphadenitis in infected people (44, 47). Under natural conditions, transmission of VSV occurs by direct contact and insect vector (48). VSV can be biologically transmitted by insects, such as blackflies and culicoides where the virus replicates, invades the salivary glands and is transmitted during insect feeding (49). Experimentally, other transmission routes have been used such as intranasal, intravenous, intradermal, scarification of the skin or oral mucosa and direct animal transmission (see references cited by 46).

VSV cause vesicular lesions and erosion of various epithelial sites including the mouth, feet and teats (44, 50). Lameness may also occur (44). Vesicular lesions disrupt animals feeding behavior, limit gain of weight and reduce milk production (50). In humans, acute febrile disease has been described sporadically (44). The lesions are clinically indistinguishable from those of FMD (50, 51). During vesiculation, the infiltration of inflammatory cells, including granulocytes and monocytes, eventually results in cellular lysis. Vesicles develop when the necrotic, edematous mucosa breaks free from underlying tissue, forming a cavity filled with cellular exudates (52). In addition, ulcerative lesions are frequently accompanied by secondary bacterial infections that delay healing and required antibiotic therapy (44).

Generally, VS lesions are restricted to inoculation or bite site. This is evidenced in a study with cattle infected by fly bite where the animals inoculated in the neck skin did not develop pyrexia or any other clinical sign of disease. They only displayed

multiple small focal areas of hyperemia at the bite site. In this study lesions developed only when the inoculation was in the coronary band, with only evidence of dissemination to regional lymph nodes (53).

In pigs infected with VSV serotype New Jersey (NJ), the virus has been recovered from tissues near the site of infection for as long as 6 days after infection. VSV isolations have also been made from nasal cavity or palatine tonsil of the soft palate but not lung in swine infected with VSV NJ (54). Direct tests failed to demonstrate persistence of virus after infection; however the humoral and cellular immune response remained elevated for months. Titer of serum-neutralizing antibodies peaked 3-5 weeks after infection (55). Viral shedding from tonsils is known to occur in pigs infected with VSV (55).

VSV proteins and genome organization

VSV genome organization is simple. A bullet-shaped virion contains a linear, single stranded, negative sense RNA genome (44).VSV sequentially encodes 5 genes from a single polymerase entry site (56). These genes are: nucleocapsid (N), phosphoprotein (P), matrix (M), glycoprotein (G) and polymerase (L) (42, 57-59) (Fig 1B). The ribonuclear proteins (RNP) function as the transcription and replication unit and it is composed by the L, P and N proteins (60). The location of the genes in the genome is conserved for gene regulation as relative molar ratios of RNP are crucial for optimal VSV replication (41, 57). The RdRP (L protein) uses the genome as a template for (i) transcription of a short leader RNA (Le+) and the 5 mRNAs and (ii) replication of the full-length anti-genomic template and then genomic strands (58). During VSV

transcription L enters the genome at a single site and that transcription of a downstream gene depends on termination of transcription of the upstream gene (58). L protein responds to cis-acting signals present within the leader region, at the leader-N junction, and at the internal gene junctions (61).

Nucleocapsid (N)

In infected cells, the N protein abundant (62) and protects the viral genome from nuclease degradation (63). Thus, translocation or reduction in N expression causes a decrease in genomic replication (41). Translocation of the N gene away from the unique transcriptional promoter caused viral attenuation and abolished disease manifestations in swine, a natural host (57).

Phosphoprotein (P)

The P protein facilitates L protein and N protein-RNA complex binding. Also, it is a crucial transcription factor for the L polymerase (63, 64).

Matrix (M)

Expression of M protein in the absence of other viral components inhibits expression of co-transfected genes (42). Also viruses that contain mutations in M protein are defective in their ability to inhibit host gene expression. M protein has also functions in virus assembly. Rae I and Nup98 are host component shown to interact directly with M protein in the inhibition of host gene expression. Overexpression of either Rae I or Nup98 counteracts the inhibitory activity of M protein to a large extent. M protein-Rae1 complexes serve as platforms to promote the interaction of M protein with other factors

involved in host transcription. Silencing Rae1 expression reduced the ability of VSV to inhibit host transcription (65)

Glycoprotein (G)

The glycoprotein is a determinant of VSV virulence in a natural host as evidence by an study using a mutant VSV serotype Indiana virus in which the glycoprotein (G) was substituted by a copy of G from a more pathogenic strain (New Jersey strain) caused more severe lesions and replicated to higher titers than the parental virus (50). The glycoprotein is first found in endocytic vesicles after the start of the infection, but it progressively moves to the nucleus (66).G protein is synthesized by membrane-bound ribosomes, associates with the chaperon proteins to ensure proper folding and it experiences several co-translational modifications (44).

Polymerase (L)

The large (L) protein is the main component of the multifunctional RNA dependent-RNA polymerase (RdRP) which executes the mRNA processing and the genome replication and (67, 68).

VSV epidemiology

VSV is endemic solely in regions of the American continent. The disease is present from northern regions of South America to southern locations in Mexico where outbreaks of clinical disease occur annually. In endemic areas, VS outbreaks are usually associated to the transitions between the rainy and dry seasons (51). There are two serotypes of VSV are NJ and Indiana (IN) (-1,-2, or -3). NJ and IN-1 occurs from USA to Central and South America. IN-2 (or Cocal) is found in Southern Brazil and

Argentina. IN-3 serotype (also known as Alagoas) is reported in North, Northeast and Central Brazil. NJ is the serotype responsible of the majority of clinical cases, followed by IN-1 (46, 69). Outbreaks of VS happened in Europe during the World War I and South Africa from horses exported from the US, but VSV is no longer present in these areas (44).

VSV has been reported in the United States with 2 patterns of occurrence (i) sporadic reports occurring approximately every ten years in the southwestern states caused both by VSV New Jersey and VSV Indiana 1, and a (ii) endemic-like pattern reported in the southeastern states (51). An enzootic focus of VSV NJ has been reported in on Ossabaw Island, Georgia, and evidence suggests that the vector for this virus is a sand fly (*Lutzomyia shannoni*) (54). In Texas, VSV is sporadically reported due to natural cycles involving livestock, wild animals, and insect vectors and its proximity to endemic areas. In fact, the US Animal and Plant Health Inspection Service (APHIS) have confirmed cases in Texas and New Mexico in past years. Outbreaks in western US caused losses to the horse industry due to animal quarantines and cancellation of events such as horse shows (51). Therefore, efforts to avoid VSV outbreaks in the US are relevant to reduce economic impact of the viral infection on the livestock industry and the impact on animal health.

Insects are capable of infecting animals with VSV in enzootic areas (44, 51). Some insects such as sand flies (70), black flies (*Simulium vittatum*), mosquitoes (Diptera: *Culicidae*), and culicoides (Diptera: *Ceratopogonidae*) (49) have been reported

as VSV vectors. Also, a study followed lesion development and replication kinetics during early bovine infection after direct black fly bite (53).

CHAPTER II

INNATE IMMUNE RESPONSE AGAINST VIRUSES

The antimicrobial host defense relies both on innate and adaptive components (71). The innate immunity is the first line of host defense against pathogens; it discriminates between self and a variety of pathogen antigens via a limited number of pattern-recognition receptors (PRRs) (72). Acquired immunity occurs in the late phase of infection and involves specific development of lymphocytes bearing antigen-specific receptors and the generation of immunological memory (72). The innate system responds rapidly to infection because it uses mechanisms that are constitutively present in the body that become active shortly after exposure to pathogens. The innate immune system entails of barriers at the surface of the body and specialized molecules and cells inside the body (73). The innate immune response involves diverse cellular sensors and signal transducing pathways that stimulates host defense mechanisms in response to pathogen invasion, and frequently these cellular reactions lead to type I interferon (IFN) production (74) or a second pathway that is elicit during non-viral and certain viral infections that leads to induction of tumor necrosis factor (TNF), interleukin 6 (IL-6), IL-12 and IFN type II (75).

The ability of the innate immune system to identify and limit pathogen replication during early infection relies predominately on phagocytosis, autophagy, complement activation, and immune awakening by different families of PRRs (76). Cells of the innate immunity include macrophages, antigen-presenting dendritic cells (DCs),

cytotoxic natural killers (NK), granulocytes, and γδ T lymphocytes (73). The complement system is composed by different auto-proteolytic proteases that interact to opsonize pathogens and induce an inflammatory response (77). Three pathways of complement activation namely, the classical pathway; the mannan-binding lectin (MBL) pathway; and the alternative pathway (reviewed by (77)), can be initiated independently of antibody secretion as part of innate immunity (77).

The molecular mechanisms of the innate response involve the recognition of specific pathogen-associated molecular patterns (PAMPs) or danger-associated molecular patterns (DAMPs) by PRRs (73, 76, 78). Pattern recognition molecules are expressed constitutively in the host and distinguish global patterns of molecules rather than specific features and recognize related pathogen types rather than a specific type (73), which makes the response faster but less specific. Each type of PRR reacts with specific PAMPs, activates specific signaling pathways, and lead to distinct anti-pathogen responses (72). Viral PAMPs are essential molecules for the infectious cycle of the invading virus (72) such as viral DNA, RNA and/or capsid proteins. Enveloped viruses also contain a phospholipid envelope holding viral glycoproteins that are frequently recognized as a PAMP. In addition, replicative intermediates such as double-stranded RNA (dsRNA) can function as PAMP (79). PRRs induce a cascade of molecular pathways that lead to the production of expression of cytokines, chemokines, reactive oxygen, species antimicrobial peptides which together coordinate the early host response to infection. Signaling through PRR is crucial for the subsequent recruitment and activation of adaptive immunity (73, 76).

Diverse pathogen patterns, including viral PAMPs, are precisely recognized by sensory molecules, including TLRs, cytosolic RIG-I-like receptors [RLRs: retinoic acid-inducible gene I (RIG-I); melanoma differentiation-associated gene 5 (MDA5); and laboratory of genetics and physiology 2 (LGP2)] and nucleotide-binding oligomerization domain (NOD) like receptors (NLRs) (76, 80, 81). A comprehensive list of specific viral PAMPs and the mechanism involved in their recognition are reviewed elsewhere (79). While TLRs are located in the plasma membrane or in endocytic compartments of specific cells (such as DCs and macrophages), RLRs can recognize viral nucleic acids in the cytoplasm of most cell types. RLRs sense viral RNA and results in immunological responses, including the production of type I interferon and inflammatory cytokines (80). Simultaneously, activated antigen presenting cells (APCs) initiate adaptive immunity, which has the ability to terminate the infection and inflammation (80).

Toll-like receptors (TLR)

The family of TLRs is the major and most comprehensively studied class of PRRs. It includes type I integral membrane glycoproteins members of a larger superfamily that includes the interleukin-1 receptors (IL-1Rs) (72, 76). Cells prominently expressing TLRs include APCs such as DCs and macrophages, which ingest and degrade pathogens (72). Twelve functional TLRs have been identified in mice and 10 in bovine (82) and humans. TLRs are divided into two subgroups depending on cellular localization: TLR1, TLR2, TLR4, TLR5, TLR6 and TLR11 are positioned on the cell surface and mainly recognize microbial components while TLR3, TLR7, TLR8

and TLR9 are expressed in intracellular vesicles including the endoplasmic reticulum and lysosomes, recognizing microbial nucleic acids (72, 83).

The ligands for TLR are diverse ranging from nucleic acids structures from RNA or DNA viruses to bacterial components. TLR signaling participates in multiple steps of phagocytosis, digestion of pathogens yields more molecules that activate other PRRs, induce cytokines and chemokines such as TNF-α and IFN-γ that help activate other phagocytic cells preparing against further invasion of the pathogens (76).The ability of TLRs to discriminate between normal cellular constituents and external pathogens components is extremely important to mount proper and timely immune response. A detailed review of the toll-like receptor signaling and accessory molecules is reviewed elsewhere (72, 84, 85).

TLRs dimerize and undergo conformational changes required for the recruitment of adaptor proteins containing a TIR domain after ligand binding. There are four main adaptor molecules: (i) myeloid differentiation factor 88 (MyD88), (ii) TIR-associated protein (TIRAP)/MyD88-adaptor-like (MAL), (iii) TIR-domain-containing adaptor protein-inducing IFN-β (TRIF)/TIR-domain-containing molecule 1 (TICAM1), and (iv) TRIF-related adaptor molecule (TRAM) (72). Recruitment of adaptor proteins results in the triggering of downstream signaling cascades and production of pro-inflammatory cytokines and chemokines. The differential responses induced by different TLR ligands are partially explained by the selective use of adaptor molecules.

Stimulation with TLR3, TLR4, TLR7, and TLR9 ligands induces type I IFN production and pro-inflammatory signals. The activation of these molecules leads to

expression of other co-stimulatory molecules, DCs maturation, and IFN-α/β secretion. TLR3 and TLR4 induce a MyD88-independent pathway to activate IFN-β and ISG activation (72). This pathway is mediated by TRIF which interacts with receptor-interacting protein 1 (RIP1) and activates of NF-κB (Fig 2). TRIF activates TRAF-family-member-associated NF-κB activator (TANK) binding kinase 1 (TBK1; also known as NAK or T2K) via TRAF3. Inducible IκB kinase (IKK-i, also known as IKK-ε) belongs to TBK1 family and mediates phosphorylation of IRF-3 and IRF-7 (Fig 2). Phosphorylated IRF-3 and IRF-7 form homo- or heterodimers relocate into the nucleus, and bind to the interferon stimulated responsive elements (ISREs), resulting in the expression of IFNs and IFN stimulated genes (ISGs) (72, 86).

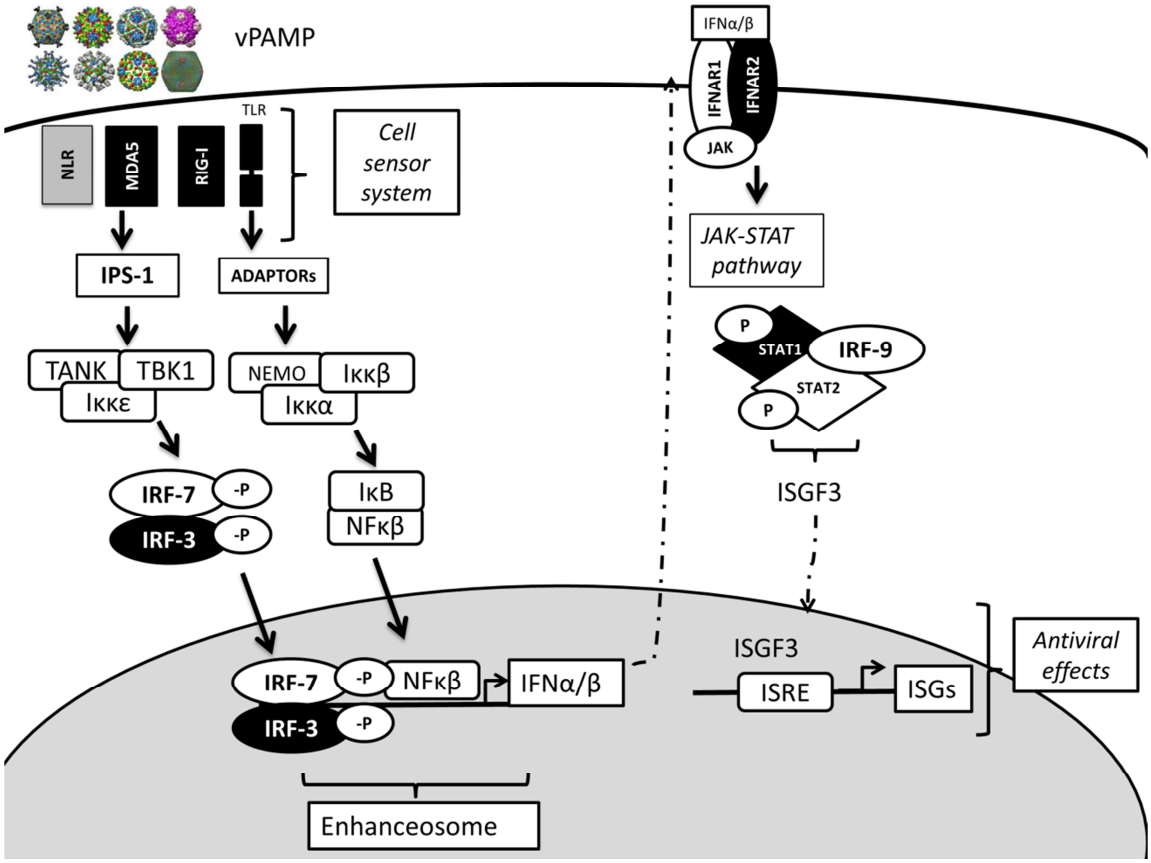

Figure. 2. Innate immune response against viral infection.
Binding of viral PAMPs to specific components of the cell sensor system, including TLR, RIG-1/MDA5 and NLR activates IFN production through adaptor molecules and transcription factors such as NFκβ, IRF-7, and IRF-3. This process involves phosphorylation, homo or hetero- dimerization and nuclear translocation of IRF-7 and IRF-3. Activated IRF proteins form higher-order protein complexes with other components of IFN enhanceosome. This protein complex sets off changes in chromatin and histone structure in the IFN gene cluster. Produced IFN then acts autocrine and paracrine through interaction with IFNα/β receptor and activation of JAK-STAT signaling pathway inducing the transcription of hundreds of ISGs. Modified from (87)

RIG-I-like receptors (RLR)

The RLR family members include RIG-I, MDA5, and LGP2 They act as cytoplasmic RNA sensors that trigger innate immune responses against infections and stimulate adaptive immunity (88). LGP2 is a positive regulator of their signaling (88).

RLRs detect RNA derived from RNA viruses and in some instances DNA viruses. RLRs are similar to TLR3, in terms of detection of viral RNA and induction of ISGs, type I IFN, and pro-inflammatory cytokines. However, nucleic acid-specific endosomal TLRs TLR3, TLR7/8, and TLR9, recognize extracellular nucleic acids having reached the endosomes through endocytosis, meanwhile RLRs detect intracellular viral RNA from actively replicating viruses (88).

RIG-I and MDA-5 contain a C-terminus DExD/H box RNA helicase domain (RNA binding) and two caspase-recruitment and activation domains (CARDs) at N-terminus (86, 88). The RNA helicase domains interacts with synthetic or viral RNA by the helicase domain and induce conformational changes to promote the CARD-mediated downstream signaling, leading to the activation of IRF-3, IRF-7, and NF-kB for the induction of type I IFN genes (Fig 2) and pro-inflammatory cytokines (i.e. IL-6). At the same time, RIG-I and MDA5 are ISGs and are involved in the positive regulatory feedback. Sensing of incoming viral RNA by RLRs is connected to downstream signaling by activation is the IFNβ promoter stimulator 1 (IPS-1) adaptor molecule, also known as mitochondrial antiviral signaling (MAVS), or CARD adaptor inducing IFNβ (Cardif) or virus-induced signaling adaptor (VISA) (78). Homologous with RIG-I and MDA5, IPS-1 also contains an N-terminal CARD (86). The transmembrane region

mediates the localization of IPS-1 in the outer mitochondrial membrane. IPS-1 interacts with signaling proteins including tumor necrosis factor receptor-associated factor 6 (TRAF6), TRAF2, TRAF3, receptor interacting protein-1 (RIP1) and Fas-associated protein with the death domain (FADD) (86). These molecules orchestrate NF-kB activation and induction of pro-inflammatory cytokine. Interacts with different TRAF adaptors is necessary for the activation of downstream kinases (86) such as TANK binding kinase 1 (TBK1; also known as T2K and NAK) and inducible IkB kinase (IKKi; or IKK3). The first one was first identified in the regulation of NF-kB activity but both kinases induce phosphorylation of IRF-3 and IRF-7 (86).

An endoplasmic reticulum associated protein referred to as STING (stimulator of interferon genes) facilitates IFN production after recognition of intracellular DNA derived from variety of pathogens (74). Studies have suggested that STING also plays an important role in RIG-I but not MDA5 signaling (74). STING associates in close proximity with mitochondria associated membrane (MAM) and may link cytosolic DNA-mediated signaling to TBK1 activation and therefore activation of NF-κβ and IRF-3 signaling, which are key regulators of IFN transcription. A review of the proposed molecular pathway is found in (74).

NOD-like receptors (NLRs)

Nucleotide-binding oligomerization domain (NOD)-like receptors (NLRs) are cytosolic pattern recognition molecules involved in innate-driven inflammatory responses, with ability to induce apoptosis (89), sensing cytosolic DNA and triggering inflammasome-dependent signaling (90, 91). The cytosolic NLRs recognize some virus

families, in particular DNA viruses (92). These proteins have a C-terminal leucine-rich repeat (LRR) domain probably involved in sensing or PAMPs or DAMPs, a central NACHT/NOD domain (nucleotide binding and oligomerization domain) and the N-terminal domain which is involved in downstream signaling (90). This pathway involves NF-κB or caspase-1 dependent processing of cytokines such as IL-1β, a key pro-inflammatory mediator that recruits DCs and macrophages and infection or injury sites and is the primary cause of chronic, acute inflammation and febrile response (93). Generally, these events are TBK1-independent and do not induce of IFN (74). The NLRP subfamily which includes NLRP1-12 and NLRC4 (90) are involved in inflammasome (caspase-activating complex comprised of caspase-1, caspase-5, Pycard/Asc, and NALP1) activation, which leads to caspase-1 mediated cleavage of IL-33, IL-1β, and IL-18 (93).

Interferons (IFNs) and Interferon stimulated-genes (ISGs)

The antiviral response is characterized by the release of type I IFNs (including IFNα and IFNβ) that induce the expression of ISGs, leading to an antiviral state (81). IFNs are a multigene family of inducible cytokines first identified by their antiviral function (94, 95 -97). These potent factors have pleotropic effects on cellular physiology, especially in cells of the immune system (75). IFNs exert anti-microbial effects by activating the transcription of hundreds of cellular anti-pathogen genes inflammatory cytokines (74). IFNs play crucial roles in surveillance of cancer cells and control of microbial pathogens such as bacteria, parasites but they are central to combat viral infections. There are three classes of IFN described, namely: type I, II, and III.

Different types and subtypes will be briefly acknowledged next to better understand the functions and the molecular pathways elicit by IFNs.

Type I IFNs includes IFN-α (which is subdivided into many different subtypes), IFN-β, IFN-δ, IFN-ε, IFN-κ, IFN-τ and IFN-ω. IFN-δ and IFN-τ have been described only for porcine and bovine, respectively (98). All type I IFNs bind the common cell-surface receptor (type I IFN receptor) composed by subunits IFNAR1 and IFNAR2. The IFNAR1 subunit associates with the tyrosine kinase 2 (TYK2) and the IFNAR2 interacts with JAK1 (98). IFNα and β can be made by any cell type in response to appropriate stimulation, and intracellular infections with viruses are potent stimulators of these factors (75). Various bacteria induce type I IFN in a TLR-independent manner. However, the role of IFN in bacterial infections is less clear (88).

Type II IFN only includes IFN-γ which plays an important role in both innate and adaptive immunity (94). It is produced by activated T cells (Th1 response) and natural killer cells and binds to different cell-surface receptor (98). It recognizes cell surface-bound viral antigens associated with the major histocompatibility complex (MHC) proteins, induces macrophages activation and triggers specific cytotoxic immunity (99). The receptor is composed by subunits IFNGR1 and IFNGR2. The IFNGR1 subunit associates with JAK1, whereas IFNGR2 is constitutively associated with JAK2 (98). IFN-γ is crucial for defense against some parasitic and bacterial pathogens (99).

Type III IFN includes IFN-λ molecules (IFN-λ1, -λ2 and -λ3, which are also known as interleukin-29, IL-28A and IL-28B, respectively) (100), (101). These

cytokines induce similar innate antiviral responses as type I IFN, but they have different structure and bind a different cell-surface receptor (98), (102). Type III IFN is recognized by a cellular receptor composed of IL28-Rα (type III IFN specific subunit), and IL10-Rβ (subunit shared by other IL10 related cytokines). IL-28R receptor subunit is expressed in a limited range of cells, including epithelial cells. It is expressed in skin and mucosae and therefore these tissues are more likely to respond to treatment with this cytokine (102), (103) and this has been suggested as a mechanisms to combat viral invasion (102).Type III IFN have been described in several species including humans, mice, chickens, swine ((101)) and more recently in bovine (102, 103). Two members, IFN-λ1 (IL29) and IFN-λ3 (IL28B) have been identified in swine (101) and boIFN-λ3/boIL28B, have been identified, cloned and characterize in bovine (102). Type III IFN signals thought the activation the signal transducer and activator of transcription (STAT) family and ultimately induces ISG expression (102, 103).

IFN response is one of the first antiviral mechanisms induced in an infected host cell (104), (75). The majority of antiviral effects of IFN are mediated by the products of ISGs, whose expression is highly induced after interferon activation (97). IFN system also induces the expression of various miRNAs that can contribute to an antiviral state by targeting viral and possibly host transcripts (105).

Hundreds of ISGs have been identified since discovery of IFNs, but only some of them have been fully characterized in terms of antiviral potential, target specificity, and mechanisms of action (104). ISG proteins usually do not have virus specificity yet they block viral proliferation by inhibiting many steps in viral replication. However, different

viruses are targeted by distinct sets of ISGs and viral species are susceptible to multiple antiviral genes (104). Conversely, some ISGs are also intrinsic virus-restriction factors that recognize specific viral components and block viral replication immediately and directly, instead of inhibit viral infection by inducing interferons and other antiviral molecules (106).

ISGs include well-studies proteins such as double-stranded RNA(dsRNA)-activated protein kinase R (PKR), 2',5'-oligoadenylate synthetase (OAS), RNAse L and Myxovirus resistance (Mx) (9). PKR is active when it binds dsRNA, a typical product of virus-infected cells, and induces inhibition of protein synthesis (9).Mx-1 inhibits protein synthesis and genome amplification. Mx1 interfered with either intra-cytoplasmic transport of influenza viral mRNAs, viral protein synthesis, or nuclear translocation of newly synthesized viral proteins (107). RNAse L reduces viral RNA synthesis upon activation by OAS RNA degradation pathway which is activated by dsRNA (108), (94)

Members of the ISG56 gene family, namely IFIT-1 or ISG56, IFIT-2 or ISG54, IFIT-4 or ISG60, and IFIT-5 or ISG58, are highly induced in response to IFN, dsRNA, or virus infection. P56 is one protein that inhibits translation of capped cellular mRNAs and viral mRNAs translated through an internal ribosomal entry sites (IRES) (97). While cellular mRNA is methylated at the 2'-O position and contains a 5'-guanosine cap, viral RNAs often contain 5'-triphosphate (5'-ppp). IFIT proteins recognize viral RNA that contains a 5'-ppp moiety or lacks 2'-O-methylation (106). In addition, expression of ISG54, independent of IFN stimulation, elicits programmed cell death via a mitochondrial pathway (109).

ISG20 encodes a 3-5’ single strand RNA exonuclease involved in the antiviral function of IFN. ISG20 interfered with VSV mRNA transcription and translation while the expression of cellular genes remained unaffected (110). Virus inhibitory protein, endoplasmic reticulum-associated, interferon-inducible (Viperin) reduces viral budding by affecting the array of lipids rafts in host cell plasma membranes (111). Theterin also known as bone marrow stromal antigen 2 (BST-2) is a lipid raft associated protein that inhibits viral infection by preventing the diffusion of virus particles after budding from infected cells. (112). Inducible nitric oxide synthase (iNOS) produces nitric oxide (NO) which has antimicrobial, antiviral, and pro-apoptotic effects helping for viral clearance. iNOS has been implicated in the activation of macrophages and the pathogenesis of autoimmune and inflammatory disease (94, 113). ISG15 encodes a 15-kDa ubiquitin-like protein (P15 or ISG15) with more than 200 candidate targets which span a diverse array of biological processes, including cell cycle regulation, cell motility, protein translation, signal transduction, glycolysis, and immune responses. However, it is still largely unknown what impact ISG15 modification has on a target proteins (97,114).

Schoggins et al (2011) tested over 380 ISGs against important viruses (including hepatitis C virus, yellow fever virus, West Nile virus, Venezuelan equine encephalitis virus, and human immunodeficiency virus) and identified widely acting effectors (such as IRF-1, RIG-I, MDA5, etc.) as well as targeted antiviral specificity. Interestingly, ISG pairs showed additive antiviral effects and a common mechanism of function involves translational inhibition for numerous effectors (104).

In summary, IFN elicit an antimicrobial response by selectively shutting off translation in infected cells, inhibiting viral protein synthesis, or degrading viral RNA. In addition to antiviral effects exerted in single cells impairing viral synthesis and yield, both IFN-α/β and IFN-γ modulate an elevation of MHC class I and II antigen levels to increase the efficiency of cellular immune responses to infections (94). Apoptosis also functions as a defense mechanism for the host cell to combat viral infection and a method of clearance of cells affected by microbial pathogens. IFNs-α/β are essential mediators of apoptosis (94). The fact that a numerous viruses encode either induce or inhibit apoptosis illustrates the importance of programmed cell death as a host mechanism to respond upon virus infection (94).

As countermeasures of host cell IFN-induced defenses, viruses elicit mechanism that interfere or block the components of the IFN response ranging from IFN synthesis, signaling or functions of IFN-induced proteins. Thus, the virus ensures efficacy in replication (115). DNA and RNA viruses contain proteins that impair the Janus-activated kinase (JAK)-STAT signaling pathway by several mechanisms (94). For instance, certain viral proteins resemble cellular components of the IFN signal transduction pathway but with antagonistic effects on the IFN signaling (94). A description of several mechanisms used by different virus to evade IFN response is reviewed elsewhere (94, 115).

Interferon dependent JAK-STAT signaling pathway

The classical pathway is the most extensively studied IFN-dependent pathway (98). Virus infection induces the synthesis of multiple IFNs that bind to cell surface

receptors in neighboring cells and activated the JAK-STAT signaling pathway (116). IFNα and IFNβ bind a transmembrane receptor termed the IFNα receptor (IFNAR), which is composed of IFNAR1 and IFNAR2 subunits (117) (Fig 2). Then, receptor-associated JAKs are activated in response to a ligand-dependent dimerization and rearrangement of the receptor subunits, followed by autophosphorylation of the associated JAKs (98). Then, JAKs phosphorylate and activate STATs. After phosphorylation STATs form homo- or heterodimers that rapidly translocate to the nucleus, bind to the promoters and induce transcription of ISGs (94, 98).

The STATs that are activated in response to type I IFNs are: STAT1, STAT2, STAT3 and STAT5. In certain cell types (endothelial or lymphoid cells), STAT4 and STAT6 can also be activated by IFN-α (98). The ISG factor 3 (ISGF3) complex is composed by the phosphorylated STAT1, STAT2 and IRF-9 (117). This complex binds to IFN-stimulated response elements (ISREs) located in the promoters of certain ISGs and initiate their transcription (98, 117). Other ISG promoters require a different element to initiate their transcription, known as an IFN-γ-activated site (GAS) element. GAS is bound by different STAT complexes.

During IFN-regulated gene transcription it is required that some STATs undergo biochemical modifications (98). The ISGs induction by type I IFNs involves chromatin remodeling, which occurs via STAT1, STAT2, and IRF-mediated recruitment of nucleosome-remodeling enzymes and histone acetyltransferases (HATs) (117). In the nucleus, STATs interact with transcriptional coactivators such as cAMP responsive-element-binding protein (CREB)-binding CRK proteins (CBP), p300, and

minichromosome maintenance deficient 5 (MCM5). NMYC and STAT interactor (NMI) improve STATS association with the co-activators CBP or p300. STAT2 interacts with the general control non-depressible 5 (GCN5) and the chromatin-remodeling factor brahma-related gene 1 (BRG1) (117). CBP and P300 have HAT activity important for chromatin remodeling to increase IFN-α- or IFN-γ-inducible transcription. Histone deacetylase 1 associates with STAT1 and STAT2. The histone-deacetylase activity is necessary for IFN-dependent gene transcription and to modify the transcriptional activity of the STATs (98).

Overall, this pathway regulates several other downstream cascades which lead to the pleiotropic biological effects of IFNs on target cells (98). Some of these pathways are JAK–STAT independent, whereas others cooperate with STATs to maximize the IFN-mediated signaling (98). Pathways that do not involve STATs have important roles in IFN mediated signaling. For example, active Crk-like protein (CRKL) binds to STAT5 in response to treatment with IFN-α/β and the resulting CRKL–STAT5 complex travels to the nucleus and binds a GAS element contained in the promoter of some ISGs (98).

FMDV and type I IFN

FMDV has developed several mechanisms to evade the host immune response including inhibition of cap-dependent host translation, inhibition IFN expression and/or IFN-signaling, presumably by virus dependent degradation of NF-κB, suppression of IRF-3 and IRF-7 activation, and deubiquitination of RIG-I, TBK1, TRAF3, and TRAF6 (see 23, 118, 119, 11, 120, 121, 122 for review). Also, 3Cpro inhibits IFN cascade by

cleaving NEMO, which is an adaptor protein crucial for activating both NF-κB- and IRF-mediated signaling pathways. Thus, this cleavage compromised NEMO functions as an adaptor of the RIG-I/MDA5 pathway and downstream IFN production (123). FMDV 3Cpro also interferes with the JAK-STAT signaling pathway by blocking nuclear translocation of STAT1/STAT2 through a mechanism that involves degradation of karyopherin α1 (KPNA1), the nuclear localization signal receptor for active STAT1 (124).

Bovine and swine cell cultures produce type I IFN mRNA when infected with either WT or LLV, but IFN activity was only detected in LLV infected cells (125, 126). Consistent with the Lpro inhibition of capped mRNAs translation, the capped IFN mRNA was not translated in the WT FMDV-infected cells even when IFNs mRNA were produced in cells infected with either virus (125,126).

Differential analysis of bovine genes from LLV versus WT infected cells by microarray demonstrated that Lpro plays a central role in the FMDV evasion of the innate immune response by inhibiting NF-κβ dependent gene expression as evidenced by up-regulation of several ISGs, chemokines, or transcription factors genes in LLV infected cells as compared to WT (127).

IFN proteins are still detected in serum and tissues of animals infected with FMDV WT, suggesting that inhibition of translation induced by the virus might be temporal and tissue or even cell specific (103). Animals that over-express IFN delivered by inoculation of a replication-defective human adenovirus type 5-based vector (Ad5) are protected against clinical manifestations of disease and in some cases protected from

primary infection in a dose dependent manner (128, 129, 96, 103, 130), suggesting that strength, timing and location of virus-host interactions are critical determinants for the outcome of the disease. In any case, high doses of Ad5-IFNs are required to achieve protection resulting in an expensive approach to control FMD; therefore there is a need to enhance the potency of this approach.

VSV and type I IFN

The ability of VSV to evade the host mechanism of defense is a critically important aspect of viral pathogenesis. Vesiculoviruses replicate rapidly and to high levels, generating high levels of potent inducers of host antiviral responses but at the same time they have rapid and potent means of inhibiting these responses, involving the general shut-off of nearly all host gene expression (42).

To counteract host antiviral responses, VSV inhibits host gene expression at a) transcription of host mRNA,(b) transport of host mRNA from the nucleus to the cytoplasm and (c) translation of host mRNA into proteins (42), (65). *In vivo* studies show that IFN induces inhibition of VSV protein synthesis by regulating the host translational machinery (131-133). In fact, IFN treatment increased mice survival even when treatment was administered 4 days after VSV intranasal inoculation (134). However, this effect is reversed by IFN neutralization (135) or IFNα/β receptor blocking (136). These studies demonstrate that animals are very sensitive to VSV in the absence of functional IFNα/β response (136) and highlight the importance of the enhancement of IFN response to counteract VSV infection.

CHAPTER III

REGULATION OF ANTIVIRAL RESPONSES BY 4EBPS

Type I IFNs are essential components of the host innate antiviral responses, however, its regulation is also critical to ensure that the response does not become excessive as IFN have either protective or damaging roles in bacterial infections and autoimmune diseases (137). Type I IFN production is regulated by members of the IFN regulatory factor (IRF) family of transcription factors, with IRF-7 being "the master regulator" for IFNα expression (138). IRF-7 is expressed at low levels in most cells, but its expression is up-regulated by viral infections. In spite of the low constitutive expression levels of IRF-7 in cells, it plays a crucial role in regulation of IFN induction through a positive feedback loop (139, 140).

IRF-7 expression and activation is altered by multiple mechanisms, for instance a cross-regulation between the IFN response and the cellular integrated stress response upon viral infection was evidenced by the IRF-7 mediated up-regulation of ATF4, which in return inhibits IRF-7 activation (141). Another study showed that Epstein-Barr virus induced receptor 2 (EBI2) negatively regulates type I IFN response in plasmacytoid DC (pDCs) and CD11b (+) myeloid cells through a mechanism that involves IRF-7, as EBI2-deficient mice expressed higher levels of IRF-7 (142).

IRF-7 is naturally regulated because excessive expression can trigger the oncogenic properties of IRF-7 (143). In mice, 4eBPs (144) and OASL-1 (145) have been described as translational regulators of IRF-7. There are three 4eBP isoforms, termed

4eBP-1, 4eBP-2 (146) and 4eBP-3 (147). 4eBPs are important regulators of overall translation levels in cells (148). 4eBPs regulate initiation of eukaryotic translation by preventing association of eIF4E with eIF4G to form the eIF4F complex (147). Interestingly, 4eBP-1 is present in both the nucleus and the cytoplasm in various cell lines (149).

Murine target of rapamycin (mTOR)-dependent pathways are important for IFN signaling (150). Although type I IFNs usually suppress translation, IFNs activate phosphoinositide 3-kinase (PI3K)-AKT- mTOR signaling in certain cell lines (150, 151), (105). mTOR is a kinase essential to the pathways that induce cell growth in mammals (152). This kinase associates with adaptor proteins raptor (153) or rictor (154) to form mTORC1 or mTORC2 complexes (154). mTOR is inhibited by the drug rapamycin, however association of mTOR with Rictor induces a rapamycin-insensitive pathway that regulates the cytoskeleton (154). S6 kinase (S6K, formerly known as p70s6K) and 4eBP-1 (also called eIF4EBP-1) are the major regulators of protein synthesis downstream of mTORC1 (152).

In the presence of serum, growth factors, or hormones, mTOR1 also phosphorylates 4eBP-1 causing release of eIF4e and allowing initiation of 5′-cap-dependent mRNA translation (152, 155). The presence of active (non-phosphorylated) 4eBPs prevents association of eIF4E with eIF4G to form the eIF4F complex, reversibly inhibiting association of the 43S ribosomal pre-initiation complex to the mRNA (147). Thus, due to the involvement of PI3K and downstream effector mTOR kinases in 4eBP-1 phosphorylation, its hyperphosphorylation is wortmannin- and rapamycin sensitive

(see Fig 3). Also, over-expression of 4eBP-1 or -2 in cells previously transformed by increased expression of eIF4e, partially reverts their transformed phenotypes (156).

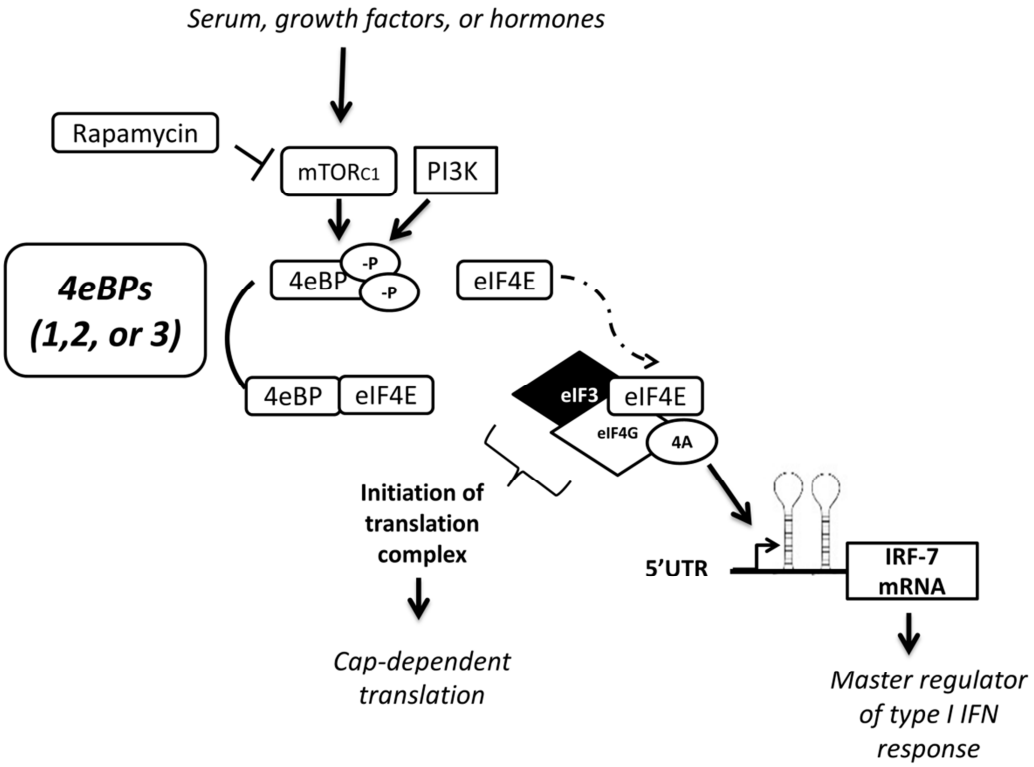

Figure. 3. Model depicting 4E-BPs translational suppression of IRF-7.
Activation of mTOR or PI3K leads to inactivation (hyperphosphorylation) of 4eBPs causing release of eIF4E. eIF4E then binds to eIF4G to form the eIF4F translation initiation complex. Increase in eIF4F allows the translation of IRF-7 mRNA, that otherwise would be inefficiently translated under 4eBPs active state (hypophosphorylation). Modified from (158, 258).

Colina et al. (2008) first described how the synthesis of IRF-7 is regulated by the repressor genes 4eBPs (144). This regulatory mechanism is supported by the correlation of increased IRF-7 mRNA translation, enhanced type I IFNs production and viral suppression in 4eBP-1 and -2 deficient mice (144). 4eBP-1 seems to inhibit the

translation of a particular set of mRNAs containing highly structured 5'UTR mRNAs (Fig 3). Thus, the structured and evolutionarily conserved 5' UTR of IRF7 mRNA seems to play a role in the translational repression by 4E-BPs in mice (144). Kaur et al (2007) also reported that mouse embryonic fibroblasts (MEFs) lacking 4eBP-1 (4eBP-$1^{-/-}$) stimulated with IFN-α4 had enhanced translation of some ISG15 and CXCL10 proteins as compared with wild-type (WT) 4E-$BP1^{+/+}$ MEFs (150). The same research group showed that 4eBP-$1^{-/-}$ MEFs were more sensitive to IFN treatment when challenged with encephalomyocarditis virus (EMCV) (150) Another group, also reported that 4eBP-$1^{-/-}$ mice were more sensitive to treatment with IFNß, exhibiting lower Coxsackievirus B3 viral titers and less severe viral induced myocarditis than control groups (157). Therefore, these studies identified 4eBPs as key regulators of IFN response.

Compelling data suggest two mechanisms of translational regulation of IRF-7 in murine model (144), (145). However in the case of 4eBPs mediated regulatory mechanism, the lack of IRF-7 5'UTR structure data and deletion/mutation analyses renders data not conclusively in terms of how 4eBPs orchestrate specific repression over IRF-7 translation in the presence of IRF-7 highly structured 5' UTR (158). In this chapter, porcine IRF-7 5'UTR regions folding in 4, 3, or 2 stem loops were predicted using computational RNA modeling. Structural analysis of the 5' UTR of porcine IRF-7 revealed homology with the 5'UTR of murine IRF-7. We found that 361nt from the porcine IRF-7 5'UTR is the minimum sequence that significantly repress reporter translation. Intriguingly, translational repression induced by poIRF-7 5'UTR was not selectively affected by 4eBP-1 depletion or hyperactivation. Thus, regulation of IRF-7-

mediated antiviral state involves 4eBP-1, but changes in 4eBP-1 did not affect translational repression induced by IRF-7 5'UTR in porcine cells. Since, the effect of 4eBPs reduction over IFN response has not yet been studied in cells from livestock species, we also sought to determine the mechanism of regulation of IRF-7-mediated type I IFN response by 4eBPs in porcine and bovine cells. We explored a strategy to enhance type IFN I response in cells from livestock species by decreasing 4eBPs. Interestingly, we found that partial knockdown of 4eBP-1,-2, or -3 by siRNAs in bovine or porcine cells did not enhance IFN mediated antiviral responses upon poly I:C or viral stimulation. However, swine cells completely deprived of 4eBP-1 by a CRISPR/Cas9 system stimulated by poly I:C produced higher levels of IFNβ, ISGs transcripts, and resulted in lower VSV yield. To better understand the CRISPR/Cas9 genome editing system, it will be briefly reviewed in the following section

Exogenous control of gene expression by CRISPR-Cas systems

Clustered regularly interspaced short palindromic repeats (CRISPR)/CRISPR-associated (CRISPR-Cas) associated systems have evolved to counteract invading viruses and plasmids in bacteria and Archaea (159). In these organisms the process involves three steps (i) integration of viral or plasmid DNA- into the CRISPR locus, (ii) expression of short guide CRISPR RNAs (crRNAs) (iii) interference with the invading foreign genomes (160, 161). CRISPR loci are typically adjacent to Cas genes and have regular structure: numerous noncontiguous direct repeats separated by target sequences (also known as protospacer) of constant size which are segments of captured viral and plasmid sequences (162, 159). CRISPR repeat-spacer arrays are transcribed and

processed into short crRNAs. Maturation of the active crRNAs from the CRISPR precursor transcript (pre-crRNA) is critical for CRISPR activation (160). An important feature of bacterial and Archaea CRISPR-Cas systems is the potential to incorporate new spacer sequences from foreign DNA and thus gain immunity against plasmids or viruses (163).

CRISPR-Cas systems differ in the repeat sequence, the number and type of Cas genes, and the number of repeat-spacer arrays (164). There are three types of CRISPR/Cas systems (161) (165),(164). The type I and III encompasses Cas endonucleases that process the pre-crRNAs. Each mature crRNA assembles into a multi-Cas protein complex that cleaves nucleic acids complementary to the crRNA (165). In type II systems, as exemplified by *Streptococcus pyogenes* (166), crRNAs anneals with a trans-activating crRNA (tracrRNA) complementary to the repeat sequences in pre-crRNA. The tracrRNA directs the maturation of crRNAs by a host endogenous double-stranded (ds) RNA-specific ribonuclease RNase III and the Cas9 (formerly Csn1) protein (160). In all types of CRISPR/Cas systems, the end result is sequence-specific silencing of foreign nucleic acid by Cas proteins (167).

Cas genes belong to a diverse family of proteins that contain domains typical of nucleases, polymerases, helicases, and polynucleotide-binding proteins (159). To cleave target dsDNA, the Cas9 requires a base-paired structure made between the tracrRNA and the targeting crRNA. Location of the site-specific cleavage of Cas9 is determined by base-pairing complementarity between the crRNA and the target DNA and the protospacer adjacent motif (PAM) (165). Cas9 contains a RuvC-like nuclease domain

near the amino terminus and the HNH (or McrA-like) nuclease domain in the middle of the protein (161).

Jinek et al (2012) demonstrated *in vitro* that the Cas9 can be programmed to cleave specific DNA sites by heterologous expression of synthetic guide RNA (gRNA), consisting of a fusion of crRNA and tracrRNA. This work proved the versatility of RNA-directed system to generate dsDNA breaks for genome targeting and editing (165). Further studies demonstrated the application of engineered CRISPR/Cas9 systems *in vitro* in mouse and human cells (166) or *in vivo* to induce targeted genetic modifications in zebrafish embryos (167). In mammalian cells engineered RNase III was not necessary for cleavage of the protospacer, maturation of pre-crRNA, or processing of the tracrRNA suggesting that there may be endogenous mammalian RNases that contribute in pre-crRNA maturation (166). Cong et al (2013) observed that sequence homology for up to 11 bp at the 5′ of the PAM are critical for genomic cleavage by Cas9 (166). Also, in mammalian DNA, double-stranded breaks induced by Cas9 are partially repaired by the indel-forming non-homologous end joining (NHEJ) pathway (166). The efficiency of the CRISPR/Cas9 system was similar to those obtained using other genome editing techniques such as zinc finger nucleases (ZFNs) (167) and transcription activator–like effector nucleases (TALENs) for the same genes (166,167). Thus, RNA-Guided Endonucleases (RGENs) have evolved as innovative, programmable genome engineering tools that are adapted from CRISPR/Cas system (166). In this chapter we describe the used of this system to knock out genes of interest and enhance the antiviral state in porcine cells.

Materials and methods

RNA structure analysis and modelling

A consensus sequence of the porcine IRF-7 5' UTR was predicted by alignment of *Sus scrofa* expressed sequence tag (EST) (AK235035.1) with the complete DNA sequence of porcine IRF-7 (AB287430.2) using ClustalW (168). Porcine consensus sequence was also compared to the murine IRF-7 5'UTR (NM_001252601.1). RNA folding predictions were performed for fragments of the poIRF-7 5'UTR consensus sequence using default parameters in the RNA fold software, (Vienna RNA web suite) (169).

Cell and reagents

Primary fetal bovine fibroblasts (FBF) were isolated from fetal skin following protocols for primary tissue isolation (170). Briefly, using aseptic technique ~0.5 cm^2 sections of skin were cut from calf fetuses acquired from the slaughter house. Pieces of skin were washed 3 times with PBS containing antibiotic. Tissue sections were minced, pooled, and cultured in several 10cm^2 tissue culture dishes with culture media containing Dulbecco's modified minimum essential media (DMEM) F12, 20% Fetal bovine serum (FBS), 2% antibiotics and antimitotic (Life technologies Carlsbad, CA), and supplemented with bovine fibroblast growth factor (Sigma- Aldrich, St. Louis, MO). Culture dishes were incubated at 37˚C in a humidified 5% CO2 and check daily. After 4-7 days cells started to grow in the dish surface surrounding the pieces of skin. Pieces of tissue were removed and the remaining cells were tripsinized and transferred into several T75 flasks. When T75 flasks were confluent, cells from several flasks were pooled and

frozen in aliquots denominated FBF passage 1 (P1). Cells were maintained in DMEM containing 10% FBS and supplemented with 1% antibiotics and non-essential amino acids. IFN competence in the FBF was evaluated by IFN bioassay. FBF cells P3 were used for transfections with siRNAs and subsequent challenge assays with VSV.

Swine kidney cells (SK-6 and IBRS-2) were obtained from APHIS at Plum Island Animal Disease Center (PIADC), Greenport, NY. Primary porcine kidney cells were kindly provided by USDA-ARS (Iowa, USA) and used for siRNAs transfections. Cells were cultured under standard tissue culture conditions, using minimum essential media (MEM) containing 10% FBS and supplemented with 1% antibiotics and 1% non-essential amino acids. Vero cells (ATCC CCL-81), were purchased from the American Type Culture Collection (ATCC, Rockville, MD) and were used for viral titrations. Cells were also cultured under standard tissue culture conditions as explained above. In some transfections, polyinosinic: polycytidylic acid (poly I:C) (Invivogen, San Diego, CA) (1-0.1 µg/ml) as an inducer of the IFN pathway.

Viral infections

A laboratory-adapted VSV serotype Indiana kindly provided by Judith Ball (Texas A&M University) was used for infections under BSL-2 conditions. Cells were infected at specified hours-post transfection (hpt) at the indicated multiplicity of infection (MOI). VSV was adsorbed for 1 h at 37^{o} C and infection continued for the time specified in each figure legend. Virus was released by one freeze-thaw cycle. Viral titers were calculated using the method of Reed and Muench (171) by microtitration. Results were expressed as log10 of the $TCID_{50}$/ml.

For some experiments FMDV A12 or LLV viruses were used. Viruses were obtained by using infectious clones $pRMC_{35}$ or pA12LLV2 (18, 172). Experimental infections using these viruses were conducted at the USDA-ARS Plum Island Animal Disease Center under biosafety level (BSL)-3Ag. Viral titers in FMDV infected cells were determined by plaque assay, using standard procedures (173) and expressed as pfu/ml.

siRNA design and transfections

Double stranded RNA sequences of 18-22 nt in length complementary to the coding region of bovine 4eBP-1 (GI:112362105), 4eBP-2 (GI:300793659), 4eBP-3 (GI:323510621) and porcine 4eBP-1 (GI:346644789), predicted 4eBP-2 (GI:545870436), and predicted 4eBP-3 (335283582) were selected to design siRNAs (Table 1). SiRNAs were transfected with lipofectamine RNAimax (Life technologies Carlsbad, CA) following the manufacturer's directions. Cells were transfected for 48h with different concentrations of the siRNAs as indicated in each figure legend. Control groups included mock transfected cells (negative control), and cells transfected with a non-targeting siRNA labeled with a fluorescent dye (Cyanine 3) (referred as siRNA control in figures) to control for unspecific silencing, unintended induction of IFN expression, and transfection efficiency.

Table 1. siRNAs used to target 4eBPs in bovine and porcine cells.

Identification	Targeted species	Sequence 5'-3'
si4eBP-1	Porcine	AACTCACCTGTGACCAAAAC
si4eBP-1	Bovine	CAGGATCATCTATGACCGGAA
si4eBP-2	Porcine	AAGACTCCAAAGTAGAAGTAA
si4eBP-2	Bovine	CTCGAATCATTTATGATCGAA
si4eBP-3	Porcine/bovine	ATGTCACTTTCTGACTGCTTA

Plasmids, constructs, and reagents

Different size fragments of regions of 5'UTR of porcine IRF-7 were cloned at Nhe I site of the psiCHECK™-2 (Promega, Madison,WI) plasmid located upstream of renilla luciferase ORF. Control groups included an empty psiCHECK™-2 vector (plasmid control) and a psiCHECK™-2 containing the 5'UTR of human IRF-2 (5'UTR IRF-2).

For some experiments, 4eBPs were dephosphorylated and consequently activated using rapamycin (174) at 10 µM for 4h.

Renilla luciferase assays

SK-6 or IBRS-2 cells were seeded in 12-well plates at $2x10^5$cells/well the day before the transfection. Five hundred ng of psiCHECK™-2 plasmids expressing different size fragments of the 5'UTR of IRF-7 were transfected for 24h into duplicate wells. Twenty-four hours later, cells were stimulated with poly I:C (1µg/ml) for 8h followed by passive lysis according to dual-luciferase assay's (Promega, Madison,WI) instructions. Renilla and firefly luciferase chemiluminescence was measured using a Cary Eclipse fluorescence spectrophotometer (Agilent technologies). Relative

luminescence units (RLU) were calculated and expressed as a percentage of the expression in plasmid control.

Generation of 4eBP-1$^{-/-}$ cells using CRISPR/Cas9 system

Three distinct guide strands were designed to target different genomic regions of porcine 4eBP-1 (Table 2). The guide strands were cloned into the pX330-U6-Chimeric_BB-CBh-hSpCas9 plasmid (Addgene plasmid 42230) which was modified by incorporation of an IRES-GFP cassette (px330-U6-IRES-GFP). SK-6 cells were seeded in 6-well plates ($1x10^6$ cells/well) the day before the transfection. In separate wells, cells were transfected with one microgram of each of the px330-U6-IRES-GFP plasmids containing the guide strands. On the next day, GFP expression was confirmed by microscopy examination and GFP-positive cells were sorted using a MoFlo Astrios Cell Sorter (Beckman Coulter, Brea, CA) into single 96-wells. Populations derived from a single cell were expanded using conditioning media. Total genomic DNA was isolated using DNA wizard (Promega, Madison,WI) from a homogenous population of cells derived from single cell colony. The DNA regions targeted by the guide strands were PCR amplified, subcloned into a PGEM sequencing vector (Promega, Madison,WI) and verified by sequencing using primers listed in Table 3.

Table 2. Sequence of guide strands targeting porcine 4eBP-1 including the PAM sequences.

Identification	Sequence 5'-3'
gs4eBP-1_ NaeI	GTAGCCCAGACGACAAGCGG
gs4eBP-1_ MseI	GTCACAGTTTGAGATGGACATTTAAAGG
gs4eBP-1_ noRE	TACCAGGATCATCTATGACCGG

Table 3. Primers used for amplification of a partial 4eBP-1 sequence from gDNA.

Identification	Sequence 5'-3'
4eBP-1 exon 3-F	GTAGGAAAACCTGCCACCTG
4eBP-1 exon 3-R	GAAAGCTGGTTGGGATGAAA

Antibodies and western blot

Cross-reacting antibodies against porcine 4eBP-1 and tubulin were purchased from Abcam (Cambridge, MA). Cell lysates were prepared using a modified RIPA buffer (25mM Tris pH7.5, 250mM NaCl, 1% NP40, 1% deoxycholate, 0.1% SDS), followed by centrifugation. Western blotting was performed according to standard procedures and proteins were visualized using supersignal west pico chemiluminescent substrate (Thermo Fisher Scientific Waltham, MA) using FluorChem E (Protein simple, Santa Clara, CA).

Analysis of mRNA expression by quantitative real time RT-qPCR

Total RNA was isolated from cell lysates using a commercially available extraction kit (Qiagen, Valencia, CA). Five hundred ng of RNA was used to synthesize cDNA using random hexamers with qScript kit mix (Quanta Biosciences, Gaithersburg, MD) according to the manufacturer's instructions. cDNA was diluted tenfold and used as template for qPCR with PerfeCTa® SYBR® Green FastMix, ROX (Quanta Biosciences, Gaithersburg, MD). Samples were run in StepOne Real-Time PCR Systems (Applied Biosystems, Carlsbad, CA).

Relative quantification was performed for IRF-7 and indicated ISGs using primer sequences previously published (96, 97). Bovine and porcine 4eBP-1, 4eBP-2 and 4eBP-

3 transcripts were detected using primers indicated in Table 4. The expression of the genes of interest was normalized using GAPDH or β-actin. RT-qPCR analysis was performed following MIQE Guidelines (175). Data was analyzed using the comparative ΔΔCt method (176).

Statistics and data analysis

Statistical analysis was performed using JMP software, version 8.0.2. Values are expressed as mean ± standard error (SEM), and statistical significance determined using Student's t-test or Wilcoxon test (*$p < 0.05$ or ** $p < 0.001$) is indicated.

Table 4. Primers used in RT-qPCR to detect porcine and bovine 4eBPs transcripts.

Identification	Target species	Sequence 5'-3'
po 4eBP-1-F	Porcine	TGTGACCAAAACGCCCCCGA
po 4eBP-1-R	Porcine	AACTGTGACTCTTCACCGCCCG
po 4eBP-2-F	Porcine	TAGGGAGGTTGGATGGGTTC
po 4eBP-2-R	Porcine	TGAGCAAGACAAGGAGAGACAGA
po 4eBP-3-F	Porcine	AGGAGCTGAAGGGGCAGAAGGA
po 4eBP-3-R	Porcine	AGGTAGCGGCAGCAGCATGA
bo 4eBP-1-F	Bovine	TCCTGATGGAGTGTCGGAAC
bo 4eBP-1-R	Bovine	CATCGCCTGTAGGGCTAGTG
bo 4eBP-2-F	Bovine	GAGGTTTGATGGGTTCAGCA
bo 4eBP-2-R	Bovine	CTGGGCAAGACAGTGAGGAG
bo 4eBP-3-F	Bovine	CTGGAAGGGGGTGATATGTTG
bo 4eBP-3-R	Bovine	TTGGGAGGAGTGGCTACAGA

Results

Knockdown of 4eBPs on bovine or porcine cells does not modify antiviral state

Previous studies have shown that obliteration of 4eBP-1 and 4eBP-2 in mice enhances IRF-7 mediated induction of type I IFN (144). To test whether knockdown of 4eBP-1 and 2 in bovine cells could also enhance antiviral response prior to viral infection, FBF (P3) were transfected with siRNAs targeting bovine 4eBP-1 or -2 (Table 1) and transcripts were analyzed by RT-qPCR. SiRNAs targeting 4eBP-1 or -2 significantly and specifically reduced their transcripts by approximately 60% ($p < 0.001$) as compared to siRNA control (Fig 4A-B), however this reduction in 4eBP-1 or 2 transcripts did not increase the levels of RIG-I or ISG15 transcripts (Fig 4C). Additionally, knockdown of 4eBP-1 or -2 prior to VSV infection did not reduced viral yield when cells were infected at MOI=0.1 (not shown).

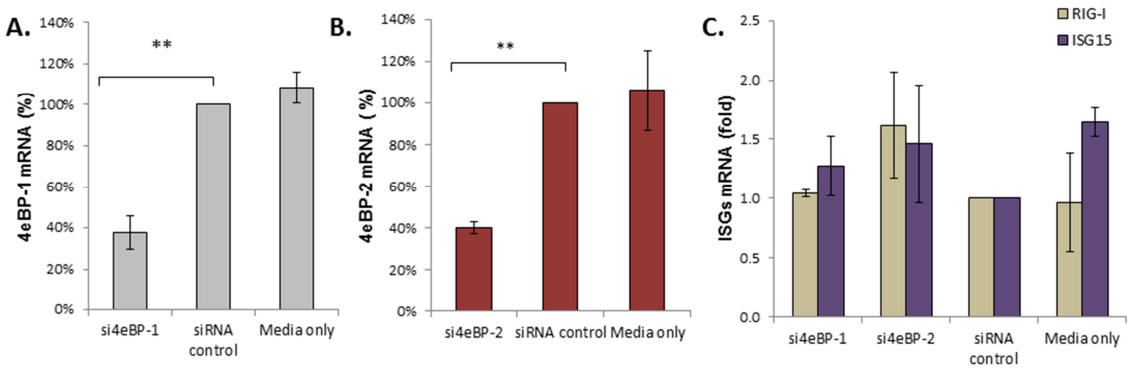

Figure. 4. Knockdown of 4eBP-1 or -2 in bovine cells has no effect on unstimulated ISGs levels.

FBF were mock transfected or transfected with 200 nM of siRNA control, si4eBP-1 or si4eBP-2. Forty eight hours later, RNA was extracted and (A) 4eBP-1, (B) 4eBP-2 or (C) ISG 15 and RIG-I transcripts levels were determined by RT-qPCR. Transcript levels in A and B are represented as a percentage relative to the media control. Statistics: Student's t-test (** $p < 0.001$)

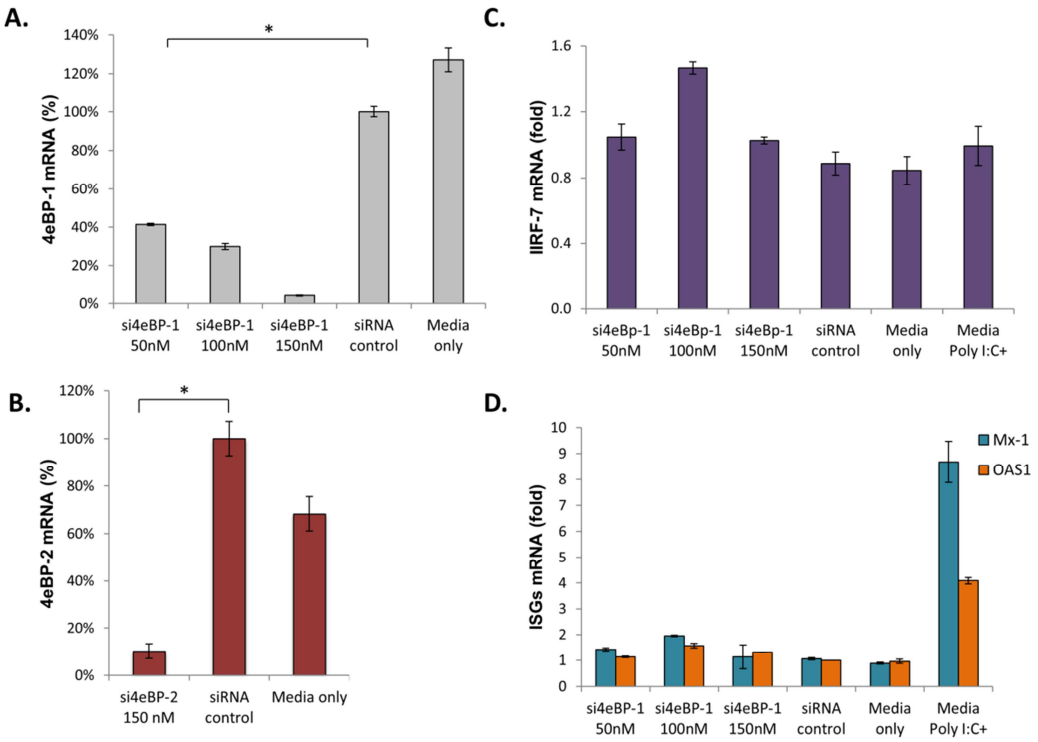

Figure. 5. Knockdown of 4eBP-1 or -2 in porcine cells has no effect on basal ISGs RNA levels.
SK-6 cells were mock transfected or transfected with 150 nM of siRNA control, (A) 50, 100 nM or 150 nM of siRNA 4eBP-1, or (B) 150 nM of siRNA 4eBP-2. Forty eight hours later, RNA was extracted and 4eBPs levels or (C) IRF-7 or (D) OAS-1 and Mx-1 relative gene expression was determined by RT-qPCR. Cells transfected with 1µg/ml of poly I:C were used as positive control. Transcript levels in A and B are represented as a percentage relative to the siRNA control. Statistics: Wilcoxon test (* $p < 0.05$)

Similarly to bovine cells, transfection of SK-6 cells with a siRNA targeting porcine 4eBP-1 induced significant dose dependent reduction of target transcripts by 60 ($p < 0.0043$), 70, or 96 % when 50, 100 or 150 nM were used, respectively (Fig 5A). Consistent with the results observed in bovine cells, knockdown of 4eBP-1 or -2 (Fig 5A-B) did not increase IRF-7 or ISGs transcripts levels (Fig 5C-D) nor enhance the antiviral response upon VSV infection (not shown). However, SK-6 cells transfected

with poly I:C (1µg/ml) showed significant increase in ISGs expression, demonstrating that IFN pathway is functional in this cell line. These results suggest that knockdown of 4eBPs without prior induction of IFN pathway has no effect on antiviral state in porcine and bovine cells.

Knockdown of 4eBP-1 or -2 on porcine cells does not induce antiviral response during FMDV A12 or LLV infection

Since knockdown of 4eBP-1 or -2 failed to enhance the antiviral response, we next reasoned that IFN pathway could be activated by using a low MOI (0.1) of FMDV LLV for 18h, a virus particularly susceptible to type I IFN and we would be able detect any difference in ISGs induction and virus yield. We also infected cells using wild type FMDV A12 virus. As shown in Fig 6, efficient and specific knockdown of 4eBP-1 in IBRS-2 was detected by western blot (Fig 6A) or RT-qPCR (Fig 6B). However, knockdown in 4eBP-1 or -2 was not associated with significant changes in transcript levels of Mx-1, RANTES, or OAS-1 in FMDV LLV infected cells as compared to mock infected cells (Fig 6C-E). Consistently, no biologically relevant differences (less than 1log) in FMDV A12 or LLV viral titers were observed after knockdown of 4eBP-1 or -2 (Table 5). These results suggest that the antiviral state was not enhanced prior to viral infection in groups with lower 4eBPs levels.

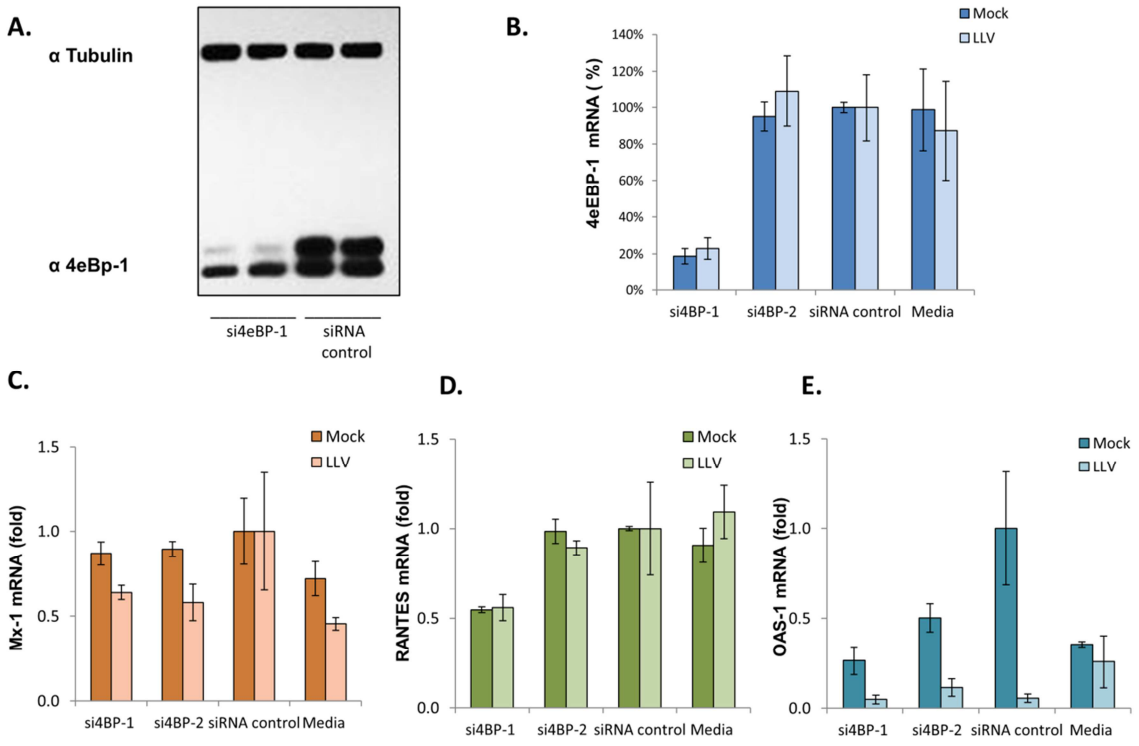

Figure. 6. Knockdown of 4eBP-1 or -2 in porcine cells has no effect on ISGs levels in LLV or mock infected porcine cells.

IBRS-2 were transfected with 200 nM of siRNA control or siRNA 4eBP-1 in duplicates. (A) Forty eight hours later 4eBP-1 and α-tubulin were detected by western blot in cell lysates. A representative blot is showing 1 out of 3 replicates.

IBRS-2 cells were transfected with 200 nM of siRNA control, si4eBP-1, si4eBP-2 or non-transfected (media). Forty eight hours later, cells were mock or LLV infected for 18h. RNA was extracted and (B) 4eBP-1 (transcript levels are represented as a percentage relative to the siRNA control), (C) Mx-1, (D) RANTES or (D) OAS-1 transcript levels were compared by RT-qPCR. Competence of IBRS-2 cells to produce IFN was tested and discussed in Chapter 5.

Table 5. Viral titers recovered from IBRS-2 cells transfected with si4eBP-1, -2, siRNA control or media and challenged with FMDV A12 or LLV.

	FMDVA12 (PFU/ml)	**FMDV LLV** (PFU/ml)
si4EBP-1	$1.3x10^7$	$5.1x10^3$
si4EBP-2	$2.2x10^7$	$1.4x10^3$
siRNA control	$2.8x10^7$	$9.9x10^3$
Media	$1.0x10^7$	$1.3x10^3$

Knockdown of 4eBPs on primary porcine cells primed by poly I:C does not enhance antiviral response

Next, we tested if knockdown induced by individual or combination of siRNAs targeting all isoforms of 4eBPs will induce a change in the antiviral state co-stimulated with poly I:C. The knockdown efficiencies of individual siRNAs were estimated by RT-qPCR and corresponded to 86, 68, and 93% for 4eBP-1, -2, and -3, respectively (Fig 7A-C). In groups stimulated with poly I:C a drastic reduction in VSV titers (~7 logs) was observed as compared to media control. However no differences among the groups were detected, suggesting that the effect was exclusively due to poly I:C stimulation and not by knockdown of 4eBPs by the siRNAs (Fig 7D). Consistent with these results, expression of ISG54 and Mx-1 transcripts was highly up-regulated by poly I:C treatment but no difference was detected among groups with reduced 4eBPs (Fig 7E).

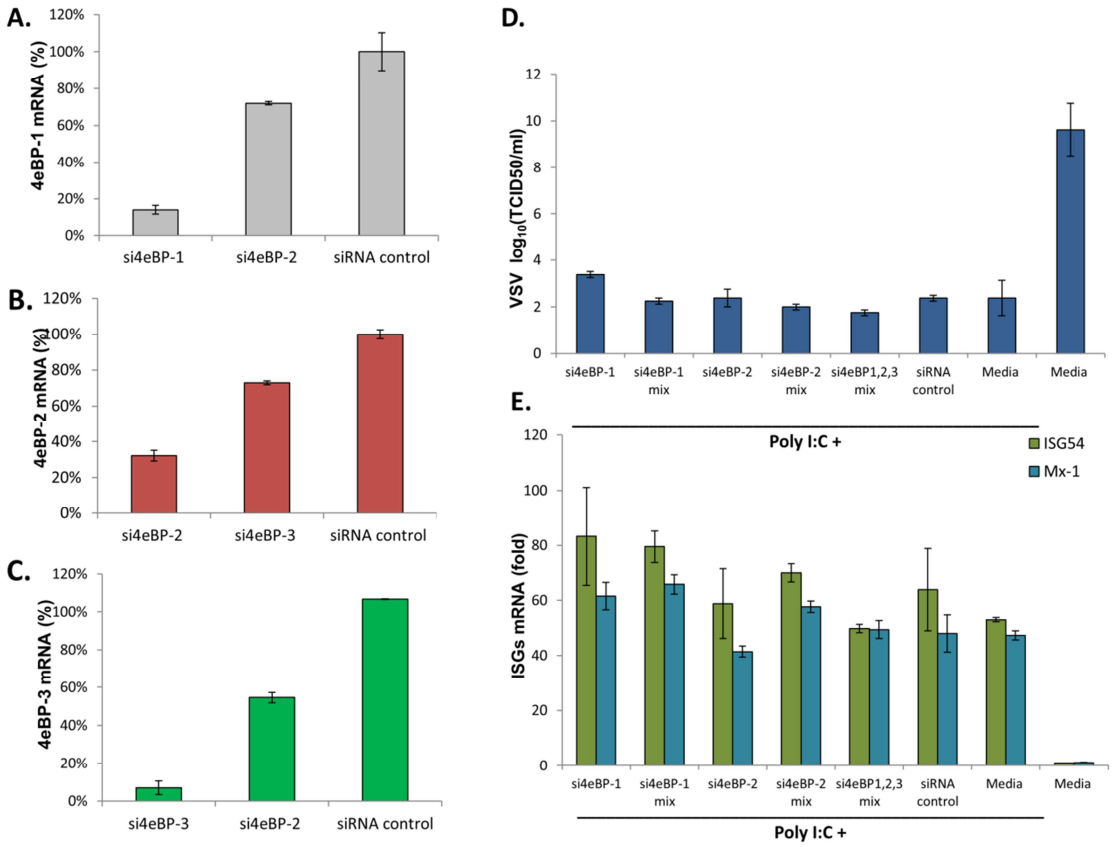

Figure. 7. Knockdown of 4eBP-1,-2 or -3 in primary porcine cells induced no differences on ISGs transcripts.

Knockdown efficiencies were determined by qPCR analysis of (A) 4eBP-1, (B) 4eBP-2, or (C) 4eBP-3 transcripts after transfection of primary porcine cells with 50pmol of indicated siRNAs. (D) Primary porcine cells were transfected with si4eBP-1, si4eBP-2, siRNA control, or a combination of 2 siRNAs (si4eBP-1 mix or si4eBP-2 mix), or a combination porcine siRNAs targeting all 4eBPs (4eBP-1,-2,-3 mix). Twenty four hours later, cells were stimulated with poly I:C (100 ng/ml). Total RNA was extracted and samples were processed for ISG54 or Mx-1 by RT-qPCR (E) VSV infection at MOI=0.01 for 24h was done after poly:IC and siRNA treatment. Viral titers were determined by $TCID_{50}$ method.

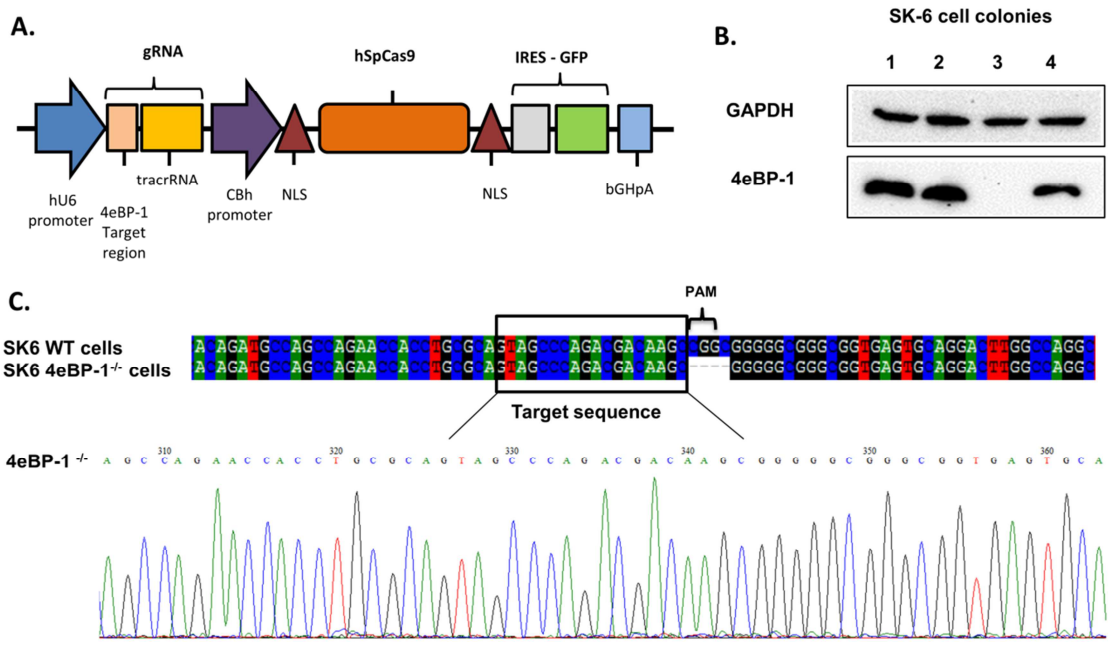

Figure. 8. Generation of a 4EBP-1$^{-/-}$ porcine cell line using CRISPR/Cas9.
(A) CRISPR/Cas9 construct contains the U6 promoter driving the expression of 4eBP-1 specific guide strands (gRNA). Human codon optimized Cas9 expression is driven by CBh promoter. Porcine SK-6 cells were transfected with the CRIPR/Cas9 construct depicted followed by GFP-FAC sorting 24 hpt. Single cell colonies were expanded. (B) Total cell lysates from each colony were resolved by PAGE and analyzed by western blotting using α-GAPDH or α-4eBP-1 antibodies. (C) Sequencing was used to verify 4eBP-1 knockout (KO) cells.

Effective knockout of 4eBP-1 by CRISPR/Cas9 system

RNAi is limited to induce partial knockdown of target genes, however new genome editing systems permit efficient generation of gene knockout. CRISPR/Cas9 system was used to generate a porcine cell line lacking 4eBP-1 (4eBP-1$^{-/-}$). First, guide strands designed to target porcine 4eBP-1 were cloned into px330-U6-IRES-GFP vector (Fig 8A). These constructs were used to transfect SK-6 cells, followed by FAC sorting and single cell colony screening. As shown in Fig 8B one out of 4 colonies transfected

with px330-U6-IRES-GFP showed knockout of 4eBP-1 expression by western blot (Fig 8B, colony 3). None of the colonies tested that were transfected with gs4eBP-1_MseI or gs4eBP-1_noRE produced 4eBP-1 knockouts (not shown). Genomic DNA sequence revealed 4 nucleotides deletion within the PAM region of the guide strand target sequence (Fig 8C), and together with the western blot data confirmed the 4eBP-1$^{-/-}$ nullizyous state of porcine cells.

Stronger antiviral response in 4eBP-1$^{-/-}$ porcine cells after poly I:C stimulation

The response of 4eBP-1$^{-/-}$ cells in the presence or absence of poly I:C (1µg/ml for 8h) stimulation and followed by VSV infection was tested. Poly I:C stimulation of 4eBP-1$^{-/-}$ cells (Fig 9A) increased expression of IRF-7 transcripts (Fig 9A), but no significant difference was observed between wild-type (WT) or KO cells with or without poly I:C stimulation. However, viral yields were significantly lower (~1.7 logs, p=0.047) in KO cells as compared to WT cells in groups stimulated with poly I:C (Fig 9B) and subtle reduction in CPE was evident in KO cells as compared to WT (Fig 9C).

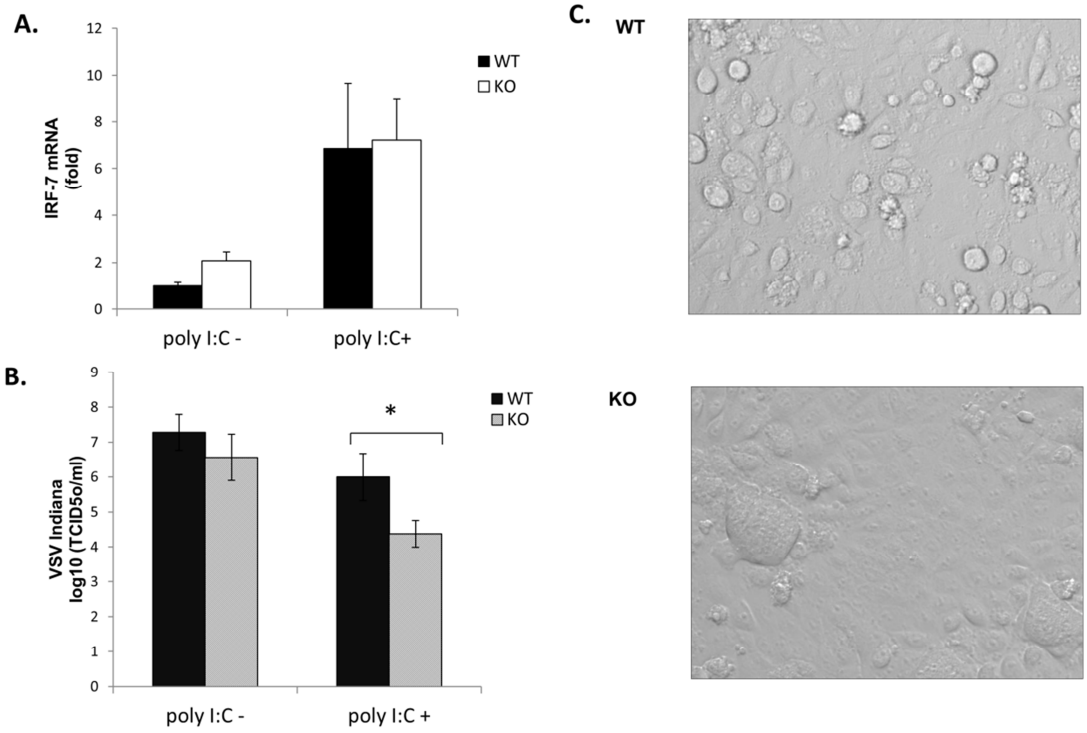

Figure. 9. 4eBP-1$^{-/-}$ cells had lower viral yield and less CPE but no changes in IRF-7 transcripts as compared to WT cells upon poly I:C stimulation.
KO or WT cells were poly I:C (0.1-1 µg/ml) or mock transfected for 12h. (A) IRF-7 transcripts were tested by RT-qPCR. (B) After poly I:C transfection, cells were infected with VSV infection at MOI=0.02. Viral yield was quantified by $TCID_{50}$ method and (C) CPE was observed at 8 hpi.

Consistent with the reduction in viral titers, IFNβ transcripts were higher in 4eBP-1$^{-/-}$ cells as compared to WT cells after poly I:C stimulation (70-fold difference), but no difference was detected between cells in which IFN was not previously stimulated (Fig 10A). Stimulation with poly I:C in WT or KO increased transcription of the ISGs tested including Mx-1, OAS-1, and ISG54 ranging from 9 to 56 fold as compared to non-stimulated controls, however KO cells showed higher induction of all ISG transcripts as compared to WT cells (Fig 10 B-D). These results suggest that the IFN

regulatory pathway involving 4eBP-1 described for mice might also play a role in regulation of IFN in porcine cells.

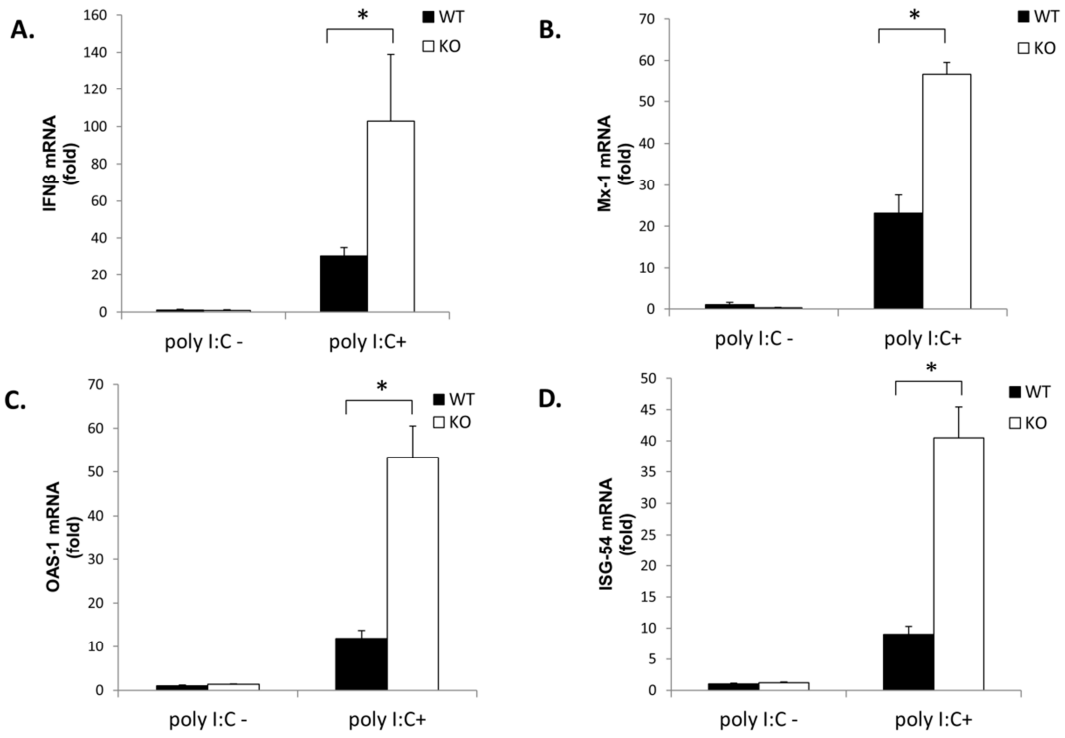

Figure. 10. 4eBP-1$^{-/-}$ cells induced higher levels of IFN and ISGs as compared to WT cells upon poly I:C stimulation.
4eBP1 KO or WT cells were poly I:C (PIC, 0.1-1 µg/ml) or mock transfected. (A) IFNβ and several ISGs transcripts including (B) Mx-1 (C) OAS-1 or (D) ISG54 were tested by RT-qPCR. Student-t test (* $p < 0.05$).

Structural models for the poIRF-7 5'UTR

The 5' UTR of IRF7 mRNA is highly structured, evolutionarily conserved, and seems to play a role in the translational repression by 4eBPs in mice (144). Analysis of the RNA secondary structure of the 5'UTR of porcine IRF-7 was performed using minimum free energy and partition function algorithms. Homologous to 420 nt of

murine 5’ UTR IRF-7 sequence previously reported (145) (Fig 11A), we reconstructed 432 nt that align to the 5’ UTR of porcine IRF-7 based on available EST sequences. Lee et al. (2013) reported 215 nt of muIRF-7 UTR that fold into 4 stem-loops (depicted boxes in Fig 11B) of which 2 stem loops (Fig 11D) are critical for IRF-7 regulation (145). By computational prediction of RNA folding, we also found 4 (Fig 11C) or 2 (Fig 11E) possible stem loop structures, similar to the ones described for murine 5’ UTR IRF-7. However, the base-pair probabilities of these stem loops structures in porcine 5’UTR were lower than in murine 5’UTR (in red probability=1, in blue probability close to 0). To test our structural predictions, fragments of different length (146, 170, 232, 361 nt) of the 5’UTR of poIRF-7 were cloned and tested in a dual renilla/luciferase reporter system (Fig 11A). We found that the reporter expression was significantly reduced (by ~75%, $p<0.05$) when 361 or 432 nt of the 5’UTR of poIRF-7 were located upstream of the reporter gene as compared to no 5’UTR or IRF-2 5’UTR controls (Fig 11F). The smaller fragments (232 bp, 170 bp, 146 bp), which all lacked the 3’ 129 bp, also reduced reporter expression (approximately 25-35%) (Fig 11F) but were not significantly different from controls.

The effect of IFN induction was tested by poly I:C stimulation, and no significant differences were in reporter expression were detected among groups in presence or absence of poly I:C. These results suggest that at least 361 nt of the 5’ region of poIRF-7 negatively regulate translation.

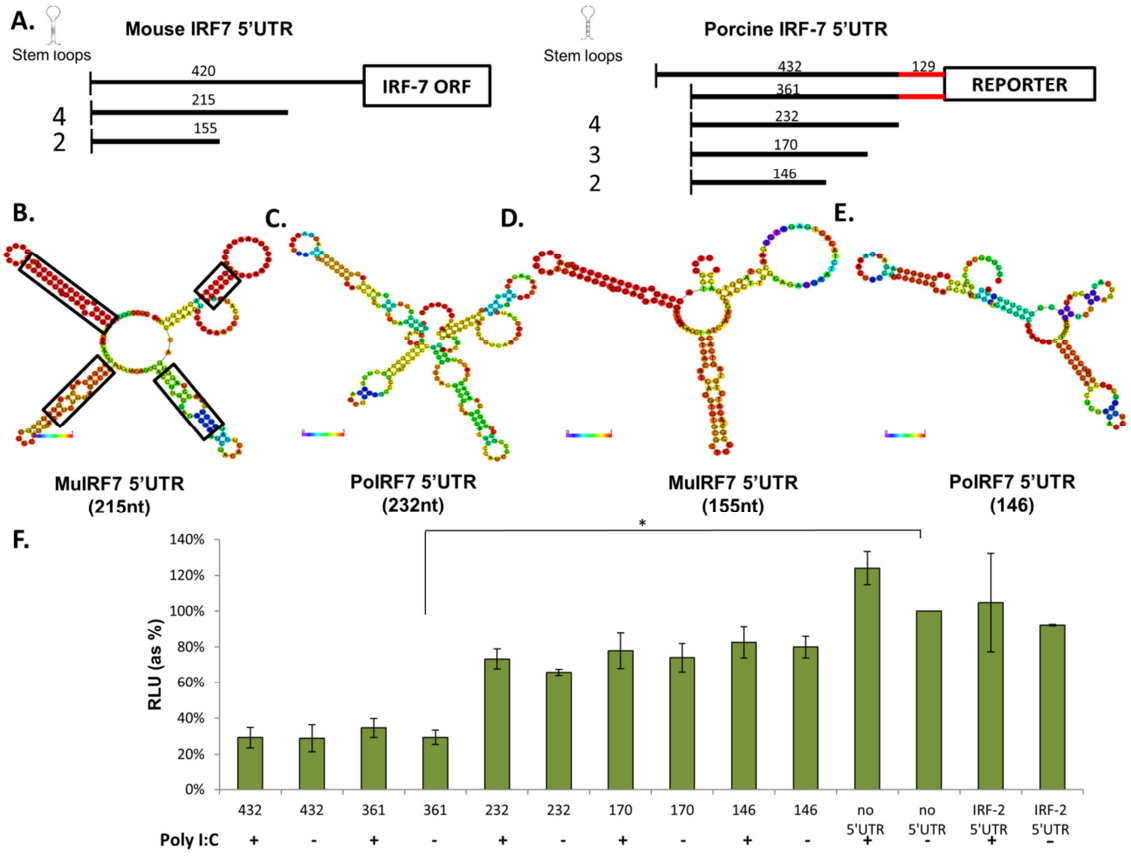

Figure. 11. Structural models for poIRF-7 5'UTR and translational repression of the 5'UTR.

(A) Different length fragments and predicted number of stem loops for murine or porcine poIRF-7 5'UTR are represented schematically. A 129 bp fragment that is only included in 432 or 361 nt 5'UTR is denoted in red. Computational prediction of RNA folding structures for (B) 215 nt of muIRF-7 5'UTR, (C) 232 nt of poIRF-7 5'UTR, (D) 155 nt of poIRF-7 5'UTR, or (E) 146 nt of poIRF-7 5'UTR. (F) SK-6 cells were transfected with dual renilla/luciferase plasmids containing fragments of the indicated size of poIRF-7 5'UTR sequence, or no 5'UTR, or IRF-2 5'UTR controls. Some groups of cells were stimulated with poly I:C (8h), followed by RLU determination. Data is represented as percentage of no 5'UTR control. Student's t-test (* $p < 0.05$)

PoIRF-7 5'UTR translational repression is independent of 4eBP-1

We tested whether the translational repression induced by the 5'UTR of IRF-7 was altered by depletion of 4eBP-1. 4eBP-$1^{-/-}$ cells or WT cells were transfected with

poIRF-7 5'UTR or with control plasmids (IRF-2 5'UTR or no 5'UTR plasmids). Using the dual reporter system and after firefly normalization, we confirmed that poIRF-7 5'UTR (432nt long) had a significant repressive effect over translation. However, 4eBP-1 depletion had no significant effect over translation of any of the groups as compared to WT cells containing 4eBP-1 (Fig 12A).

Next, we used rapamycin (the inhibitor of mTOR) to increase 4eBPs activity (174) in presence or absence of 4eBP-1 knock down. We detected efficient knock down of 4eBP-1 by siRNAs (shown in duplicate wells in the western blot) in absence of rapamycin, but rapamycin seemed to partially reverse the 4eBP-1 protein knockdown (Fig 12B).

Data from the renilla/luciferase reporter system again confirmed a strong reduction in reporter translation in groups that were transfected with poIRF-7 5'UTR (432nt long) upstream renilla reporter as compared to no 5'UTR control ($p = 0.04$) (Fig 12C). Knockdown of 4eBP-1 tended to increase reporter translation as compared to siRNA control in cells transfected with no 5'UTR control (Fig 11C, compare bars 2 to 4, $p = 0.054$). Rapamycin treatment, however, tended to decrease reporter translation in cells transfected with si4eBP-1 ($p = 0.053$) (Fig 12B, compare bars 1 to 2). However, 4eBP-1 knockdown had no effect over reporter translation in presence of poIRF-7 5'UTR with or without rapamycin treatment (Fig 12C, in graph bars 5-8).

Our results showed that 4eBP-1 depletion or activation of 4eBP-1 by rapamycin treatment did not affect translation of the reporter containing poIRF-7 highly structured mRNA (5'UTR renilla).Unexpectedly, the translational regulation IRF-7 by 4eBP-1

might involve mechanisms not selectively mediated by the highly structured 5'UTR IRF-7 in swine cells.

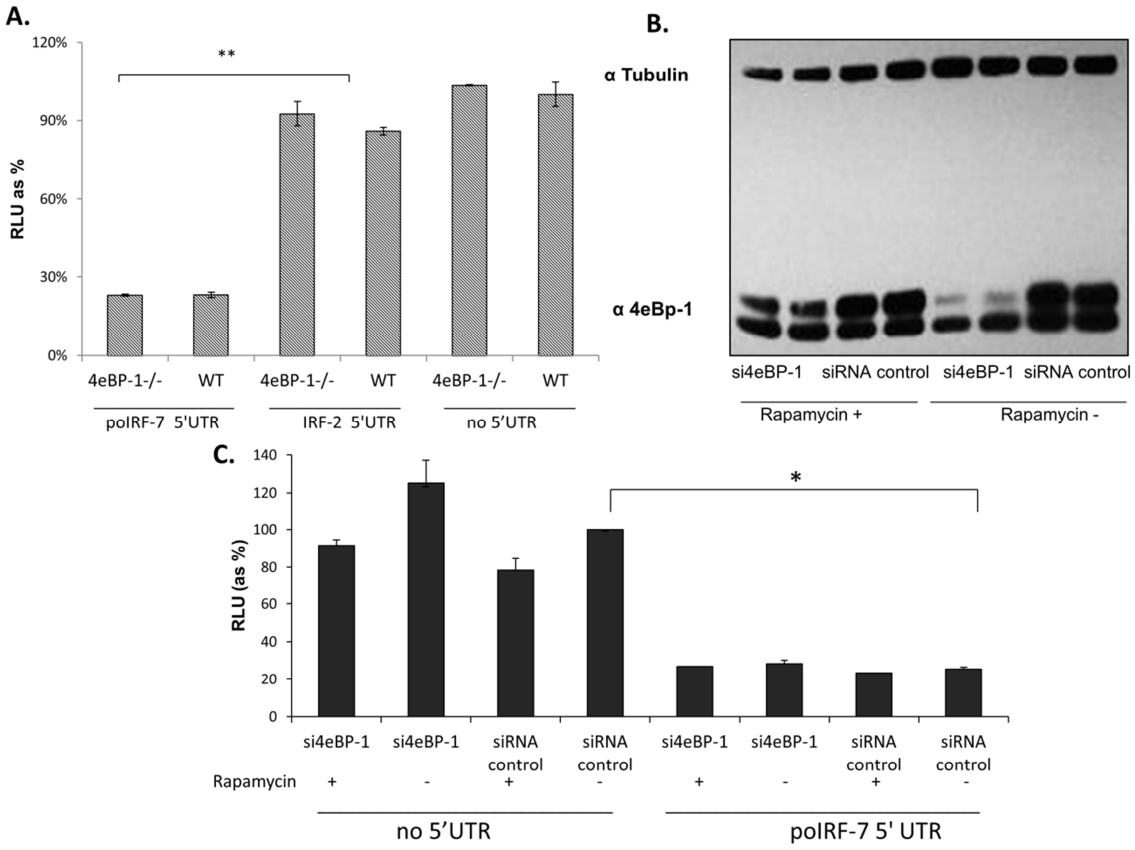

Figure. 12. Depletion or hyperactivation of 4eBP-1 in porcine cells did not specifically alter translation of a reporter containing the highly structured poIRF-7. 5'UTR sequence (A) 4eBP-1 KO or WT cells were transfected with 500 ng of poIRF-7 5'UTR psicheck (432 nt), IRF-2 5'UTR psicheck, or no 5'UTR psicheck plasmids. Twenty-four hours later cells were lysed and renilla/luciferase activities were determined. (B) IBRS-2 cells were transfected with si4eBP-1 or control for 48h, followed by rapamycin treatment for 4h. Total cell lysates were resolved by PAGE and analyzed by western blotting using α-tubulin or α-4eBP-1. (C) IBRS-2 cells were co-tranfected with combinations of si-4eBP-1 or siRNA control and poIRF-7 5'UTR psicheck (432 nt) or control plasmid for 48h, followed by rapamycin treatment for 4h. Then, cells were lysed and renilla/luciferase activities were determined

Discussion

Previous reports described 4eBP-1 and 4eBP-2 as negative regulators of IRF-7 translation in murine model (144), consistent with the characterized role of 4eBP-1 as repressors of cell growth (156). Here, we found that partial knockdown of 4eBP-1, -2 or -3 by RNAi was not sufficient to alter host antiviral response with or without previous activation of IFN pathway by either synthetic nucleic acids or by direct viral infection. Decreased protein levels of 4eBP-1 after siRNA treatment were detected which rules out the possibility that knockdown of 4eBP-1 was not effective. Surprisingly, knockdown of 4eBP-2 or -3 or the combination of several si4eBPs did not improve IFN stimulated response before or during viral infection, but we were unable to confirm effective knockdown of 4eBP-2 or -3 proteins due to a lack of functional antibodies for bovine and porcine.

Previous studies found 4eBP-2 to be important in IRF-7 regulation, but even when 4eBP-3 exhibits the similar effects on translation as 4eBP-1 (177), the role of 4eBP-3 in IRF-7 translation regulation remains unclear (177). Tissue expression and nuclear localization of 4eBP-3 (178) differs from the other 4eBPs and a regulatory motif critical for phosphorylation is absent from 4eBP-3 (179), (177). Based on these observations, it is reasonable to hypothesize that 4eBP-3 may play a different role or may not play a role in the regulation of IRF-7. Further studies are required to elucidate any possible alterative regulatory role of 4eBP-3 in porcine and bovine.

We also found that when 4eBP-1 was abolished from porcine cells using CRIPR/Cas9 system, higher antiviral activity and significant reduction in VSV titers in

KO cells as compared to WT controls were detected (Fig 9). These findings suggest that in the experiments with siRNAs even when si4eBP-1 knockdown was significant, low levels of 4eBP-1 present in the cell prevented enhancement in IFN-induced antiviral state. Most interestingly, these results indicate that 4eBPs have a repressive effect on ISG and antiviral activity in porcine cells.

Enhancement of the antiviral effects in 4eBP-$1^{-/-}$ SK-6 cells was significant (Fig 9) ($p<0.05$) but not as drastic as observed by Colina et al (2008) in MEF, who reported absence of VSV viral proteins and CPE up to 12 hpi and ~700 fold reduction in viral titer (144).The difference in the results observed could be explained by the fact that in Colina's experiments MEF were derived from double 4eBP-$1^{-/-}$ and 4eBP-$2^{-/-}$ mice (which naturally lack 4eBP-3), while in 4eBP-$1^{-/-}$ SK-6 the other 4eBPs might still function as negative regulation of IRF-7 translation.

Even though we were unable to confirm a direct effect of 4eBP-1 knockout over porcine IRF-7 translation due to lack of an effective antibody to detect porcine IRF-7, we gained insights into the effect of 4eBPs over translation in swine cells using a dual renilla luciferase reporter system. Analysis of the RNA structure of the 5'UTR of porcine IRF-7 shows homology with mice UTR. However, the poIRF-7 5'UTR fragments (232 bp, 170 bp, 146 bp long) predicted to fold into 4, 3, or 2 stem loops did not significantly modify reporter translation as compared to controls. Only 432 or 361 nt long sequences of poIRF-7 5'UTR induced significant decrease in reporter translation (Fig 3.8F). Smaller fragments (232 bp, 170 bp, 146 bp), which all lacked the 3' 129 bp of the IRF-7 5'UTR, induced reduced reporter expression but the change was not

significantly different from control levels. Therefore, our results indicate that the last 129 bp at the 3'end IRF-7 5'UTR or the full length region (361 bp) play a repressive role in the IRF-7 regulation.

These results are consistent with previous findings in which cap-dependent ribosomal scanning is severely hampered on long 5'UTRs that contain AUGs, secondary structure, and that are often found in mRNAs encoding regulatory proteins (180). In accordance with the cap-dependent scanning model for translation initiation, 5'UTRs with these characteristics are inefficient in assembling an initiation complex (180).

We also detected slight increase in reporter translation after 4eBP-1 knockdown/knockout in IRF-2 5'UTR or no 5'UTR control groups (Fig 12C). This result is consistent with the reduction of a host translation repressor. Partial reversion in the effect of the si4eBP-1 was expected as rapamycin is a stimulator of 4eBP-1 activity. Thus, IBRS-2 cells treated with rapamycin showed reduction in translation as rapamycin is a potent translational repressor (181). However, we did not evaluate 4eBP-1 phosphorylation upon treatment with rapamycin. In this regard, evidence of an alternative mTOR independent but PI3K dependent regulation of 4eBP-1 (182) confounds manipulation of 4eBP-1 phosphorylation state. Also, Choo et al (2008) reported that the effects of rapamycin varied among cell lines, in some cells treated with this inhibitor 4eBP-1 recovered phosphorylation within 6 hours despite initial inhibition. Re-emerged 4eBP-1 phosphorylation was rapamycin-resistant and might explain how cap-dependent translation can be maintained even after rapamycin treatment (181).

Findings from Choo et al. (2008) might explain the subtle effect of rapamycin over translation in our experimental setting.

Lastly, we did not observe specific effects over the translation of the reporter containing the highly structured 5'UTR of poIRF-7 when 4eBP-1 expression (by si4eBP-1 or in 4eBP-1$^{-/-}$) or activity (rapamycin treatment) were manipulated. Thus, our results partially contradict previous findings in mice in which 4eBPs preferably repress IRF-7 translation by a mechanism involving its highly structured 5'UTR (144).

Overall, we demonstrated that partial knockdown of 4eBP1,2 or 3 is not sufficient to enhance the antiviral state in bovine or porcine cells but data from 4eBP-1 knockout supported the involvement of 4eBP-1 in the regulation of the antiviral state. However, in porcine cells there could be a translational regulatory mechanism that involve the 5'UTR IRF-7 region but is not controlled by porcine 4eBP-1. Alternatively, IRF-7 mRNA might belong to a described subset of mRNAs that has evolved to be translated via an unconventional mechanism (180). Further studies will elucidate other possible mechanisms of specific translational regulation of porcine IRF-7 through its highly structured 5'UTR.

CHAPTER IV

PORCINE OASL AND THE ANTIVIRAL STATE

The 2'-5'-Oligoadenylate Synthase (OAS) proteins are among the first characterized IFN-induced antiviral proteins (183) described as dsRNA-induced inhibitors of protein synthesis (184). OAS family transcription is induced by type I and type II IFNs and requires dsRNA for activation (184-187), by interaction within the RNA binding groove (188). DsRNA that is produced during viral replication is identified by OAS proteins (188) resulting in the synthesis of 2′-5′-linked oligoadenylates (2-5A) using ATP. Then, 2-5A binds to the RNase L, inducing its dimerization and activation, which degrades viral and cellular RNAs leading to suppression in protein synthesis and viral growth (184). Thus, the 2′-5′-A produced by OAS after viral infection is responsible for the activation of RNase L that represses viral propagation. There are many isoforms of 2-5(A) synthases, however it is not clear the reason of their existence, for instance the 9-2 isozyme of 2-5(A) synthase has a role in induction of apoptosis though a Bcl-2 homology 3 (BH3) domain (189).

OAS proteins are a highly conserved (187) members of an ancient class of template-independent RNA polymerases (188). The four major types of these genes (OAS1, OAS2, OAS3, and OASL) are conserved (190). However, during mammalian evolution other OAS genes have been lost or transformed to pseudogenes (190). In humans, the OAS gene family is composed of four genes. The OAS1, OAS2, and OAS3 genes encode enzymatically active OAS proteins (191) and the OAS-like (OASL)

encodes a two-domain protein (also known as p59) composed of an N-terminal OAS domain fused to an ubiquitin-like domain (184, 187). The pig and cattle genomes contain single copies of the OAS1, 2, or OASL genes and no OAS3 gene have been reported (190). Analysis of the crystal structure of porcine OAS1 protein revealed several activities such as 2-5A oligoadenylate synthase, ATP binding, dsRNA interaction, metal ion binding, zinc ion binding activities (186, 188). Porcine OAS1 interacts with dsRNA at regions 12-59 and 199-209 (187, 188).

The mouse 2-5 OAS gene family consists of at least 11 genes. Murine OAS1 and OASL type genes have been multiplied and duplicated as compared to single gene that occurs in humans (185). The OASL loci in mice revealed two genes, murine OASL1 (mOASL1) and OASL2 (mOASL2). OASL lacks 2-5A synthase activity possibly attributed to changes in the amino acid sequence within the active domains of OAS (187, 192) suggesting that OASL1 might have obtained a novel function independent of 2’5A synthesis (186).

OASL1 can interact with double-stranded RNA and displays antiviral activity via an alternative antiviral pathway independent of RNase L (185, 186). The mOASL1 gene is the orthologous of the human OASL gene but mOASL2 is a possible intermediate between the active OAS species and human OASL1/mOASL1 proteins (186). Sequence alignment data from human, equine, canine, and bovine OASL-1 compared to mOASL2 and chicken OASL (isoform A) reveals that mOASL2 and the chicken OASL genes encode active 2′-5′ OAS enzymes whereas all the OASL1 proteins are apparently

inactive. Moreover, the ubiquitin-like motif is highly conserved among the mammalian OASL1 genes but is different from the chicken OASL and mOASL2 (192).

The physiological role of the distinct non-enzymatic OASL1 was largely unknown (185, 186). However, several studies have suggested that OASL is highly induced by lipopolysaccharide (LPS) stimulation, bacterial infection (193), and it is among the signature genes induced (IRF-3 dependent) (194) in response to virus infection (104). A distinct human isoform of OASL (OASL d) was reported from a spliced variant and it contains the same N-terminus and C-terminal ubiquitin-like domain as OASL a. OASL d was highly induced by IFNγ and IFNβ and suppressed RNA virus infection in similar extent as OASLa (193).

Lee et al. (2013) described that mOASL1 specifically inhibited translation of IRF-7 and negatively regulated viral induced production of type I IFN, thus OASL1$^{-/-}$ mice were resistant to infection with various viruses (145, 195). OASL1 interacts with two contiguous long stem loops present at the 5' end of the muIRF7 UTR. This probably prevents IRF-7 mRNA to be loaded into the 43S pre-initiation complex and inhibits the initiation of translation. The inhibitory mechanism of OASL1 seems to be distinct from that of 4eBP-1, while the last one inhibits the loading of 43S ribosomal complex by preventing the assembly of the eIF4F complex on the 5' cap of the IRF-7 message, OASL1 seems to inhibit the scanning process of the 43S complex without affecting loading of the 43S complex onto the message (145). In opposition to the results from (145), the human homolog of OASL1 has antiviral effects against encephalomyocarditis virus, but not against herpes simplex virus 1 (a large DNA virus) (192). Human OASL

and mOASL1b are incapable of activating RNase L, nevertheless, both proteins display antiviral activity if expressed in mammalian cells. Also, induction of human OASL does not need a functional type I IFN response, but is sensitive to a viral inhibitor of IRF-3 (194), consistent with the presence of putative ISRE sites in the promoters of all OAS genes (194, 196). This evidence suggests the existence of RNase L-independent antiviral pathways associated to OASL (188).

Targeting negative regulators of type I IFN, including OASL1, to prevent viral infection (195) represents a promising avenue to explore in species other than in-bred mice, as these outcomes need to be validated in livestock, the actual hosts of viruses such as FMDV that require protection. Because most mammals, including equine, swine, and cattle, have an ortholog of OASL (192), it is important to elucidate the role of OASL during antiviral state in livestock species. In this chapter we analyzed the functions of the only OASL protein described in swine and we explored its role in regulation of IFN response in porcine cells. We confirmed that porcine OASL (poOASL) transcripts were highly induced after poly I:C stimulation, but poOASL knockdown by siRNAs had only a minor effect on VSV replication, even when IFNβ and several ISGs transcripts were reduced in association with poOASL transcript reduction. Consistently, expression of synthetic poOASL in swine cells did not affect viral replication or ISGs stimulation. Discrepancies between our data and previous reports of OASL function in mouse or human might be explained by the absence of the ubiquitin-like domain in poOASL. Further studies will be required to explore the existence and possible functions of undescribed isoforms of OASL in cattle and swine.

Material and methods

Phylogenetic analysis

In order to identifying possible distantly related proteins to poOASL, a PSI-BLAST search was performed with three iterations. Twenty-two protein sequences were used for multiple sequence analysis using MUSCLE (197) (Table 6). Phylogenetic analyses were conducted using MEGA version 6 using the maximum likelihood (ML) method (198). Bootstrap test was performed and adjusted to 500. The results of bootstrap analysis are shown as the number associated with each branch in a tree.

Cells and reagents

Swine kidney cells (SK-6) were obtained from the Foreign Animal Disease Diagnostic Laboratory (APHIS) at Plum Island Animal Disease Center (PIADC), Greenport, NY and were cultured under standard conditions as explained in previous chapter and used for transfections. Vero cells were also maintained under standard tissue culture conditions and were used for viral titrations. In some transfections, poly I:C (Invivogen, San Diego, CA) was used at the specified concentration (figure legends).

siRNA design and transfections

Three sequences of 22 nt in length complementary to the coding region of porcine OASL-1 (GenBank: AY594645.1) were chosen to design siRNAs. SiRNAs were transfected with lipofectamine RNAimax (life technologies, Carlsbad, CA) into SK-6 cells previously seeded in 12-well plates and following the manufacturer's directions. The cells were transfected with specified concentrations of siOASL shown in Table 7 using RNAimax (Life technologies, Carlsbad, CA). Control groups included cells

transfected with a non-targeting siRNA (siRNA control) to account for nonspecific silencing, or unintended induction of IFN expression. Transfection efficiency was estimated by microscopic examination of fluorescein tagged to siOASL-254 24 hpt.

Table 6. NCBI reference sequence identification for OAS proteins of indicated species used in the phylogenetic analysis.

ID	Protein	NCBI Reference Sequence	Species
1	OASL-1	NM_145209.3	mouse
2	OASL	AY594645.1	Pig
3	OAS-1B	NP_653353.2	Rat
4	OAS-1B	NP_001077394.1	mouse
5	OAS-1A	NP_660212.2	mouse
6	OAS-1A	NP_620268.1	rat
7	OAS-2	NP_660262.2	mouse
8	OAS-2	NP_001019728.1	bovine
9	OAS-2	P29728.3	human
10	OAS-1	NP_058132.2	human
11	OAS-1	NP_999468.1	pig
12	OAS-3	NP_660261.1	mouse
13	OAS-3	NP_001009493.1	rat
14	OAS-3	NP_006178.2	human
15	OASL-2	NP_035984.2	mouse
16	OASL-2	NP_001009682.1	rat
17	OASL	NP_003724.1	human
18	OASL-1	NP_001009681.1	rat
19	OAS-2	NP_001019728.1	bovine
20	OASL	NP_001075266.1	horse
21	OASL	NP_001075128.1	bovine
22	OAS-1	AAP69995.1	bovine

Table 7. siRNAs targeting poOASL.

Identification	5'-3' siRNA Sequence
siOASL-254	CCGAGGACCTCGATAACAT
siOASL-468	GGTCTATGTGGATCTGATT
siOASL-782	GGACCAACTACTACAAGTT

Plasmids construction

PoOASL (NCBI RefSeq AY594645.1) with Myc and Flag tags was synthetized using gene art services (Life technologies, Carlsbad, CA). PoOASL was sub-cloned into mammalian expression vector pcDNA 3.1 (Life technologies, Carlsbad, CA) at EcoRI and NotI restriction sites. Sequence was verified using T7 and SP6 primers. A plasmid expressing the green fluorescent protein (GFP) in the pcDNA 3.1 zeo background, kindly provided by Dr. Michael Golding (Texas A&M University), was used as a control.

Analysis of mRNA expression by quantitative real time RT-qPCR

Total RNA was isolated from cell lysates using a commercially available extraction kit (Qiagen, Valencia, CA) and processed for RT-qPCR. RNA was used to synthesize cDNA and used as template for qPCR. Relative quantification was performed for several ISGs using primer sequences previously published (96, 97). The following primers for detection of poOASL were used poOASL-F 5'-CTCCTGCGACTGGTAAAACACTGGTA- 3' and poOASL-R. 5'-CGAGGGCATAGAGAGGGGGCA-3'. Expression of the genes of interest was normalized using the geometric mean of GAPDH and β-actin values. Data was analyzed using the comparative ΔΔCt method (176).

Antibodies and western blot

Custom antibodies targeting poOASL were purchased from Genscript (Piscataway, NJ) for epitopes IEARKPPGNFSPSF and QRSFVKHRPAKLKS. Anti-GAPDH from Gene Tex (Irvine, CA) was used. Cell lysates were prepared using a RIPA buffer followed by centrifugation. Western blotting was performed according to standard procedures. Proteins were detected using supersignal West Pico Chemiluminescent substrate (Thermo scientific, Rockford, IL).

Results

OASL phylogenetic and protein sequence analysis

Multiple protein sequence alignment is a central tool in inferring function for sequence comparison (199). To study possible functional relationships among members of the 2-5A synthase family, multiple sequence alignment analysis was performed using OAS or OASL sequences derived from mouse, rat, human, pig, cow and horse available in public databases (Table 6). The analysis revealed that human, equine, rat and mouse OASL orthologs had similar sequence length, but porcine and bovine OASL proteins are shorter and lack of the C-terminal ubiquitin-like domain (Fig 13A). We also found that muOASL-1 essential residues, Arg192, Lys 196 and Lys201, are conserved in porcine and bovine OASL sequences (Fig 13A). In the alignment, these 3 conserved residues were adjacent to a region that corresponded to the dsRNA interaction domain of porcine OAS1 (highlighted in Fig 13A).

The phylogenetic analysis confirms current division of OAS family members as OAS1 (A and B). OAS2, OAS3 and OASL (1 and 2) protein sequences were located in

separate clades (shown in braces in Fig. 13B). Horse and human OASL proteins showed closer relationship to murine OASL-1 than muOASL-2. Bovine and porcine OASL form a monophyletic group located intermediate between OASL-1 and OASL-2.

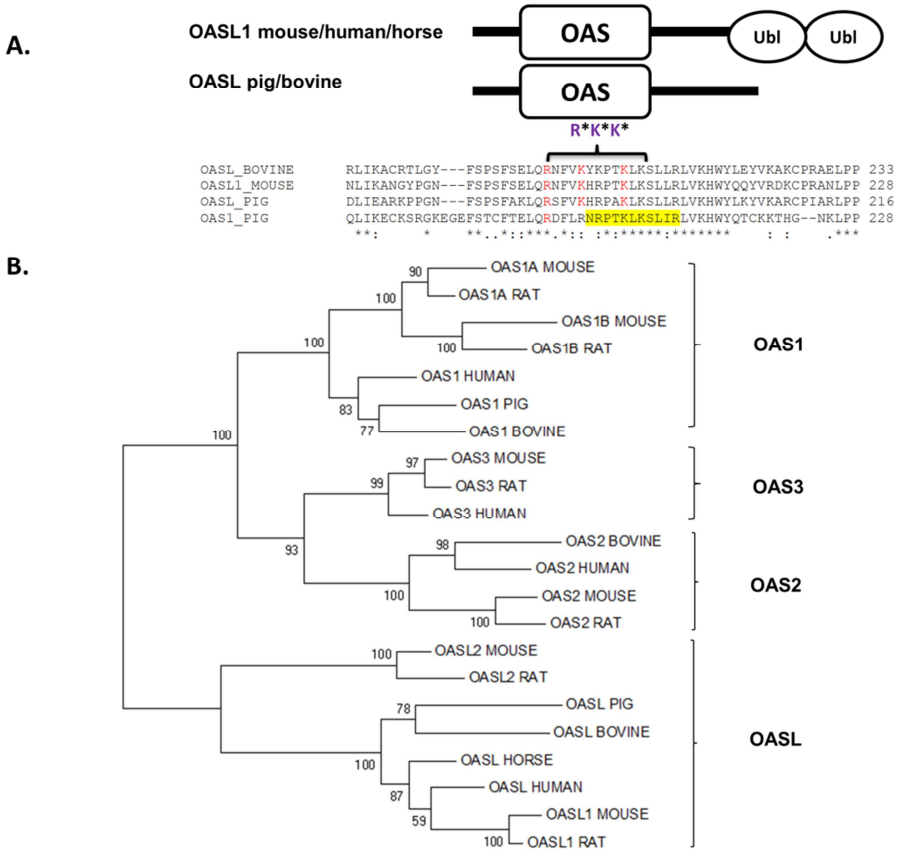

Figure. 13. Phylogenetic and protein sequence analysis of OAS family members across species reveals conserved and unique features of porcine and bovine OASL proteins.
(A) OAS and ubiquitin-like domains (Ubl) are represented schematically. A section of a protein sequence alignment of bovine, mouse, and pig OASL is shown. R*K*K essential residues are denoted in red. The RNA interaction domain of porcine OAS-1 is highlighted (B) Phylogenetic tree elaborated using ML method and protein sequences described in Table 4.1. Bootstrap values are numbers associated with each branch in the tree.

Knockdown of porcine OASL induced slight changes in antiviral state

To study the function of poOASL, we knocked it down using three siRNAs targeting distinct regions of OASL mRNA (Table 7). All three siRNAs efficiently reduced OASL transcripts by at least 75% (Fig 14A). PoOASL was highly induced after IFN by poly I:C priming yet significant fold reduction in poOASL transcripts was detected in IFN-induced cells after and siOASL knockdown (Fig 14B). The combination of three siOASL produced similar knockdown as individual siRNAs (not shown). Reduction in poOASL by siRNA was also evidenced at protein level. Densitometry analysis revealed ~50% reduction in OASL protein after siOASL468 transfection in absence of poly I:C stimulus (Fig 14C , compare lane 1 and 4). Also, there was 71% reduction poOASL expression after siOASL468 transfection in cells stimulated with poly I:C (Fig 14C compare lane 2 and 3).

To explore any possible regulatory role of poOASL over antiviral state, poOASL was knocked down and cells were mock or stimulated with poly I:C followed by VSV infection. Knockdown of poOASL in presence of poly I:C slightly increased viral yield (by ~1 log) as compared to siRNA control. However, no differences in VSV titers were detected after knockdown of OASL in absence of poly I:C stimuli at 8 hpi (Fig 14D).

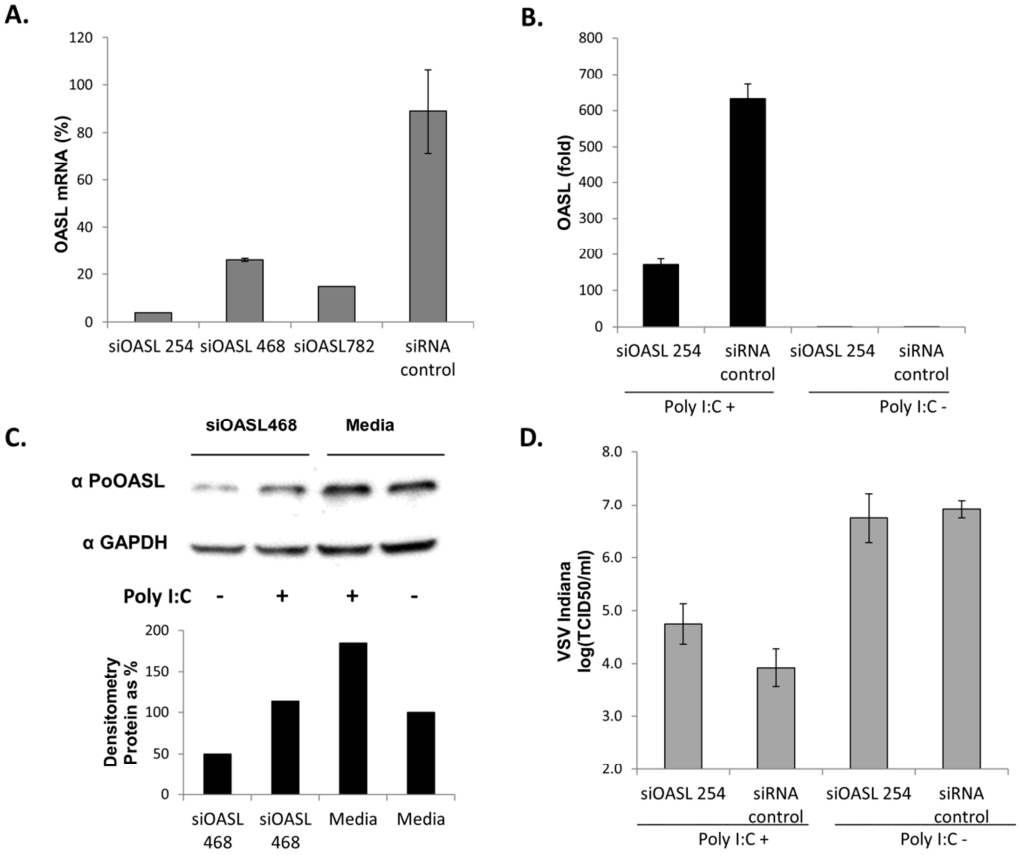

Figure. 14. Effective knockdown of poOASL induced slight increase in viral yield. SK-6 cells were transfected with indicated siRNAs (10 µM) (A) Knockdown efficiencies of poOASL determined by RT-qPCR 48h after transfection Transcript levels are represented as a percentage relative to the siRNA control (B) Fold change in poOASL transcripts in presence (+) or absence (-) of poly I:C stimulation (0.5 µg/ml) (C) Total cell lysates were resolved by PAGE and analyzed by western blotting using α-GAPDH or α-poOASL. Densitometry analysis is shown. (D)VSV yield was determined by $TCID_{50}$ method in cells siRNA or mock transfected in presence (+) or absence (-) of poly I:C stimulation (0.5 µg/ml) 8h after VSV infection (MOI=0.02).

Analysis of ISGs transcript profile revealed that knockdown of poOASL reduced IFNβ (Fig 15A) and RANTES (Fig 15B) transcripts by ~50% relative to siRNA control in cells previously stimulated with poly I:C, consistent with the slight increase in viral

yield. Mx-1 (Fig 15C) or ISG54 (Fig 15B) transcripts also seemed to be slightly reduced by OASL knockdown.

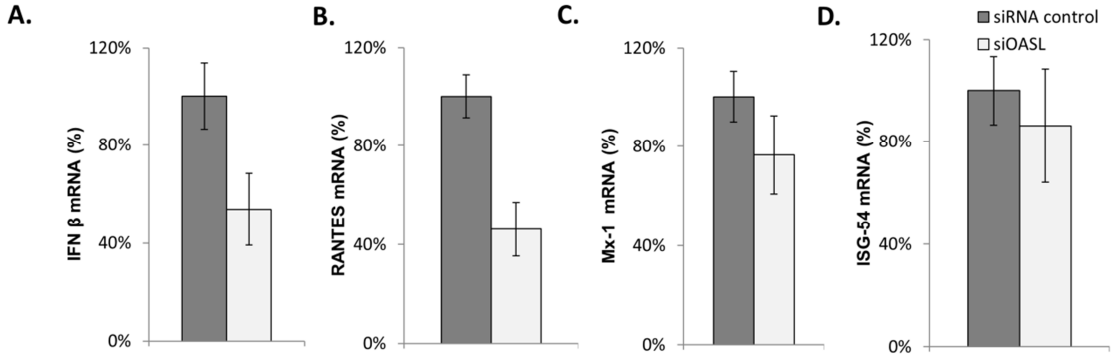

Figure. 15. Knockdown of porcine OASL induced mild change in ISG transcription profile.
SK-6 cells were transfected with siOASL 254 (10 µM) followed by poly I:C stimulation (0.5µg/ml) (A) Total RNA was extracted and analyzed by RT-qPCR. Changes in transcript levels relative to siRNA control are reported for (A) IFNβ, (B) RANTES, (C) Mx-1, or (D) ISG54 transcripts were determined 48hpt.

Overexpression of synthetic OASL-1 did not enhance antiviral state

Since the effect knockdown of poOASL over antiviral state suggests that poOASL might hold antiviral properties, we decided to express poOASL exogenously *in vitro*. SK-6 cells were transfected with a mammalian expression vector carrying poOASL gene driven by CMV promoter. Forty-hour later, transfection efficiency was estimated by GFP expression in control cells. Cells were mock or poly I:C stimulated for 12h followed by VSV infection. A prominent increase in OASL transcripts was detected in groups transfected with poOASL in presence or absence of poly I:C as compared to GFP or mock control. Overexpression of poOASL was also detected using a myc tag

(Fig 16A). However, extrinsic expression of poOASL had no effect on viral replication in presence or absence of poly I:C stimulation (Fig 16B). Analysis of ISGs transcript profile in presence of poly I:C denoted a slightly increased expression of IFNβ (Fig 17A), RANTES (Fig 17B) and OAS-1(Fig 17D) but not Mx-1(Fig 17C) as compared to the GFP or mock controls. However, differences in transcript expression were not statistically significant in the presence or absence of poly I:C stimulation (Fig 17).

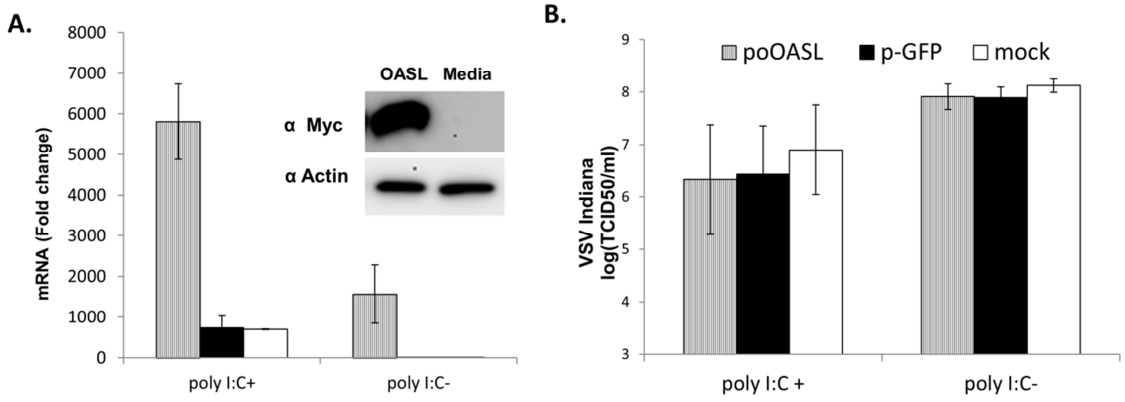

Figure. 16. PoOASL over-expression induced no change in viral replication.
SK-6 cells were transfected with poOASL, a plasmid expressing the GFP in the pcDNA 3.1 background (p-GFP), or mock transfected. Forty-hours post-transfection, cells were mock or poly I:C stimulated (0.5µg/ml) for 12h. (A) Total RNA was extracted and OASL transcripts were determined by RT-qPCR. (B) Cells were infected with VSV (MOI=0.02) for 12h. Viral titer was determined by $TCID_{50}$ method.

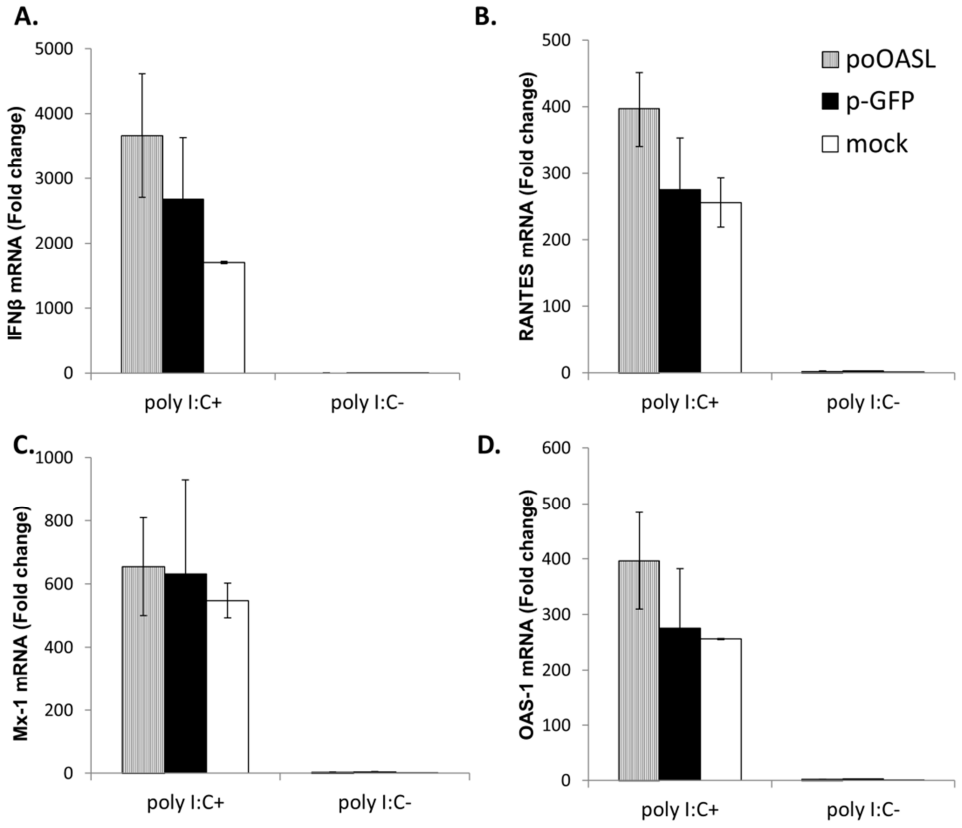

Figure. 17. PoOASL over-expression induced no change in antiviral state.
SK-6 cells were transfected with poOASL, p-GFP, or mock transfected. Forty-hours post-transfection, cells were mock or poly I:C stimulated (0.5µg/ml) for 12h. (A) Total RNA was extracted and (A) IFNβ, (B) RANTES, (C) Mx-1, or (D) OAS-1 transcript levels were determined by RT-qPCR

Discussion

The function of OASL-1 orthologs in the antiviral state is controversial. Experimental evidence suggested that huOASL-1 has antiviral properties (192), (194) while another study described mOASL-1 as a negative regulator of IRF-7 translation (145). To elucidate the possible function of the porcine OASL, we first analyzed the phylogenetic relationships among several members of the OAS family in rodent, human,

and farm species. Our results confirmed the accepted clade division among OAS-1, OAS-2, OAS-3, OASL1 and OASL2 members. Our data was supported by bootstrap values (BV) greater than 70%, which roughly corresponds to a probability greater than 95% that the true phylogeny was found (199). A protein sequence alignment of OASL from several species revealed conservation of the A2'-5'-oligoadenylate synthetase 1 domain 2 (153-333 aa, in porcine OASL, GenBank: AY594645.1) across horse, bovine, human, swine, mouse, and rat species. Likewise, our data confirmed the presence of a premature stop codon in porcine and bovine OASL. This stop codon resulted in a truncated OASL protein that lacks the ubiquitin-like (Ubl) domain (190). We also found that 3 aminoacids essential for muOALS-1 function (Arg192, Lys 196 and Lys 201) (145) are preserved in the OAS domain of porcine and bovine OASL. These 3 residues are located adjacent to one of the porcine OAS1 dsRNA interaction domains. Lee et al. (2013) reported that these 3 residues are crucial for muOASL-1 interaction with the IRF-7 5'UTR (145).

Our results suggest that down-regulation of porcine OASL-1 had minor effects on the viral replication or the ISGs stimulation. In this regard, specific poOASL transcripts knockdown was detected after siRNA treatment but only ~50% reduction in OASL protein was detected after siOASL treatment. Therefore, we cannot rule out the possibility that the mild effects were due to an inefficient OASL-1 silencing.

To our knowledge, this is the first detection of porcine OASL protein. Perelygin et al. (2006) first suggested the existence of poOASL based on sequences obtained from mRNA and genomic DNA derived from two or more unrelated animals of various

breeds (190). Since then, “evidenced at transcript level” status remained for porcine OASL (uniprot Q53B79_PIG) at Uniprot database.

Unexpectedly, transfection of porcine cells with the poOASL plasmid did not significantly alter the antiviral state. Our results do not support previous findings in which murine OASL held negative regulatory properties of the antiviral state (145, 195). Experimental evidence from Lee et al. (2013) demonstrated that the muOASL1 ubiquitin-like domain is needed for an optimal inhibitory effect of the OASL1 on IRF-7 5’UTR. However, in the same work it was shown that decreased reporter expression dependent on the 5’UTR muIRF-7 was still detected in a muOASL1ΔUbl mutant as compared to the wild type muOASL1(145). Thus, the absence of an ubiquitin-like domain probably impairs the poOASL function and consequently, it is unlikely that the poOASL regulates IRF-7 translation as it is reported for murine OASL-1 ortholog.

The ubiquitin-like domain is also required for the antiviral function of human OASL (192). This might explain why transfection with a plasmid encoding the naturally truncated poOASL had minimal effects on the ISG stimulation or the viral replication on swine cells. Intriguingly, the porcine OASL might still preserve its RNA interaction function as it was suggested *in silico* by conservation within the residues homologous to poOAS-1 RNA binding domain and as it was evidenced *in vitro* by up-regulation in presence of a synthetic RNA analog (poly I:C). Interestingly, the human OASL gene induction is IRF-3 dependent but IFN independent (194). Thus, one could speculate that poOASL might also have an IFN-independent role in the recognition of harmful nuclei acids within the cell. It is also possible that some individuals or swine breeds might not

contain a premature stop codon in their OASL gene sequence (190). Further investigations are required to explore this possibility and to elucidate any potential IFN-independent role of OASL in porcine and bovine cells.

CHAPTER V

POIRF7/3(5D) CONTROLS FMDV REPLICATION

The interferon regulatory factors (IRFs) family consists of nine members (200). IRF-1, -3, -5, -7 and -8 are positive regulators of type I IFNs (200). IRFs have roles in regulation of oncogenesis and apoptosis (200, 201) IRF-3, -5, and -7 have been identified as key transcription factors responsible for mediating the type I IFN and ISG response during viral infections (116, 202), IRF-1, however, is dispensable for IFN production during viral replication (203).

IRFs share similar structure; a highly conserved N-terminus with DNA-specific binding (DB) activity and a variable C-terminal domain or IRF association domain (IAD) that mediates oligomerization among IRF factors and other transcription factors and co-activators. All IRF proteins recognize a DNA element with a consensus sequence AANNGAAA. This sequence is found in promoters from a multitude of interferon response genes (204). IRFs act cooperatively through binding to enhancers and promoters (204).

The IRF-3 is a 50-55kDa protein that binds specifically to the IFN-stimulated response element (ISRE) but not to the IRF-1 binding site PRD-I (205). IRF-3 is expressed constitutively in many tissues and no rise in the steady-state level of IRF-3 mRNA is observed in IFN-treated or virus-infected cells (205). IRF-3 overexpression stimulates the IFN-stimulated gene 15 (ISG15) promoter (206) but not of murine IFNα4 promoter (205). Virus- and dsRNA-inducible phosphorylation of IRF-3 or -7 represents

an important post-translational modification, leading to cytoplasmic to nuclear translocation (206). Cytoplasmic IRF-3 is activated through phosphorylation of specific serine residues located in its C-terminus. Overexpression of IRF-3 enhances the virus-mediated expression of IFNα/β genes and the antiviral state (207).

IRF-3 contains a DNA-binding domain (DBD); a transactivation domain, a nuclear export element; a proline-rich region; and an IAD. To prevent nuclear translocation and DNA binding, two auto-inhibitory domains in IRF-3 closely interact and mask the IAD and the DBD (208). Upon viral infection, inducible C-terminus phosphorylation releases the association between the two auto-inhibitory domains, uncovering the IAD and the DBD. This conformational change induces dimer formation and cytoplasmic-to-nuclear translocation. IRF-3 phosphorylation also signals for its degradation thought the ubiquitin-proteasome pathway (206), (209). IRF-3 phosphorylation is performed by IKKϵ and TBK1 and occurs on Ser385 and Ser386 and on a Ser/Thr cluster located between aminoacids 396 and 405 (206, 209). V-maf avian musculoaponeurotic fibrosarcoma oncogene homolog B (MAFB) acts as a transcriptional antagonist impairing the interaction of CBP with IRF-3 (210). IRF-3 can also mediate virus-induced apoptosis by the direct interaction of IRF-3 BH3 domain with the pro-apoptotic protein Bax, resulting in activation of the mitochondrial apoptotic pathway (211).

IRF-7 is the closest family member to IRF-3; but unlike IRF-3, IRF-7 is not expressed constitutively in all tissues (143). However, IRF-7 is constitutively expressed in cell types with key immune roles such as B cells, spleen cells, pDCs, monocytes, and

peripheral blood lymphocytes (212, 143).There are four isoforms of IRF-7, namely IRF-7A, B, C and D. IRF-7A protein has a molecular size of 55kD in humans and 52kD in mice (143). IRF-7 can be stimulated by IFN, LPS, viral infection (143), TNFα, 12-o-tetradecanoylphonol-13-acetate (TPA), and reagents that alter chromatin structure such as topoisomerase II inhibitors (213). Similar to IRF-3, virus infection induces the phosphorylation of IRF-7 at its C-terminus, inducing dimerization, and translocation to the nucleus (143).

Several post-translational modifications have been described for IRF-7, but phosphorylation is the most important (143). As explained in Chapter 2, IRF-7 phosphorylation and activation is mainly mediated by IKKε and TBK1 kinases (214), but IRAK1, and IKKα can also mediate phosphorylation (143). The potential residues targeted for inducible phosphorylation are Ser425 and Ser426 in murine IRF-7 and aminoacids 411 to 453, which are indispensable for nuclear translocation (143).

IRFs are also regulated by ubiquitination (209). IRF-7 activity is increased following Lys 63 ubiquitination by TRAF-6 (215). Both, IRF-3 and IRF-7 are targeted for proteasome-dependent degradation by polyubiquitination introduced by RTA-Associated Ubiquitin Ligase (RAUL). (216). IRF-3 and IRF-7 are also sumoylated in response to virus infection by host SUMO1, 2, and 3 (217). Sumoylation negatively regulates the transcriptional activity of IRF-7 and -3 (143, 217). DNA binding activity of IRF-7 is modulated by acetylation at lysine 92 (located in the DBD) performed by the histone acetyltransferases p300/CREB-binding protein-associated factor (PCAF) and

GCN5 (218). Lastly, methylation of a CpG island in the IRF-7 promoter results in IRF-7 gene silencing (219,143).

Upon activation, IRF-7 forms an enhanceosome together with IRF3, c-Jun, NFκB, activating transcription factor 2, and p300/CREB-binding protein on the IFN β gene promoter (98, 143). Qing et al (2004), reported that TGF-β/Smad3 signaling modulates the transcriptional activity of IRF-7 at the IFN-β promoter and that Smad3 physically interacts with IRF-7 (220). Even though no transcriptional co-repressor has been identified for IRF-7, MAFB might inhibit IRF-7-dependent transcriptional activation by interfering with IRF-7 binding to target promoters (210, 143).

The major source for IRF-7 expression in the cell comes from the positive regulatory feedback between IRF-7 and type I IFNs during antiviral immune responses (140, 143). At the early stage of virus infection, PRRs mediated signaling triggers phosphorylation and activation of NFκB, IRF-3, and IRF-7, these transcription factors bind to the virus-responsive elements in the IFNα and IFNβ promoters and induces secretion of small amounts of type I IFNs, which act in autocrine and paracrine manner. Binding of IFNs to IFN receptor results in the activation of JAK–STAT signaling pathway (reviewed in Chapter II) which leads to more IRF-7 synthesis (140, 143).

IRF-7 has a short half-life of 0.5~1 h in infected cells and approximately 5 h in uninfected cells (221, 143). Stability seems to be controlled by the ubiquitin-proteasome system (216). Oncogenic properties have been associated to IRF-7 related to Epstein Barr viral infections, for instance increased IRF-7 expression was detected in EBV-immortalized B cells (222, 143). However, IRF-3 and IRF-7 also display antitumor

properties in human macrophages (223). Apoptosis was observed in macrophages transduced with Ad-IRF-3, but Ad-IRF-3 or Ad-IRF-7 transduction also down-regulated specific protumorigenic genes transcription (223).

IRF-3 and -7 are necessary for efficient IFN production in most immune cells. Cells that lack of both factors fail to induce IFNα or β (224). Mice deficient in IRF-3 and IRF-7 have higher mortality after Chikungunya virus (CHIKV) infection (225). However, functions of IRF-3 and IRF-7 are not redundant (139). IRF-7 induces multiple IFNα genes but IRF-3 activates predominantly IFNβ and IFNα1 (139). After, IRF-3 is degraded, the low constitutive levels of IRF7 are critical for the priming and feedback loop of IFNα and IFNβ by newly synthesized IRF-7 (143). In addition, IRF-3 and -7 can bind cooperatively to regulate the IFNβ promoter (86, 143). The crucial roles of IRF-7 and -3 during IFN induction is evidenced by the multiple counteraction strategies of numerous viruses targeting these IRFs (reviewed by 226)

A constitutively active fusion construct containing 246 amino acids from IRF-7 (DNA binding and constitutive activation domains) and 295 amino acids from IRF-3(5D) (transactivation and signal response domains) denominated IRF-7/3A was previously described using human sequences (116). Expression of this construct in cultured human cells induced activation of IFN promoters *in vitro* (116). Adjuvant properties of the plasmid were also described in mice but gene transfer in mice muscle was not efficient (227). Here, analogous to IRF7/3A construct, we designed a constitutively active fusion construct using porcine IRF-7 and IRF-3 sequences and termed poIRF7/3(5D). We tested poIRF7/3(5D) in different cell types and found that

poIRF7/3(5D) is a potent inducer of several type I IFNs (but not type III IFNs) in cells from several species, including porcine, murine, and bovine cell types. Expression of poIRF7/3(5D) also enhanced the antiviral activity of Ad5-poIFNβ against FMDV. Lastly, we tested the properties of poIRF-7/3(5D) *in vivo* using mouse model and found that mice inoculated with an Ad5 vector expressing poIRF7/3(5D) (Ad5-poIRF7/3(5D) developed no viremia after FMDV A24 challenge, correlated with high antiviral activity with increased systemic levels of muIFNα/β.

Material and methods

Cell and reagents

SK-6 and IBRS-2 were obtained from APHIS at PIADC, Greenport, NY. Madin-Darby bovine kidney (MDBK, ATCC CCL-22), baby hamster kidney (BHK-21, clone 13, ATCC CCL-10), and mouse L929 (ATCC CCL-1) cells were purchased from the ATCC (Rockville, MD) and used for plasmid transfection or Ad5 vector transduction. Human 293 cells (ATCC CRL-1573) were also purchased from ATCC and were used to propagate recombinant Ad5 vectors (228). Mouse embryonic fibroblasts (MEFs) were propagated from original clones kindly provided by Dr David E. Levy (New York University) (129). Cells were cultured under standard tissue culture conditions, maintained in MEM containing 10% FBS and supplemented with 1% antibiotics and non-essential amino acids. Ten percent tryptose phosphate broth was included in the media of BHK-21 cells.

B18R inhibitor (eBioscience, San Jose, CA) was used to block the IFN type I receptor. Prior to transfection or infection, cells were incubated for 1 h at room

temperature in complete media containing B18R inhibitor at a concentration of 20-200ng/ml. B18R inhibitor was maintained in the media during transfection and replenished after viral infection.

Anti-pig IFNα, clone K9 antibody (Ab) (PBL Interferon Source, Piscataway, NJ) was used to neutralize IFNα activity present in supernatants (3 µg of antibody/ml of supernatant) of treated cells.

In some transfections, poly I:C (Invivogen, San Diego, CA) was used at the specified concentration as an inducer of the IFN pathway.

Viral infections

A laboratory-adapted VSV serotype Indiana was kindly provided by Judith Ball (Texas A&M University). A VSV serotype New Jersey field strain (95COB) was used for some experiments. FMDV serotype A12 generated from a full-length virus infectious clone (172) was used at indicated MOI. FMDV serotype A24 isolated from the field and passed once in BHK-21 cells was used for mouse experiments. All experimental infections using VSV serotype New Jersey or FMDV (A12 or A24) were conducted at the USDA-ARS Plum Island Animal Disease Center under biosafety level (BSL)-3Ag conditions. Infections with VSV serotype Indiana were performed at Texas A&M under BSL-2 conditions.

Cells were infected at specified times post-transfection or Ad5-transduction at the indicated MOIs. In all cases FMDV or VSV were adsorbed for 1 h at 37^{o} C. For FMDV, unabsorbed virus was removed by washing the cells with 150 mM NaCl–20 mM morpholineethanesulfonic acid (MES) (pH 6.0). Incubation continued for 24 h unless

otherwise specified. Virus was released by one freeze-thaw cycle. Viral titers were determined by a standard $TCID_{50}$ method using IBRS-2 cells and results were expressed as log10 of the $TCID_{50}$/ml. Viral titers in FMDV infected mice sera were determined by plaque assay, using standard procedures (173) and expressed as plaque forming units (pfu)/ml of serum.

Cell toxicity assay

Cell toxicity after transfection or transduction of plasmids or Ad5 vectors expressing poIRF7/3(5D) was determined by using the XTT based *in vitro* toxicology assay kit (Sigma, St. Louis, MO) following the manufacturer's recommendations. Optical density was read at 450 nm and filtered at 650 nm after 4 h incubation. Microscopic examination of cell morphology in the monolayer after transfection/transduction was also used as an indicator of cell toxicity.

Plasmid construction

Partial DNA sequences of porcine IRF-7 (GenBank AB287430, nucleotides 212-964) and IRF-3 (GenBank AB116563.1, nucleotides 400-1259) were used to synthesize a fusion construct poIRF7/3(5D). This fusion construct was then cloned at EcoRV/ XbaI sites of the pcDNA 3.1 zeo+ vector (Invitrogen, Carlsbad, CA). A plasmid expressing the green fluorescent protein (GFP) in the pcDNA 3.1 zeo background was kindly provided by Dr. Michael Golding (Texas A&M University) and was used as a control. IRF-7 5'UTR sequence identified in previous chapters was also cloned into poIRF7/3(5D) to generate 5'UTRpoIRF7/3(5D) construct. All constructs were verified by sequencing.

Ad5 vector construction

PcDNA 3.1 zeo+ poIRF7/3(5D) was digested with ClaI and XbaI, and the resulting DNA fragment was ligated into a pAd5-Blue vector (229) digested with the same enzymes to create recombinant Ad5-poIRF7/3(5D). Replication-defective human adenovirus type 5 (Ad5) expressing poIRF7/3(5D) was produced by transfection of 293 cells with the Pac I-linearized recombinant pAd5-poIRF7/3(5D). Viruses were isolated, propagated and purified by CsCl gradient centrifugation (229). Ad5-Blue, and Ad5-poIFNβ vectors were constructed previously (230, 129).

Antibodies and western blot

Pig cross-reacting antibodies against human IRF-3 and tubulin were purchased from Abcam (Cambridge, MA), and anti-TATA-box binding protein (TBP) from Gene Tex (Irvine, CA). For western blotting cell lysates were prepared in a modified RIPA buffer (25mM Tris pH7.5, 250mM NaCl, 1% NP40, 1% deoxycholate, 0.1% SDS), followed by centrifugation. Supernatants were kept as the cytoplasmic fraction and the nuclear fraction was prepared by sonication of the pellet. Tubulin was used as internal loading control for the cytoplasmic fraction and TBP was used as the internal loading control for the nuclear fraction. Western blotting was performed according to standard procedures and proteins were detected by chemiluminescence using BioRad Immuno-star HPS (BioRad, Hercules, CA).

Analysis of mRNA expression by quantitative real time RT-qPCR

Total RNA was isolated from cell lysates using a commercially available extraction kit (Qiagen, Valencia, CA). Approximately 1000 ng of RNA of each sample

was used to synthesize cDNA using random hexamers with qScript kit mix (Quanta Biosciences, Gaithersburg, MD) according to the manufacturer's instructions. Copied DNA was diluted tenfold and used as template for qPCR with PerfeCTa® SYBR® Green FastMix, ROX (Quanta Biosciences, Gaithersburg, MD). Samples were run in an Applied Biosystems® 7500 or StepOne Real-Time PCR Systems (Applied Biosystems, Carlsbad, CA).

Relative quantification was performed for IRF-7 and a panel ISGs using primers previously described (96, 97). Standard curves were run to standardize a SyBr-green based PCR array of the subtypes of porcine type I IFN. Sequences for detecting subtypes of porcine IFN type I (IFNα, β, κ, ε, ω, δ) were published previously (101, 231-233). The expression of the genes of interest was normalized using GAPDH and β-actin. RT-qPCR analysis was performed following MIQE Guidelines (175). Data was analyzed using the comparative ΔΔCt method (176).

IFN bioassay

Antiviral activity induced by IFN expression was tested by a VSV infection inhibition assay as previously described (11). Supernatants from samples previously transduced with Ad5 vectors, were filtered through centricon 100 columns (Millipore, Billerica, MA) to remove adenovirus particles.

Samples were two-fold diluted and incubated on IBRS-2 cells for approximately 24 h. Supernatants were then removed, and the cells were infected with VSV NJ (MOI=2) . Twenty four or 48 h later, CPE was determined by microscopic examination, followed by staining with 1% crystal violet. Antiviral activity (IFN units/ml) was

expressed as the reciprocal of the highest dilution of supernatant able to suppress VSV-induced CPE on the 50% of assayed wells.

Antiviral activity in serum samples of mice inoculated with Ad5 vectors was tested on L929 cells as previously described (234). Briefly, 2-fold dilutions of serum samples were applied to confluent monolayers of L929 cells. At 24 h cells were infected with VSV (MOI= 20) followed by 48-72 h incubation at 37°C. CPEs were scored by microscopic examination followed by staining with 1% crystal violet.

Murine IFN ELISA

Serum samples from mice infected with Ad5-poIRF7/3(5D) or Ad5-Blue control vector were tested for the presence of IFN-α and IFN-β using VeriKine mouse ELISAs (PBL Interferon Source, Piscataway, NJ) as per manufacturer's directions. The absorbance at 450 nm was measured in an ELISA plate reader (VersaMax, Molecular Devices, Sunnyvale, CA). Cytokine concentrations were calculated based on the optical densities obtained with standard curves.

Ethics statement

All animal research was conducted in agreement with the 2011 Guide for Care and Use of Laboratory Animals, the Animal Welfare Act (AWA), 2002 PHS Policy for the Humane Care and Use of Laboratory Animals, and U.S. Government Principles for Utilization and Care of Vertebrates Animal Used in Testing, Research and Training, as well as a specific animal protocol reviewed and approved by the Institutional Animal Care and Use Committee (IACUC) of the PIADC.

Mouse challenge studies

C57BL/6, 6 to 7-week-old female mice were purchased from Jackson Laboratory (Bar Harbor, ME) and acclimated for one week. In the first experiment, two groups of five mice each were inoculated with Ad5-poIRF7/3(5D) (3×10^7 or 3×10^8 PFU/mouse) or Ad5-Blue (3×10^8 PFU/mouse) subcutaneously (s.c) in the dorsal flank. One day after Ad5 treatment, serum samples were collected and mice were euthanized.

In the second experiment, groups of five mice were inoculated s.c with Ad5-poIRF7/3(5D) or Ad5-Blue (3×10^5 or 3×10^8 PFU/mouse). One day after Ad5 treatment, serum was collected and mice were anesthetized with ketamine/xylazine and infected s.c in the right rear footpad with 1×10^5 PFU of FMDV A24 in 50 ul of PBS as previously described (235). Animals were monitored for 7 days, and blood was collected at day 0 and 2 days post-challenge (dpc). Viremia was determined by plaque assay on BHK-21 cells (173) and serum was examined for the total antiviral activity as described earlier.

Statistics and data analysis

Treatment differences were determined using, Student's t-test, Dunnett's method, or Wilcoxon-rank sum test as indicated in each figure legend. Data shows representative results of three independent replicates except for figure 6 (two independent experiments) and mice experiments. Statistical analysis was performed using JMP software, version 8.0.2. Values are expressed as mean ± standard error (SEM), and statistical significance ($p < 0.05$ or $p < 0.001$) is indicated.

Results

PoIRF7/3(5D) induces high levels of ISGs expression

The IRF-7 transcription factor shares structural features with IRF-3 (204). Here, using analogous domains to human IRF7/3A, we generated a chimeric construct of porcine IRF-7 and IRF-3, poIRF7/3(5D). The construct contains the DBD and constitutive activation domain (CAD) from porcine IRF-7, but lacks the inhibitory domain (ID) (Fig 18A). It also has the proline-rich domain (Pro), transactivation domain (TAD) and SRD signal response domain from porcine IRF-3. Analogous to the human construct described previously (116), poIRF7/3(5D) contains 5 mutations in the C-terminal IRF-3 domain that mimic phosphorylation and therefore results in constitutive activation (Fig 18A).

Expression of poIRF7/3(5D) was analyzed by RT-qPCR. IRF-7 or IRF-3 transcript levels were detected using a primer set that recognizes a consensus sequence of IRF-7 and IRF-3 in both mRNA from cellular and plasmid origin (Fig 18B). IRF-7 or IRF-3 transcripts were significantly up-regulated (~40-fold and ~10 fold, respectively) in SK-6 cells transfected with poIRF7/3(5D) expressing plasmid as compared to control groups (mock and pGFP transfected), where only basal levels of IRF-7 or IRF-3 mRNA were detected ($p<0.05$). Endogenous IRF-3 (eIRF-3) transcript levels remain unchanged in all groups.

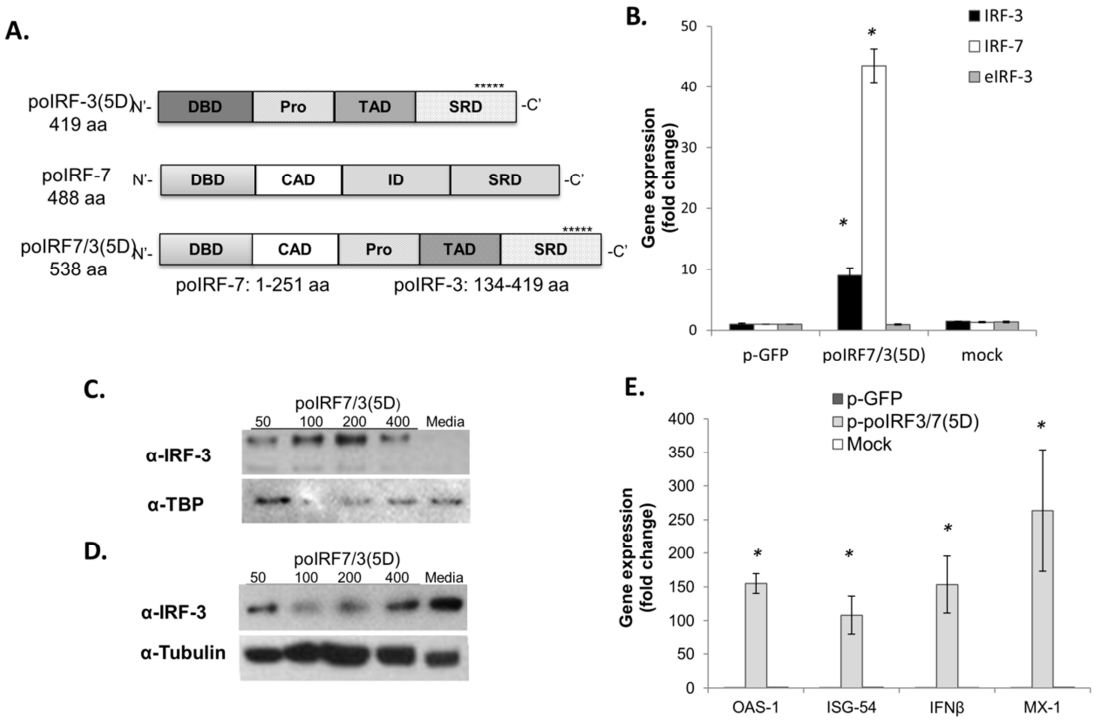

Figure. 18. Expression of poIRF3/7(5D) induces the expression of IFN and ISGs mRNA.

(A) The structures of IRF-3(5D), IRF-7 and the fusion protein poIRF-7/3(5D) are illustrated schematically. Asterisks represent five phosphomimetic aminoacid substitutions at C-terminus of IRF-3(5D). DNA binding domain (DBD); proline-rich domain (pro); transactivation domain (TAD); signal response domain (SRD); constitutive activation domain (CAD); and inhibitory domain (ID) are represented in boxes. (B) Up-regulation of IRF-7, IRF-3, but not endogenous IRF-3 (eIRF-3) transcripts in SK-6 transfected with a plasmid encoding poIRF7/3(5D). (C) Up-regulation of ISGs was also detected in SK6 cells transfected with poIRF7/3(5D) plasmid but not in a control plasmid with the same backbone but expressing green fluorescent protein (p-GFP), or mock transfected. Transcript levels were quantified using RT-qPCR and expression levels were expressed as fold induction relative to p-GFP transfected cells. Statistical analysis was performed using the Wilcoxon-rank sum test method (* $p<0.05$). SK6 cells were transfected with 50-400ng of plasmid poIRF7/3(5D). (D) Nuclear or (E) cytoplasmic fractions were resolved by PAGE and analyzed by western blotting using α-IRF-3, α-TATA-box binding protein (TBP), or α-Tubulin.

We also looked at expression of the fusion protein by western blot using an antibody against human IRF-3 (Fig 18C-D). At the plasmid concentrations used, 25-400 ng, a dose-dependent expression was not evident in cytoplasmic extracts; however, translocation to the nucleus was only detected in cells transfected with the poIRF7/3(5D) plasmid (Fig 18C), consistently with the presence of a constitutively active form of the fusion protein.

To determine if the overexpression of poIRF7/3(5D) also induced changes in host gene expression, three known ISGs, OAS-1, ISG54 and Mx-1 as well as IFNβ were analyzed by RT-qPCR. While little or no induction was detected in SK-6 cells mock treated or transfected with pGFP, a significant up-regulation was detected in cells transfected with 25 ng of the poIRF7/3(5D) fusion protein (Fig 18E). Inductions varying from 100 to 250 fold were detected for all analyzed genes indicating that the fusion poIRF7/3(5D) protein was active.

PoIRF7/3(5D) expressed in porcine cells has antiviral properties against FMDV and VSV

To test the biological functions of the fusion protein poIRF7/3(5D) in the context of a viral infection, SK-6 cells were mock transfected or transfected with 25 ng of poIRF7/3(5D), or pGFP and later infected with either FMDV or VSV. A striking reduction (5-6 log10) in virus yield of FMDV (Fig 19A) or VSV (Fig 19B) ($p<0.001$, in all cases) was observed in cells transfected with poIRF7/3(5D), while no effect was detected in cells transfected with the control pGFP. Consistently, antiviral activity was only detected in supernatants from poIRF7/3(5D) transfected cells and this activity was

greatly decreased, but not completely neutralized, when cells were treated with an anti-poIFNα antibody (Table 8).

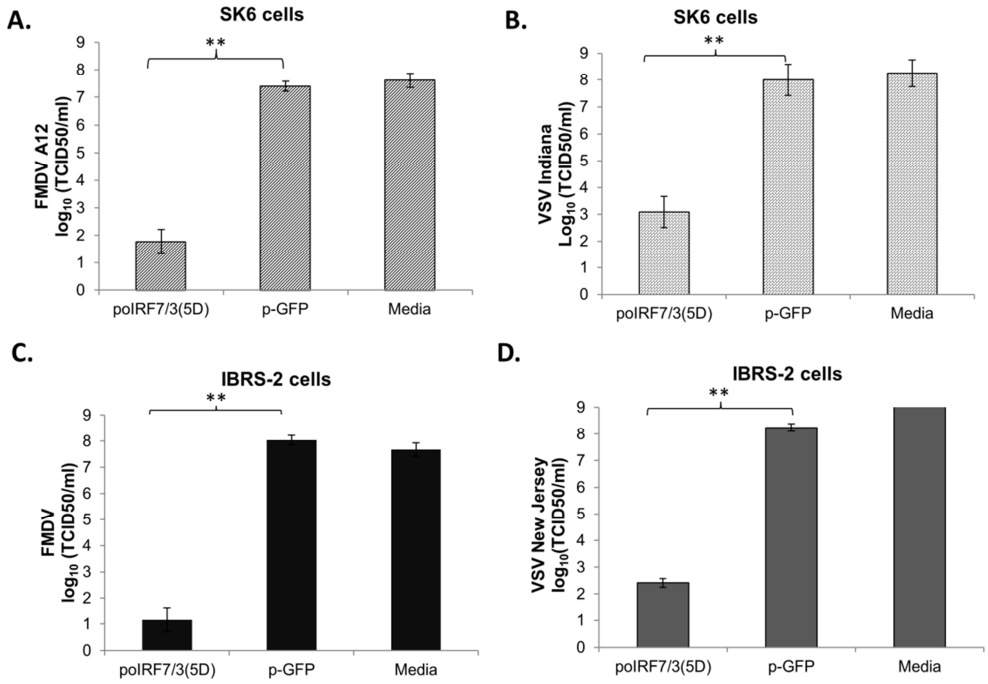

Figure. 19. PoIRF7/3(5D) has significant antiviral activity against FMDV and VSV in porcine cell lines.
(A-B) SK-6 or (C-D) IBRS-2 cells were transfected with 25 ng of plasmids poIRF7/3(5D), p-GFP, or mock. Twenty-four hours post transfection cells were infected with FMDV A12 or VSV Indiana at a MOI=0.1 for 24h. Viral titers were determined by $TCID_{50}$. Statistical analysis was performed using Student's t-test (** $p<0.001$).

Antiviral activity against FMDV and VSV was also evaluated in supernatants of IBRS-2 cells transfected with plasmids expressing the poIRF7/3(5D) construct (Fig 5.2D). Similar to SK-6 cells, there was a substantial reduction of viral titers (FMDV and VSV) varying from 4-6 log_{10} after transfection with plasmids expressing the poIRF7/3(5D) with no inhibition detected in the p-GFP transfected cells. However,

significantly less (6x) antiviral activity was detected in the supernatants of transfected IBRS-2 as compared to SK-6 cells (Table 8). Most of the detected antiviral activity was neutralized by addition of an anti-porcine IFNα antibody, suggesting that poIRF7/3(5D) mainly induced this type of IFN in swine cells (Table 8).

Table 8. Antiviral activity in the supernatants of porcine SK-6 and IBRS-2 cells after transfection with poIRF7/3(5D)[a].

		SK-6		IBRS-2	
Treatment	Neutralization[b]	IFN (Units/ml)	SEM	IFN (Units/ml)	SEM
poIRF7/3(5D)	-	135.9	39.8	22.8	10.8
poIRF7/3(5D)	anti-IFNα	10.5	4.4	1.6	0.6
p-GFP	-	<1	0.0	<1	0.0
p-GFP	anti-IFNα	<1	0.0	<1	0.0
Mock	-	<1	0.0	<1	0.0
Mock	anti-IFNα	<1	0.0	<1	0.0

[a] Antiviral activity bioassay was performed in supernatants of SK-6 or IBRS-2 collected 24 h post transfection of 25 ng of plasmid DNA.
[b] In some supernatants, a neutralizing mouse anti-porcine IFNα antibody was added to the cell supernatants prior to testing of VSV antiviral activity.

PoIRF7/3(5D) steadily reduces viral yield and enhances Ad5-poIFNβ and it is negatively regulated by IRF-7 5'UTR

To determine if poIRF7/3(5D) could induce a sustained reduction of viral titers, IBRS-2 cells were transfected with poIRF7/3(5D) and infected with FMDV A12 at different hours post-transfection (hpt). No differences in viral yields were detected earlier that 6 hpt with poIRF7/3(5D), pGFP, or mock transfected (Fig 20A). However, by 24 hpt the reduction in virus yield was sustained for up to 120 h.

In Chapter III the inhibitory effect of poIRF-7 5'UTR over reporter translation was demonstrated. In order to test whether IRF-7 5'UTR also affects antiviral effects induced by poIRF7/3(5D), we generated and compared the induction of IFNβ and several ISGs by poIRF7/3(5D) and a construct containing poIRF-7 5'UTR (5'UTR poIRF7/3(5D) (Fig 20B). Induction of all ISGs tested by 5'UTR poIRF7/3(5D) was lower as compared to poIRF7/3(5D), in particular expression of Mx-1 was significantly decreased in presence of 5'UTR, which confirms that 5'UTR has a negative regulatory role over IRF-7 (Fig 20B).

In order to deliver poIRF7/3(5D) more efficiently, we cloned its coding sequence in a replication defective human Ad5 vector (Ad5-Blue) previously developed (229). Infection of IBRS-2 cells with Ad5-poIRF7/3(5D) at MOI 2 resulted in a reduction of approximately 5 log10 in FMDV $TCID_{50}$/ml (Table 9). Addition of IFN neutralizing reagents (B18R inhibitor and anti-IFNα) neutralized most of the antiviral activity although some residual activity (about 1 log_{10}) was still detected (Table 9).

Table 9. Antiviral activity induced by Ad5-poIRF7/3(5D)[a].

Treatment	B18R- Anti-IFNα -		B18R + Anti-IFNα +	
	Log ($TCID_{50}$/ml)	SEM	Log($TCID_{50}$/ml)	SEM
Ad5 poIRF7/3(5D)	< 0.1	0.0	4.1	0.4
Media	5.5	0.0	6.3	0.0
Ad5 Blue	5.1	0.4	5.4	0.4

[a] FMDV viral titers (log $TCID_{50}$/ml) recovered from supernatants of IBRS-2 cells 24 h after infection with Ad5-poIRF7/3(5D) in presence (+) or absence (-) of IFN neutralizing agents (B18R and anti-porcine IFNα antibody).

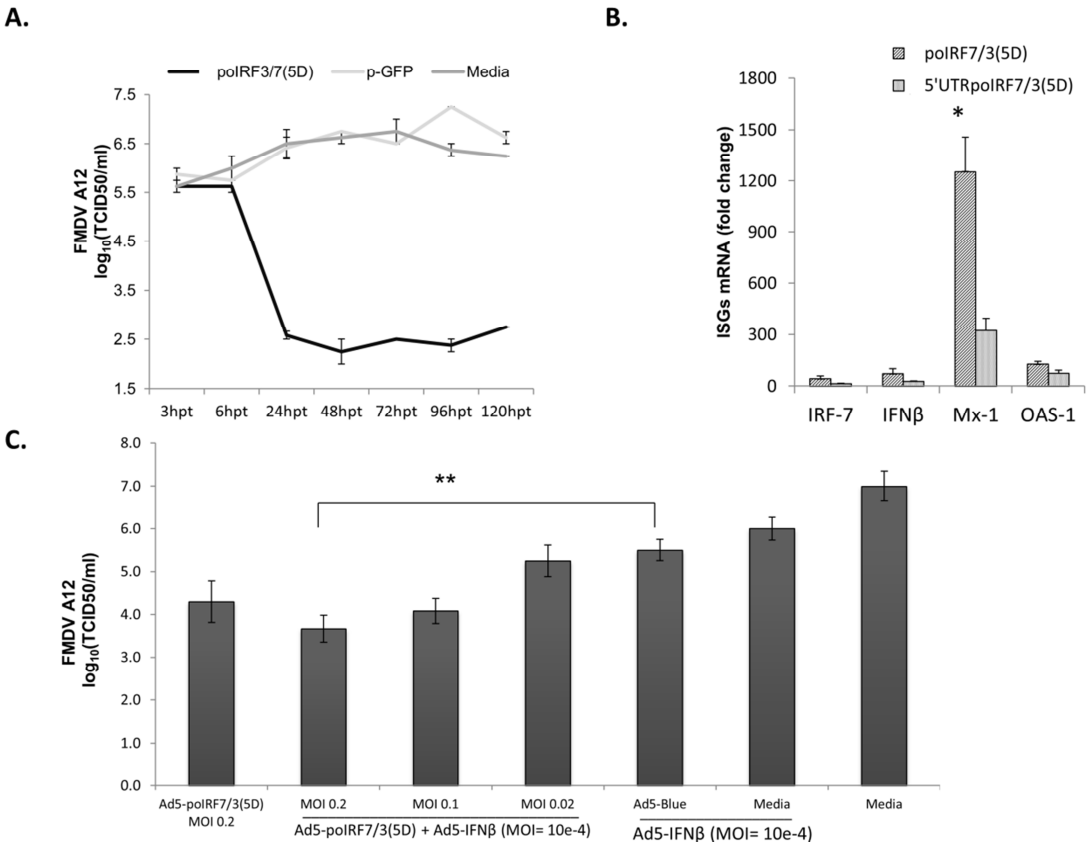

Figure. 20. PoIRF7/3(5D) induces sustained antiviral activity and potentiates Ad5-IFNβ effects.

(A) IBRS-2 cells were transfected with 25 ng of plasmids poIRF7/3(5D), p-GFP, or mock transfected. At specified times post-transfection, cells were infected with FMDV A12 at MOI=1. Twenty-four hours post-infection, supernatants were collected for viral titration by $TCID_{50}$. (B) IBRS-2 cells were co-transfected with a renilla plasmid and p-poIRF7/3(5D) or p-UTRpoIRF7/3(5D) plasmid. Twenty-four hours later, cell were lysed, RNA extracted and used for transcript analysis. Renilla expression was used to account for differences in transfection efficiencies and expression of endogenous reference genes was used for normalization (C) SK-6 cells were co-infected with Ad5-poIFNβ (MOI=10e-4) and Ad5-poIRF7/3(5D) at three different MOIs (0.2; 0.1 or 0.02); or Ad5-poIFNβ (MOI=10e-4) and Ad5-Blue (MOI=0.2), or mock infected. At 24h cells were challenged with FMDV MOI=0.1 for 24h followed by determination of viral titers by $TCID_{50}$. Statistical analysis was performed using student's t-test (** $p<0.01$).

Next, we evaluated whether Ad5-poIRF7/3(5D) could enhance Ad5-poIFNβ antiviral activity (130). SK-6 cells were infected with combinations of Ad5-poIFNβ and Ad5-poIRF7/3(5D) or Ad5-Blue (empty vector) 24 h prior to FMDV challenge. A dose dependent decrease in viral yield, 2 to 3.5 log10, was observed when cells were co-infected with low MOIs (0.02, 0.1, and 0.2) of Ad5-poIRF7/3(5D) and very low amounts of Ad5-poIFNβ (MOI=10e-4) and compared to mock treatment (Fig 5.3C). Combinations of Ad5-poIRF7/3(5D) (MOI=0.2) and Ad5-poIFNβ (MOI=10e-4) resulted in significant reduction ~2 log10 ($p<0.01$), when compared to cells treated with our control vector Ad5-Blue combined with Ad5-poIFNβ at similar MOIs. At the highest MOI used (0.2), Ad5-blue did not significantly contribute to the reduction in virus titer induced by Ad5-poIFNβ ($p>0.1$). These results indicated that treatment with Ad5-poIRF7/3(5D) enhanced the antiviral activity of Ad5-poIFNβ against FMDV.

PoIRF7/3(5D) induces antiviral responses in vitro in species other than swine

Since IRFs family members share some homology across species, we studied the effect of poIRF7/3(5D) expression *in vitro* in several species. Phylogenetic relationships among several IRF-3 protein sequences from some species available in public databases were deduced by ML analysis (Fig 21A) and verified by Bayesian inference. We confirmed that species from more closely related taxonomical groups such as bovine, swine, and sheep form a monophyletic group based on IRF-3 sequences while primates, carnivores and rodents are more distantly related.

Interestingly, poIRF7/3(5D) induced a functional antiviral response *in vitro* in cell lines from several species including MDBK (bovine), BHK-21 (hamster), or L929

(mouse) (Fig 21). After infection with Ad5-poIRF7/3(5D) or transfection with poIRF7/3(5D) and subsequent challenge with FMDV or VSV these cell lines exhibited a drastic reduction in viral yield as compared with mock treated cells. The antiviral effect in mouse cells, L929 (Fig 21B) or MEF (not shown), was lower as compared to porcine (Fig 5.2 A-D) and bovine cell lines (Fig 21C). Consistent with a previous report (234), transduction with Ad5-poIFNβ did not protect murine cell lines from FMDV infection (Fig 21B). Reduction in FMDV yield in BHK-21 cells treated with the fusion protein (Fig 21D) was similar to the effect observed for SK-6 cells (Fig 19A) but BHK-21 cells did not develop an antiviral response after poly I:C stimulation.

Characterization of antiviral response induced by poIRF7/3(5D) in swine cells

The antiviral activity elicited by transfection of the plasmid expressing poIRF7/3(5D) in SK-6 or IBRS-2 cells was not fully neutralized by addition of an anti-IFNα antibody (Table 8). To determine whether the residual antiviral activity could be attributed to the expression of other subtypes of porcine type I IFN, we quantitated relative transcript levels of the IFN type I subtypes (IFNα, β, κ, ε, ω, δ) in cells treated with the Ad5-poIRF7/3(5D). Infection with Ad5-poIRF7/3(5D) induced expression of IFNα, β, and ω in IBRS-2 (Fig 22) and in SK-6 cells (data not shown). However IFNκ, ε, δ or IL28B (IFN λ3) mRNAs were not up-regulated.

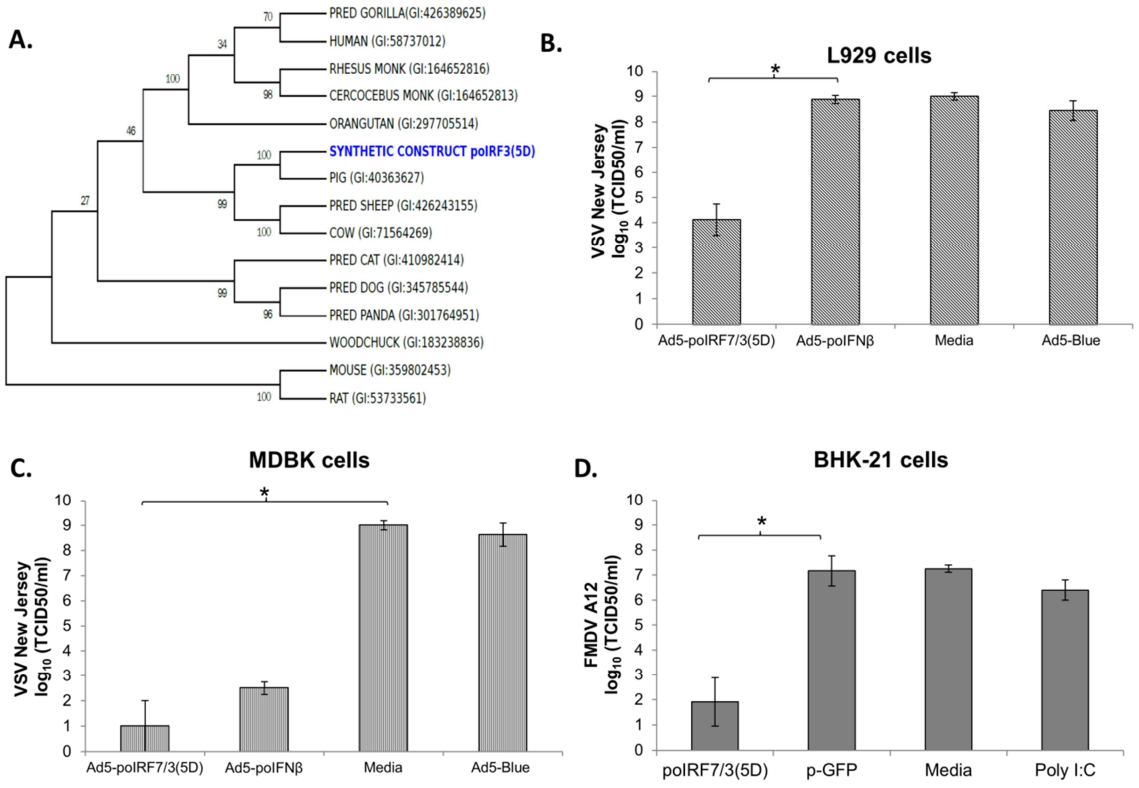

Figure. 21. PoIRF7/3(5D) induces antiviral response *in vitro* in cells from several species.

(A) Consensus tree generated using ML. Bootstrapping values are displayed in each branch (B) L929 or (C) MDBK cells were infected with Ad5-poIRF7/3(5D), Ad5-poIFNβ or Ad5-Blue at MOI= 20 , or mock treated (media). Twenty four hours post treatment, cells were infected with VSV new Jersey MOI= 1 for 24h. Viral titers were determined by $TCID_{50}$. (D) BHK-21 cells were transfected with plasmids poIRF7/3(5D), p-GFP, mock transfected (media), or treated with poly I:C (100ng/ml). Twenty four hours post treatment cells were infected with FMDV A12 at a MOI= 0.1 for 24h. Viral titers were determined by $TCID_{50}$. Statistical analysis was performed using student's t-test (* $p<0.05$).

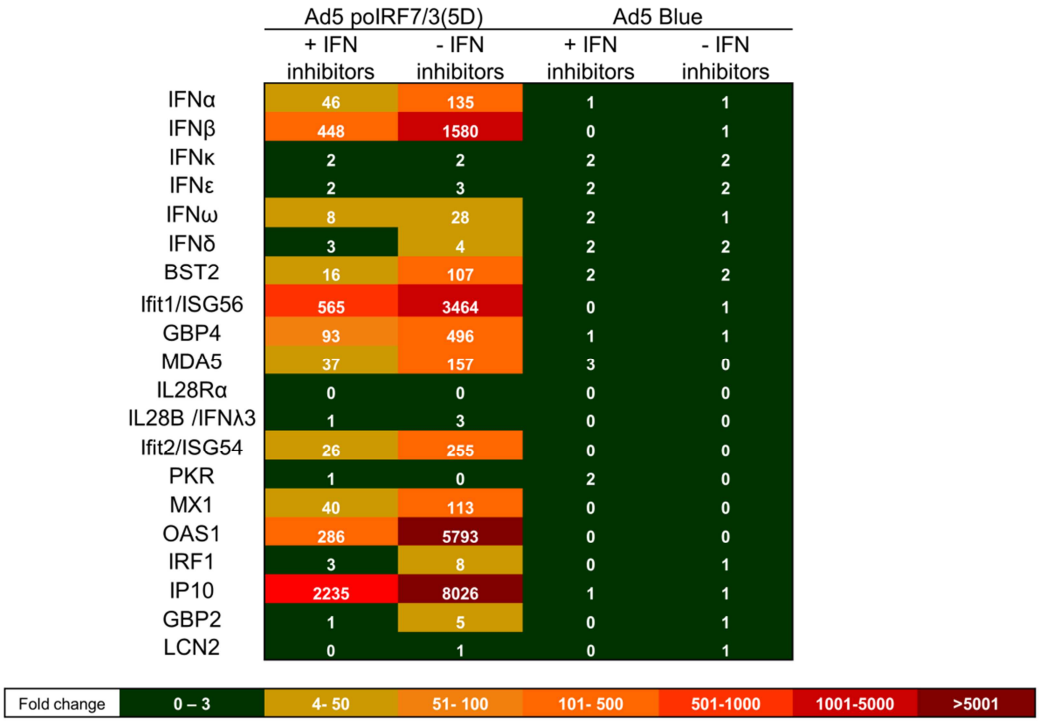

Figure. 22. Characterization of several type I IFNs and other genes with antiviral functions induced by Ad5-poIRF7/3(5D) in porcine cells.
Analysis of gene expression in IBRS-2 cells infected with Ad5-poIRF7/3(5D) or Ad5-Blue was performed by qPCR. Relative gene expression was analyzed in cells infected with Ad5-poIRF7/3(5D) or Ad5-Blue in the presence (+) or absence (-) of B18R inhibitor and an anti-IFNα antibody. Mock treated cells were used as reference to calculate relative gene expression using the ΔΔ Ct method.

Table 10. Antiviral activity from IBRS-2 cells filtered supernatants after treatment with Ad5-poIRF7/3(5D) in presence (+) or absence (-) of IFN neutralizing treatment [a].

Treatment	B18R- Anti-IFNα - IFN U/ml	B18R+ Anti-IFNα+ IFN U/ml
Ad5-poIRF7/3(5D)	11.3	0.0
Media	0.0	0.0
Ad5-Blue	0.0	0.0

[a] Antiviral activity bioassay was performed in supernatants of IBRS-2 collected 24 h after infection with Ad5-poIRF7/3(5D) in presence (+) or absence (-) of IFN neutralizing agents (B18R and anti-porcine IFNα antibody).

We also questioned if an antiviral effect independent of type I IFN might be involved in the strong antiviral response of IBRS-2 cells even when these cells showed lower ability to induce antiviral responses as compared to SK-6 cells (Table 8). To neutralize the IFN induced response we used B18R inhibitor, a vaccinia virus encoded product that competes with IFN for binding to the type I IFN receptor. Based on the production of antiviral activity induced by poIRF7/3(5D) in SK-6 or IBRS-2 cells (Table 8), we used a dose of B18R that was sufficient to neutralize up to 500 IFN units of IFNα without causing toxicity. Transduction of IBRS-2 with Ad5-poIRF7/3(5D) completely blocked FMDV replication, and this effect was only partially reversed by the addition of the B18R inhibitor (Table 9). Although, antiviral activity in the supernatants of the cells was fully neutralized by B18R (Table 10), inhibition of FMDV replication was partially reversed (Table 9) and up-regulation of 46-, 448-fold, and 8-fold for IFNα, β and ω transcripts, respectively (Fig 22) was observed even in the presence of the B18R inhibitor combined with an anti-IFNα. Even though treatment with B18R inhibitor in combination with anti-IFNα markedly reduced the expression of all the ISGs tested, several ISGs including BST2, IP10, ISG56, ISG54, GBP4, MDA5, and OAS1 were up-regulated to relatively high levels in cells maintained with the IFN neutralizing treatment (Fig 22). Fold change in transcripts level of genes such as IP10, OAS1 and ISG56 dropped from 8026 to 2235, 5793 to 296 and from 3464 to 565, respectively. These results suggested that poIRF7/3(5D) may stimulate genes with antiviral function even when type I IFNs are neutralized. However, the identity of antiviral genes induced by

poIRF7/3(5D) fully independent of IFN stimuli in a porcine system remains to be determined.

Ad5-poIRF7/3(5D) induced levels of IFN capable of preventing FMDV viremia

We tested the ability of Ad5-poIRF7/3(5D) to induce immune responses *in vivo* and confer protection against FMDV challenge. It has been previously shown that high doses of FMDV can cause fatal disease in adult (6 to 7 weeks old) C57Bl/6 mice (235), (234). To determine if Ad5-poIRF7/3(5D) induced the production of systemic IFN, we inoculated mice with two doses of Ad5-poIRF7/3(5D) and compared these animals to those treated with Ad5-Blue control. We found that mice inoculated at the higher dose ($3x10^8$PFU/mouse) of Ad5-poIRF7/3(5D) had statistically significantly higher levels of IFNα ($p<0.001$), β ($p<0.05$), and total induced antiviral activity ($p<0.001$) as compared to an equivalent dose of Ad5-Blue control (Fig 23A-C). Notably, Ad5-Blue induced some antiviral activity and production of IFNα or β, when it was used at a high dose ($3x10^8$ PFU/mouse). Mice treated with the high dose of Ad5-poIRF7/3(5D) produced on average 21,195 pg/ml of IFNα as compared to 210 pg/ml produced by mice treated with an Ad5-Blue control. Also mice treated with the high dose of Ad-poIRF7/3(5D) produced on average 171 pg/ml of IFNβ as compared to 85 pg/ml produced by mice treated with an Ad5-Blue control.

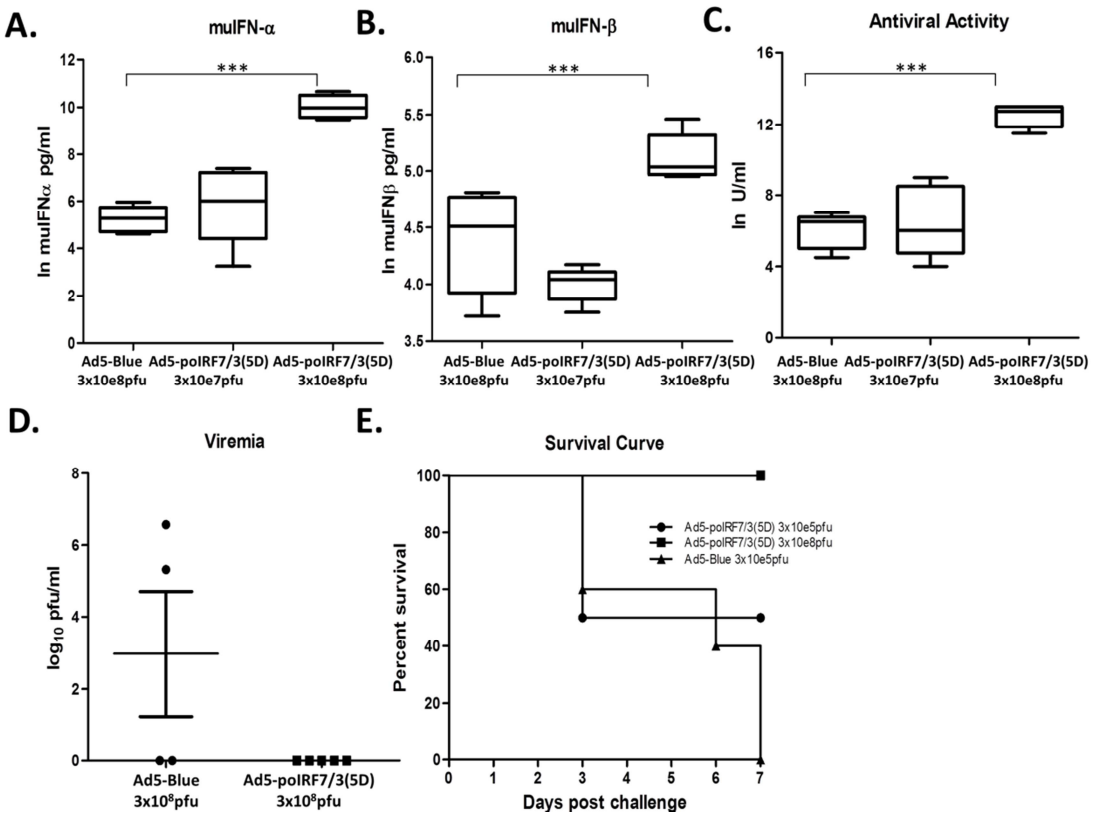

Figure. 23. Ad5-poIRF7/3(5D) induced antiviral activity with production of IFNα/β that blocks FMDV viremia.

Groups of five mice were inoculated with Ad5-poIRF7/3(5D) or Ad5-Blue at indicated doses. (A) MuIFNα or (B) MuIFNβ levels present in serum were tested by ELISA. Values are represented as natural logarithm [ln] of IFN concentration in pg/ml. (C) Antiviral activity was measured by a VSV bioassay in serum. Values are represented as natural logarithm [ln] of IFN U/ml. (D) FMDV viremia at 2dpc determined by $TCID_{50}$ in mice treated with Ad5-poIRF7/3(5D) or Ad5-Blue control at high dose (3x108 PFU/mouse). (E) Survival curve of mice treated with Ad5-poIRF7/3(5D) or Ad5-Blue control at lowest dose (3x105 pfu/mouse) or high dose (3x108 pfu/mouse) for 24h followed by FMDV challenge. Statistical analysis in panels (A), (B) and (C) was performed using Student's t-test (*** $p<0.001$).

In a second experiment, four groups of mice were treated with two different doses of Ad5-poIRF7/3(5D) or control Ad5-Blue (high dose=$3x10^8$ PFU/mouse or low

dose=$3x10^5$ PFU/mouse) and challenged with FMDV 24 h later. Animals were monitored for 7 days, and blood drawn daily to determine viremia. All mice treated with a high dose ($3x10^8$PFU/mouse) of Ad5-poIRF7/3(5D) had no viremia and were protected from FMDV challenge (Fig 23D-E). Consistent with the production of IFNα/β, the antiviral activity induced by the group treated with Ad5-Blue at high dose (3x108PFU/mouse) was sufficient to prevent mortality in mice but not viremia (Fig 23C-E). In the groups treated at a 1000X lower dose ($3x10^5$ PFU/mice), Ad5-poIRF7/3(5D) conferred 50% protection while Ad5 blue did not. Protected mice did not developed viremia (Table 11) and survived after 7 days monitoring. In contrast, all animals inoculated with Ad5-Blue at similar dose ($3x10^5$PFU/mice) died by 7 days and developed viremia at 2 dpc (Fig 23D-E; Table 11). These results indicate that the levels of antiviral activity induced *in vivo* by Ad5-poIRF7/3(5D) are sufficient to completely block FMDV replication.

Table 11. FMDV A24 viremia two days post challenge in mice treated with Ad5-poIRF7/3(5D) or Ad5-Blue at low dose ($3x10^5$ PFU/mice).

	Ad5 poIRF7/3(5D) (PFU/ml)	Ad5 Blue (PFU/ml)
Mouse 1	$8.5x10^5$	$2.1 x10^6$
Mouse 2	0.0	$1.4 x10^7$
Mouse 3	$3.4 x10^6$	$9.5 x10^6$
Mouse 4	0.0	$9.5 x10^6$
Mouse 5	D	$8.0 x10^6$

D= Died due to anesthesia complication

Discussion

Over-expression of IFNs delivered with an Ad5 vector is effective in protecting swine and cattle against different serotypes of FMDV (128-130, 230). However, high amounts of Ad5-IFNs are required to fully protect swine and partially protect bovine. Thus, this strategy can be very expensive to protect large animals. To circumvent this limitation, a number of strategies have been examined, including use of a combination of type I and II IFN which results in enhanced activity at lower doses (230), use of type III IFN (102, 103), use of adjuvants/modulators of innate immunity such as polyICLC (236) or use of Venezuelan equine encephalitis replicon particles (VRPs) (234). Here, we report an additional strategy that involves a fusion construct generated from porcine sequences of IRF-7 and IRF-3, namely poIRF7/3(5D). The resulting protein induced activation of type I IFNs and consequently ISGs. We demonstrated that poIRF7/3(5D) is a powerful inducer of antiviral activity against FMDV and VSV.

Even though a low amount (25 ng) of the poIRF7/3(5D) construct was transfected into porcine cells, IRF-7 transcripts were significantly increased (Fig 18B) and there was a significant induction of ISGs (Fig 18E) and antiviral activity. These results suggested that even a low expression of this fusion protein is sufficient to induce innate responses in porcine cells. Importantly, the expression of this construct *in vitro* or *in vivo* did not result in cytotoxicity (not shown) at doses that were able to reduce viral replication by as much as ~6 $\log_{10}$.

Administration of inactivated FMD vaccine or an Ad5 vector expressing the FMDV capsid requires approximately 7 days to induce protective immunity (237,238). As a result, vaccinated animals exposed to virus within the first 7 days after vaccination are still susceptible to the disease (234, 239, 240). Here, we have shown that the impairment in viral replication by using the poIRF7/3(5D) construct *in vitro* was detected as early as 1 day after treatment and it was sustained for at least 5 days post treatment. Our results *in vitro* suggest that Ad5-poIRF7/3(5D) may not only induce rapid innate immunity, but also a sustained response that is needed for protecting animals until the vaccine induced adaptive immunity is effective. Importantly, we have also shown that poIRF7/3(5D) enhances the function of poIFNβ. This information is instrumental in supporting additional experiments to explore if Ad5-poIRF7/3(5D) will allow for Ad5-poIFN dose-sparing to protect animals from FMD.

IBRS-2 cells have been traditionally used to grow FMDV in cell culture. Apparently, high levels of viral replication are achieved in this cell line because no induction of IFN-α/β mRNA is detected (126). In this study, we confirmed that IBRS-2 cells are somewhat impaired in their ability to induce IFNs as compared to another porcine cell line, SK-6 cells. Unexpectedly, we detected antiviral activity (partially neutralized by an anti-IFNα) in the supernatants of IBRS-2 cells transfected with poIRF7/3(5D) suggesting that other IFNs or IFN-independent genes with direct antiviral activity might have been induced by the fusion protein.

Previous reports found that expression of IRF-3 alone does not induce the synthesis of endogenous IFNα1 and IFNβ (241, 242). However, a subset of genes were

activated in cells expressing the constitutively active form IRF3(5D) combined with neutralizing antibodies against IFNα/β (242). This result led us to investigate whether poIRF7/3(5D) could induce genes with antiviral function independently of IFN. We neutralized the antiviral activity in the supernatants of IBRS-2 cells by combining an anti-swine IFNα antibody (clone K9) and B18R inhibitor, a vaccinia virus encoded product prevents the binding of type I IFN to its natural receptor (IFN α/β receptor) (243). The B18R protein has broad activity across species (244), is soluble outside the cell and present on the cell surface thus blocking type I IFN autocrine and paracrine functions (243). In the presence of B18R and anti-swine IFNα at doses that fully neutralized antiviral activity in supernatants of cells infected with Ad5-poIRF7/3(5D), induction of IFNα, β, and ω transcripts was still highly up-regulated. In accordance with findings from Grandvaux et al. (2002) we found that ISG54 and ISG56 were still highly up-regulated in the presence of IFN neutralization treatment. Other ISGs including GBP4, (but not GBP2), IP10, MDA-5, Mx-1, and OAS-1 genes were also highly up-regulated in the presence of the IFN neutralization treatment after transduction with Ad5-poIRF7/3(5D). This is consistent with a predominantly positive transcription signature described for IRF-7 (245) or a STAT1-independent mechanism of induction as previously reported for IP10 during HIV infection of astrocytes (246). A possible explanation to the high up-regulation of IFN transcription in the presence of B18R inhibitor could be the two-step positive feedback loop that IFNs α/β employ to amplify their own expression (140, 247). While B18R inhibits signaling through the IFN α/β receptor (second wave), earlier expression of IFNβ and IFNα-4 (247) remains unaffected

by the use of B18R inhibitor. Alternatively, our treatments with B18R and anti IFNα might have not been sufficient to neutralize all subtypes of type I IFN induced by the fusion protein. The high induction of IFN transcripts in the presence of IFN neutralizing treatment does not necessarily conclude that induction of genes with antiviral function by poIRF7/3(5D) is fully independent of IFN.

Another study using B18R to block the IFN response has shown induction of a lipid raft associated protein BST-2 (also known as tetherin or CD317) independently of IFN. Tetherin inhibits viral infection by preventing the release of viral particles after budding from infected cells (112). Here, we confirmed that transcript levels of BST-2 were induced by 16-fold in the presence of Ad5-poIRF7/3(5D) and IFN neutralizing treatment. This antiviral protein inhibits the release of diverse enveloped virus particles and it plays a role in neutralizing VSV (248). However, a role in controlling infection of non-enveloped viruses such as FMDV remains to be elucidated.

Similarly, we have also demonstrated that poIRF7/3(5D) induces potent antiviral effects in cell lines derived from multiple species including bovine, hamster and murine. In the case of murine cells (L929), the Ad5-poIRF7/3(5D) seemed to be less efficient to reduce viral yield, a result that was also observed when the Ad5-poIRF7/3(5D) was tested in mouse embryonic fibroblasts (data not shown). This observation is consistent with a more distant phylogenetic relationship between mouse and porcine sequences. However, contrary to the case in murine cells, reduction in antiviral properties of Ad5-poIRF7/3(5D) in hamster cells was not observed. In fact, it was surprising to detect a strong antiviral activity induced by Ad5-poIRF7/3(5D) in cell lines previously reported

as defective in IFNα/β sensing or signaling (249, 250) that are used routinely for viral expansion and production of FMD vaccine (251). BHK-21 cells did not respond to poly I:C stimulation (or viral infection), but responded to treatment with the poIRF7/3(5D) protein suggesting that expression of this protein bypasses certain limitations in antiviral pathways. Treatment with poIRF7/3(5D) in BHK-21 or IBRS-2 cells might bypass a defect in PAMP sensing or transduction pathways and directly induce strong transcription of IFN or other genes with antiviral activities. Further studies are required to characterize the plethora of responses that could be induced by the fusion protein in these cell lines.

Characterization of the antiviral activity induced by poIRF7/3(5D) in porcine cells led us to identify type I but not type III IFNs (IFNλ3 or IL28B) as major players in the induced antiviral effect. Contrary to our findings using poIRF7/3(5D) in porcine cells, it has been reported that human IFN-λ2/3 gene expression is mainly controlled by IRF-7 (252). In accordance with our results, another study suggested that type III IFNs are induced through independent actions of IRFs and nuclear factor-kappa B (NF-κB) (253). Another report also suggested c-REL/p65 NF-κB heterodimer and IRF-1 are the main transcriptional regulators of type III IFNs (254). Further studies are needed to study the regulation of type III IFN in porcine cells.

We found that expression of poIRF7/3(5D) induced the expression of various but not all type I IFN mRNAs including IFNα, β, or ω. These results are consistent with previous reports in which IFNε was mainly associated with cells of reproductive function and IFNκ expressed in epidermal keratinocytes (255). IFNδ has been shown to

have high antiviral activity in porcine cells and a relevant biological role during early pregnancy when it is secreted by the trophectoderm of the pig conceptus (256).

Finally, the results *in vitro* prompted us to evaluate the effectiveness of poIRF7/3(5D) in protecting mice from FMDV infection. Confirming the results from our *in vitro* studies, mice treated with Ad5-poIRF7/3(5D) at high dose produced on average 100 times more IFNα than the control group. Ad5-poIRF7/3(5D) at high dose also induced up regulation of IFNβ to a lesser extent than the induction of IFNα. These results were consistent with the rapid antiviral activity detected in mice sera 24 hpt. In contrast, IFNβ transcripts were induced at approximately 10-fold higher levels than IFNα in cultured epithelial porcine cells infected with Ad5-poIRF7/3(5D). Nevertheless, when IFNβ transcripts were highly up-regulated *in vitro*, antiviral activity accounted for only less than 10% after neutralization with IFNα specific antibodies. Further analysis of IFN transcripts and protein from *in vivo* experiments using porcine tissues and serum is necessary to make a more relevant comparison.

Altogether, our results demonstrated that poIRF7/3(5D) is a robust inducer of innate immunity in porcine cells. Furthermore, poIRF7/3(5D) inhibits viral replication in cell lines from several species including porcine, murine, and bovine, suggesting that a single poIRF7/3(5D) construct might hold biotherapeutic properties across species of interest thus potentially inducing protection against FMDV, a virus that affects a wide range of livestock and more than 70 species of wildlife.

CHAPTER VI

SUMMARY AND FUTURE DIRECTIONS

Continuous efforts to control and eradicate the viral diseases of veterinary importance worldwide have faced many challenges. In the case of VSV, the presence of neutralizing antibodies is not sufficient to prevent clinical disease under natural conditions and animals can be re-infected following recovery (44). In the case of FMDV, the constant emergence of numerous field variants in addition to the seven serotypes and multiple subtypes has prevented the design of a single vaccine that provides protection (37). In order to prevent fast spread of FMDV during outbreaks, it is imperative to develop new methods that rapidly enhance immune innate responses in susceptible animals and help to contain viral transmission.

In this dissertation, first we reviewed the pathogenesis, epidemiology, genome and protein organization of FMDV and VSV. Understanding virus-specific properties, molecular pathogenesis, and identifying virulence factors should allow a better design of biotechnological approaches to diminish the consequences of viral diseases on the animal health and international economy. In addition, these two viruses were models used to determine the antiviral activities from several strategies described in the chapters III, IV and V.

In the chapter II, we reviewed the key components and mechanisms involved in the innate immune antiviral response. We studied the critical role of the pathogen recognition receptors such as TLR, RIG-I, MDA-5, and NLR in detection viral PAMPs.

Next, the different types of IFNs were reviewed, highlighting the importance of type I IFN to counteract viral infections through the activation of hundreds of ISGs. Lastly, we described the molecular components of the IFN-activated classic signaling pathway and some virus-specific interactions of FMDV and VSV viral proteins with the IFNs.

In subsequent chapters, we tested several methods to enhance the antiviral response and possibly counteract viral tactics to evade innate immunity. In the chapter III, we explored the role of eIF4e-binding proteins in the regulation of the antiviral state in bovine and porcine cells. We found that the partial reduction in 4eBP-1, 4eBP-2 or 4eBP-3 expression did not induce changes in the antiviral state, however fully 4eBP-1 depletion resulted in higher levels of IFNβ, ISGs and correlated with lower viral yields (~2 logs, $p<0.05$) after IFN induction.

To generate 4eBP-$1^{-/-}$ porcine cells, we used the novel CRISPR/Cas9 genome editing strategy. CRISPR/Cas9-mediated homology-directed repair has been demonstrated in a limited range of eukaryotic models and until recently it has been applied to livestock species (257). In the chapter III, we validated a new swine genome target with agricultural and biomedical relevance.

We also gained new insights in the regulation of porcine IRF-7 thought its 5'UTR using a renilla/luciferase reporter system. Even though, we found no correlation between our predicted secondary structure of poIRF-7 5'UTR and their regulatory roles in reporter translation, we identified a 361nt region of poIRF-7 5'UTR that partially represses translation. A better understanding of the control of the interferon response

through 4E-BP translational suppression of IRF-7 regulation (258) could contribute to develop better biotherapeutic approaches to control viral diseases in the livestock.

In the chapter IV, the role of porcine OASL in antiviral state was explored. We found that down-regulation or overexpression of porcine OASL-1 had minor effects on the viral replication or the antiviral response. In accordance to previous reports, we confirmed that poOASL is a truncated protein (190) compared to murine, human, or horse OASL. We reasoned that the absence of the ubiquitin-like domain probably impairs any antiviral or IRF-7 regulatory function of the poOASL. However, poOASL might still retain its RNA binding function. These findings justify new investigations to elucidate a possible unique physiological role of bovine and porcine OASL. Also, future work will clarify if some bovine or porcine individuals or livestock breeds might encode a non-truncated OASL protein.

Lastly, chapter V describes the results of the characterization of a constitutively active fusion protein of IRF-3 and IRF-7. Low doses of poIRF7/3(5D) *in vitro* were effective to reduce 4 -6 logs of the FMDV and VSV viral yield, for up to 5 days and correlated with the induction of several ISGs. In addition, mice inoculated with an Ad5poIRF7/3(5D) showed high antiviral activity, increased the systemic levels of muIFNα and β at 1dpi, and survived the FMDV challenge. Using this strategy, the ability of host cell to prevent viral infection was enhanced. However, a more precise understanding of the role of the poIRF7/3(5D) in blocking FMDV replication *in vivo* will come from future studies in livestock.

Overall, the work presented here confirmed the role of porcine 4eBP-1 but not poOASL in the regulation of IFN responses in swine cells. Further investigations will clarify if the 4eBP-1 depletion in bovine cells will also enhance the antiviral response. Our studies also validated for the first time the expression of IRF-7/3(5D) to enhance IFN response against FMDV and VSV. Future investigations might elucidate possible IFN-independent antiviral pathways stimulated by poIRF7/3(5D) or poOASL. Results described in this dissertation, may contribute to develop better tools to defend our agriculture animal resources against FMD and possibly other viral diseases.

REFERENCES

1. **Pinto, A. A.** 2004. Foot-and-mouth disease in tropical wildlife. Ann. N. Y. Acad. Sci. **1026:**65-72. doi: 10.1196/annals.1307.008.

2. **Grubman, M. J., and B. Baxt.** 2004. Foot-and-mouth disease. Clin. Microbiol. Rev. **17:**465-493.

3. **Arzt, J., B. Baxt, M. J. Grubman, T. Jackson, N. Juleff, J. Rhyan, E. Rieder, R. Waters, and L. L. Rodriguez.** 2011. The pathogenesis of foot-and-mouth disease II: viral pathways in swine, small ruminants, and wildlife; myotropism, chronic syndromes, and molecular virus-host interactions. Transbound Emerg. Dis. **58:**305-326. doi: 10.1111/j.1865-1682.2011.01236.x.

4. **Arzt, J., N. Juleff, Z. Zhang, and L. L. Rodriguez.** 2011. The pathogenesis of foot-and-mouth disease I: viral pathways in cattle. Transbound Emerg. Dis. **58:**291-304. doi: 10.1111/j.1865-1682.2011.01204.x.

5. **Arzt, J., J. M. Pacheco, and L. L. Rodriguez.** 2010. The early pathogenesis of foot-and-mouth disease in cattle after aerosol inoculation. Identification of the nasopharynx as the primary site of infection. Vet. Pathol. **47:**1048-1063. doi: 10.1177/0300985810372509.

6. **Burrows, R.** 1966. Studies on the carrier state of cattle exposed to foot-and-mouth disease virus. J Hyg. (Lond.). **64:**81-90.

7. **Alexandersen, S., Z. Zhang, A. I. Donaldson, and A. J. Garland.** 2003. The pathogenesis and diagnosis of foot-and-mouth disease. J. Comp. Pathol. **129:**1-36. doi: S0021997503000410 [pii].

8. **Whitton, J. L., C. T. Cornell, and R. Feuer.** 2005. Host and virus determinants of picornavirus pathogenesis and tropism. Nat. Rev. Microbiol. **3:**765-776. doi: 10.1038/nrmicro1284.

9. **Grubman, M.J., Rodriguez, L.L., and de los Santos, T.** 2010. Foot-and-mouth disease virus, p397-410. *In* Ehrenfeld, E., Domingo E., and Roos, R. P. (eds.), The Picornaviruses, ASM publisher. DC, USA.

10. **Racaniello, V. R.** 2007. Picornaviridae: The viruses and their replication, p. 839. *In* Howley, D. Griffin Knipe P. (ed.), Fields' virology,5th ed., vol. I. Lippincott Williamms & Wilkins, PA, USA.

11. **Rodriguez-Pulido, M., B. Borrego, F. Sobrino, and M. Saiz.** 2011. RNA structural domains in noncoding regions of the foot-and-mouth disease virus genome trigger innate immunity in porcine cells and mice. J. Virol. **85:**6492-6501. doi: 10.1128/JVI.00599-11.

12. **Robertson, B. H., M. J. Grubman, G. N. Weddell, D. M. Moore, J. D. Welsh, T. Fischer, D. J. Dowbenko, D. G. Yansura, B. Small, and D. G. Kleid.** 1985. Nucleotide and amino acid sequence coding for polypeptides of foot-and-mouth disease virus type A12. J. Virol. **54:**651-660.

13. **Nayak, A., I. G. Goodfellow, and G. J. Belsham.** 2005. Factors required for the uridylylation of the foot-and-mouth disease virus 3B1, 3B2, and 3B3 peptides by the RNA-dependent RNA polymerase (3Dpol) *in vitro.* J. Virol. **79:**7698-7706. doi: 10.1128/JVI.79.12.7698-7706.2005.

14. **Mason, P. W., M. J. Grubman, and B. Baxt.** 2003. Molecular basis of pathogenesis of FMDV. Virus Res. **91:**9-32.

15. **Strebel, K., and E. Beck.** 1986. A second protease of foot-and-mouth disease virus. J. Virol. **58:**893-899.

16. **Foeger, N., W. Glaser, and T. Skern.** 2002. Recognition of eukaryotic initiation factor 4G isoforms by picornaviral proteinases. J. Biol. Chem. **277:**44300-44309. doi: 10.1074/jbc.M208006200.

17. **Foeger, N., E. Kuehnel, R. Cencic, and T. Skern.** 2005. The binding of foot-and-mouth disease virus leader proteinase to eIF4GI involves conserved ionic interactions. Febs j. **272:**2602-2611. doi: 10.1111/j.1742-4658.2005.04689.x.

18. **Piccone, M. E., E. Rieder, P. W. Mason, and M. J. Grubman.** 1995. The foot-and-mouth disease virus leader proteinase gene is not required for viral replication. J. Virol. **69:**5376-5382.

19. **Jackson, T., F. M. Ellard, R. A. Ghazaleh, S. M. Brookes, W. E. Blakemore, A. H. Corteyn, D. I. Stuart, J. W. Newman, and A. M. King.** 1996. Efficient infection of cells in culture by type O foot-and-mouth disease virus requires binding to cell surface heparan sulfate. J. Virol. **70:**5282-5287.

20. **Ryan, M. D., G. J. Belsham, and A. M. Q. King.** 1989. Specificity of enzyme-substrate interactions in foot-and-mouth disease virus polyprotein processing. Virology. **173:** 35- 45. doi: 10.1016/0042-6822(89)90219-5.

21. **De Felipe, P., G. A. Luke, J. D. Brown, and M. D. Ryan.** 2010. Inhibition of 2A-mediated 'cleavage' of certain artificial polyproteins bearing N-terminal signal sequences. Biotechnol. J. **5:**213-223. doi: 10.1002/biot.200900134.

22. **Moffat, K., C. Knox, G. Howell, S. J. Clark, H. Yang, G. J. Belsham, M. Ryan, and T. Wileman.** 2007. Inhibition of the secretory pathway by foot-and-mouth disease virus 2BC protein is reproduced by coexpression of 2B with 2C, and the site of inhibition is determined by the subcellular location of 2C. J. Virol. **81:**1129-1139. doi: 10.1128/JVI.00393-06.

23. **Grubman, M. J., M. P. Moraes, F. Diaz-San Segundo, L. Pena, and T. de los Santos.** 2008. Evading the host immune response: how foot-and-mouth disease virus has become an effective pathogen. FEMS Immunol. Med. Microbiol. **53:**8-17. doi: 10.1111/j.1574-695X.2008.00409.x.

24. **Sweeney, T. R., V. Cisnetto, D. Bose, M. Bailey, J. R. Wilson, X. Zhang, G. J. Belsham, and S. Curry.** 2010. Foot-and-mouth disease virus 2C is a hexameric AAA+ protein with a coordinated ATP hydrolysis mechanism. J. Biol. Chem. **285:**24347 - 24359. doi: 10.1074/jbc.M110.129940.

25. **Gladue, D. P., V. O'Donnell, R. Baker-Branstetter, L. G. Holinka, J. M. Pacheco, I. Fernandez-Sainz, Z. Lu, E. Brocchi, B. Baxt, M. E. Piccone, L. Rodriguez, and M. V. Borca.** 2012. Foot-and-mouth disease virus nonstructural protein 2C interacts with Beclin1, modulating virus replication. J. Virol. **86:** 12080 - 12090. doi: 10.1128/JVI.01610-12.

26. **O'Donnell, V., J. M. Pacheco, M. LaRocco, T. Burrage, W. Jackson, L. L. Rodriguez, M. V. Borca, and B. Baxt.** 2011. Foot-and-mouth disease virus utilizes an autophagic pathway during viral replication. Virology. **410:**142-150. doi: 10.1016/j.virol.2010.10.042.

27. **Pacheco, J. M., T. M. Henry, V. K. O'Donnell, J. B. Gregory, and P. W. Mason.** 2003. Role of nonstructural proteins 3A and 3B in host range and pathogenicity of foot-and-mouth disease virus. J. Virol. **77:**13017-13027. doi: 10.1128/JVI.77.24.13017-13027.2003.

28. **O'Donnell, V. K., J. M. Pacheco, T. M. Henry, and P. W. Mason.** 2001. Subcellular distribution of the foot-and-mouth disease virus 3A protein in cells infected with viruses encoding wild-type and bovine-attenuated forms of 3A. Virology. **287:**151-162. doi: 10.1006/viro.2001.1035.

29. **Gonzalez-Magaldi, M., R. Postigo, B. G. de la Torre, Y. A. Vieira, M. Rodriguez-Pulido, E. Lopez-Vinas, P. Gomez-Puertas, D. Andreu, L. Kremer, M. F. Rosas, and F. Sobrino.** 2012. Mutations that hamper dimerization of foot-and-mouth disease virus 3A protein are detrimental for infectivity. J. Virol. **86:**11013-11023. doi: 10.1128/JVI.00580-12.

30. **Clarke, B. E., and D. V. Sangar.** 1988. Processing and assembly of foot-and-mouth disease virus proteins using subgenomic RNA. J. Gen. Virol. **69:**2313 -2325. doi: 10.1099/0022-1317-69-9-2313.

31. **Belsham, G. J., G. M. McInerney, and N. Ross-Smith.** 2000. Foot-and-mouth disease virus 3C protease induces cleavage of translation initiation factors eIF4A and eIF4G within infected cells. J. Virol. **74:**272-280.

32. **Tesar, M., and O. Marquardt.** 1990. Foot-and-mouth disease virus protease 3C inhibits cellular transcription and mediates cleavage of histone H3. Virology. **174:**364- 374. doi: 10.1016/0042-6822(90)90090-E.

33. **Zhou, Z., M. M. Mogensen, P. P. Powell, S. Curry, and T. Wileman.** 2013. Foot-and-mouth disease virus 3C protease induces fragmentation of the Golgi compartment and blocks intra-Golgi transport. J. Virol. **87:**11721- 11729. doi: 10.1128/JVI.01355-13.

34. **Ferrer-Orta, C.** 2004. Structure of foot-and-mouth disease virus RNA-dependent RNA polymerase and its complex with a template-primer RNA. J. Biol. Chem. **279:**47212 - 47221. doi: 10.1074/jbc.M405465200.

35. **Bentham, M., K. Holmes, S. Forrest, D. J. Rowlands, and N. J. Stonehouse.** 2012. Formation of higher-order foot-and-mouth disease virus 3Dpol complexes is dependent on elongation activity. J. Virol. **86:**2371-2374. doi: 10.1128/JVI.05696-11.

36. **Ferrer-Orta, C., R. Agudo, E. Domingo, and N. Verdaguer.** 2009. Structural insights into replication initiation and elongation processes by the FMDV RNA-dependent RNA polymerase. Curr. Opin. Struct. Biol. **19:**752-758. doi: 10.1016/j.sbi.2009.10.016.

37. **Rodriguez, L. L., and C. G. Gay.** 2011. Development of vaccines toward the global control and eradication of foot-and-mouth disease. Expert Rev Vaccines. **10:**377-87.

38. **Rodriguez, L. L., and M. J. Grubman.** 2009. Foot and mouth disease virus vaccines. Vaccine. **5;27 Suppl 4:**D90-4. doi: 10.1016/j.vaccine.2009.08.039.

39. **Ludi, A., and L. L. Rodriguez.** 2013. Novel approaches to foot-and-mouth disease vaccine development. Dev Biol (Basel). **135:**107-16. doi: 10.1159/000313913.

40. **Grubman, M. J., M. P. Moraes, C. Schutta, J. Barrera, J. Neilan, D. Ettyreddy, B. T. Butman, D. E. Brough, and D. A. Brake.** 2010. Adenovirus serotype 5-vectored foot-and-mouth disease subunit vaccines: the first decade. Future Virology. **5:**51- 64. doi: 10.2217/fvl.09.68.

41. **Wertz, G. W., V. P. Perepelitsa, and L. A. Ball.** 1998. Gene rearrangement attenuates expression and lethality of a nonsegmented negative strand RNA virus. Proc. Natl. Acad. Sci. U. S. A. **95:**3501-3506.

42. **Lyles, D., and C. Rupprecht.** 2007. Rhabdoviridae, principles of virology, p. 26, 1364. *In* Howley, D. Griffin Knipe P. (ed.), Fields' virology., 5th ed., vol. I. Lippincott Williamms & Wilkins, PA, USA.

43. **Stillman, E. A., J. K. Rose, and M. A. Whitt.** 1995. Replication and amplification of novel vesicular stomatitis virus minigenomes encoding viral structural proteins. J. Virol. **69:**2946-2953.

44. **Letchworth, G. J., L. L. Rodriguez, and J. Del cbarrera.** 1999. Vesicular stomatitis. Vet. J. **157:**239-260. doi: 10.1053/tvjl.1998.0303.

45. **Murphy, A. M., D. M. Besmer, M. Moerdyk-Schauwecker, N. Moestl, D. A. Ornelles, P. Mukherjee, and V. Z. Grdzelishvili.** 2012. Vesicular stomatitis virus as an oncolytic agent against pancreatic ductal adenocarcinoma. J. Virol. **86:**3073-3087. doi: 10.1128/JVI.05640-11.

46. **Reis, J. L., D. G. Mead, L. L. Rodriguez, and C. C. Brown.** 2009. Transmission and pathogenesis of vesicular stomatitis viruses. Braz J Vet Pathol. **2:**49-59.

47. **Patterson, W. C., L. O. Mott, and E. W. Jenney.** 1958. A study of vesicular stomatitis in man. J. Am. Vet. Med. Assoc. **133:**57-62.

48. **Stallknecht, D. E., D. E. Perzak, L. D. Bauer, M. D. Murphy, and E. W. Howerth.** 2001. Contact transmission of vesicular stomatitis virus New Jersey in pigs. Am. J. Vet. Res. **62:**516-520.

49. **Sudia, W. D., B. N. Fields, and C. H. Calisher.** 1967. The isolation of vesiculay stomatitis virus (Indiana strain) and other viruses from mosquitoes in New Mexico, 1965. Am. J. Epidemiol. **86:**598-602.

50. **Martinez, I., L. L. Rodriguez, C. Jimenez, S. J. Pauszek, and G. W. Wertz.** 2003. Vesicular stomatitis virus glycoprotein is a determinant of pathogenesis in swine, a natural hos.t J. Virol. **77:**8039-8047.

51. **Rodriguez, L. L.** 2002. Emergence and re-emergence of vesicular stomatitis in the United States. Virus Res. **85:**211-219.

52. **McCluskey, B.** 2007. Vesicular stomatitis , p. 219-225. *In* D. Sellon and M. T. Long (eds.), Equine infectious diseases. Saunders, MO, USA.

53. **Reis, J. L., L. L. Rodriguez, D. G. Mead, G. Smoliga, and C. C. Brown.** 2011. Lesion development and replication kinetics during early infection in cattle inoculated with vesicular stomatitis New Jersey virus via scarification and black fly (*Simulium vittatum*) bite. Vet Pathol. **48:**547-557. doi: 10.1177/0300985810381247.

54. **Howerth, E. W., D. E. Stallknecht, M. Dorminy, T. Pisell, and G. R. Clarke.** 1997. Experimental vesicular stomatitis in swine: effects of route of inoculation and steroid treatment. J. Vet. Diagn. Invest. **9:**136-142.

55. **Redelman, D., S. Nichol, R. Klieforth, M. Van Der Maaten, and C. Whetstone.** 1989. Experimental vesicular stomatitis virus infection of swine: extent of infection and immunological response. Vet. Immunol. Immunopathol. **20:**345-361.

56. **Abraham, G., and A. K. Banerjee.** 1976. Sequential transcription of the genes of vesicular stomatitis virus. Proc. Natl. Acad. Sci. U. S. A. **73:**1504-1508.

57. **Flanagan, E. B., J. M. Zamparo, L. A. Ball, L. L. Rodriguez, and G. W. Wertz.** 2001. Rearrangement of the genes of vesicular stomatitis virus eliminates clinical disease in the natural host: new strategy for vaccine development. J. Virol. **75:**6107-6114. doi: 10.1128/JVI.75.13.6107-6114.2001.

58. **Whelan, S. P., and G. W. Wertz.** 2002. Transcription and replication initiate at separate sites on the vesicular stomatitis virus genome. Proc. Natl. Acad. Sci. U. S. A. **99:**9178-9183. doi: 10.1073/pnas.152155599.

59. **Clarke, D. K., F. Nasar, M. Lee, J. E. Johnson, K. Wright, P. Calderon, M. Guo, R. Natuk, D. Cooper, R. M. Hendry, and S. A. Udem.** 2007. Synergistic

attenuation of vesicular stomatitis virus by combination of specific G gene truncations and N gene translocations. J. Virol. **81:**2056-2064. doi: 10.1128/JVI.01911-06.

60. **Rubio, C., C. Kolakofsky, V. M. Hill, and D. F. Summers.** 1980. Replication and assembly of VSV nucleocapsids: protein association with RNPs and the effects of cycloheximide on replication. Virology. **105:**123-135.

61. **Hinzman, E. E., J. N. Barr, and G. W. Wertz.** 2002. Identification of an upstream sequence element required for vesicular stomatitis virus mRNA transcription. J. Virol. **76:**7632-7641.

62. **Rodriguez, L. L., S. J. Pauszek, T. A. Bunch, and K. R. Schumann.** 2002. Full-length genome analysis of natural isolates of vesicular stomatitis virus (Indiana 1 serotype) from North, Central and South America. J. Gen. Virol. **83:**2475-2483.

63. **Li, T., and A. K. Pattnaik.** 1999. Overlapping signals for transcription and replication at the 3' terminus of the vesicular stomatitis virus genome. J. Virol. **73:**444-452.

64. **Bitko, V., and S. Barik.** 2001. Phenotypic silencing of cytoplasmic genes using sequence-specific double-stranded short interfering RNA and its application in the reverse genetics of wild type negative-strand RNA viruses. BMC Microbiol. **1:**34.

65. **Rajani, K. R., E. L. Pettit Kneller, M. O. McKenzie, D. A. Horita, J. W. Chou, and D. S. Lyles.** 2012. Complexes of vesicular stomatitis virus matrix protein with host Rae1 and Nup98 involved in inhibition of host transcription PLoS Pathog. **8:**e1002929. doi: 10.1371/journal.ppat.1002929.

66. **Da Poian, A. T., A. M. Gomes, R. J. Oliveira, and J. L. Silva.** 1996. Migration of vesicular stomatitis virus glycoprotein to the nucleus of infected cells. Proc. Natl. Acad. Sci. USA **93:**8268-8273.

67. **Fu, Z. F.** 2005. The world of rhabdoviruses. p 208. Springer, The Netherlands.

68. **Rahmeh, A. A., A. D. Schenk, E. I. Danek, P. J. Kranzusch, B. Liang, T. Walz, and S. P. Whelan.** 2010. Molecular architecture of the vesicular stomatitis virus RNA polymerase. Proc. Natl. Acad. Sci. U. S. A. **107:**20075-20080. doi: 10.1073/pnas.1013559107.

69. **Allende, R., and P. M. Germano.** 1993. Comparison of virus neutralisation and enzyme-linked immunosorbent assay for the identification of antibodies against vesicular stomatitis (Indiana 3) virus. Rev. Sci. Tech. **12:**849-855.

70. **Tesh, R. B., P. H. Peralta, and K. M. Johnson.** 1969. Ecologic studies of vesicular stomatitis virus. I. Prevalence of infection among animals and humans living in an area of endemic VSV activity. Am. J. Epidemiol. **90:**255-261.

71. **Hoffmann, J. A., F. C. Kafatos, C. A. Janeway, and R. A. Ezekowitz.** 1999. Phylogenetic perspectives in innate immunity. Science. **284:**1313-1318.

72. **Kawai, T., and S. Akira.** 2010. The role of pattern-recognition receptors in innate immunity: update on Toll-like receptors. Nat. Immunol. **11:**373-384. doi: 10.1038/ni.1863.

73. **Mogensen, T. H.** 2009. Pathogen recognition and inflammatory signaling in innate immune defenses. Clin. Microbiol. Rev. **22:**240-273. doi: 10.1128/CMR.00046-08.

74. **Barber, G. N.** 2011. Innate immune DNA sensing pathways: STING, AIMII and the regulation of interferon production and inflammatory responses. Curr. Opin. Immunol. **23:**10-20. doi: 10.1016/j.coi.2010.12.015.

75. **Biron, C., and G. C. Sen.** 2001. Interferons and other cytokines, p. 321–351. *In* D. Knipe, P. Howley, D. Griffin, R. Lamb, M. Martin, and S. Straus (eds.), Fields' Virology, 4th ed., vol. I. Lippincott Williamms & Wilkins, PA, USA.

76. **Sotolongo, J., J. Ruiz, and M. Fukata.** 2012. The role of innate immunity in the host defense against intestinal bacterial pathogens. Curr. Infect. Dis. Rep. **14:**15-23. doi: 10.1007/s11908-011-0234-4.

77. **Janeway, C. A. J., P. Travers, and M. Walport.** 2001. The complement system and innate immunity *In* C. A. Janeway (ed.), Immunobiology: The immune system in health and disease, 5th ed., Garland Science, NY, USA.

78. **Michallet, M. C., G. Rota, K. Maslowski , and G. Guarda.** 2013. Innate receptors for adaptive immunity. Curr Opin Microbiol. **16:**296-302. doi: 10.1016/j.mib.2013.04.003.

79. **Thompson, A. J., and S. A. Locarnini.** 2007. Toll-like receptors, RIG-I-like RNA helicases and the antiviral innate immune response. Immunol. Cell Biol. **85:**435-445. doi: 10.1038/sj.icb.7100100.

80. **Yoneyama, M., and T. Fujita.** 2008. Structural mechanism of RNA recognition by the RIG-I-like receptors. Immunity. **29:**178-181. doi: 10.1016/j.immuni.2008.07.009.

81. **Whitehead, K. A., J. E. Dahlman, R. S. Langer, and D. G. Anderson.** 2011. Silencing or stimulation? siRNA delivery and the immune system. Annu. Rev. Chem. Biomol. Eng. **2:**77-96. doi: 10.1146/annurev-chembioeng-061010-114133.

82. **Menzies, M., and A. Ingham.** 2006. Identification and expression of Toll-like receptors 1-10 in selected bovine and ovine tissues. Vet. Immunol. Immunopathol. **109:**23-30. doi: S0165-2427(05)00226-6 [pii].

83. **Meyer-Bahlburg, A., and D. J. Rawlings.** 2012. Differential impact of Toll-like receptor signaling on distinct B cell subpopulations. Front. Biosci. **17:**1499-1516.

84. **Akira, S., and K. Takeda.** 2004. Toll-like receptor signaling. Nat. Rev. Immunol. **4:**499-511. doi: 10.1038/nri1391.

85. **Lee, C. C., A. M. Avalos, and H. L. Ploegh.** 2012. Accessory molecules for Toll-like receptors and their function. Nat. Rev. Immunol. **12:**168-179. doi: 10.1038/nri3151.

86. **Honda, K., A. Takaoka, and T. Taniguchi.** 2006. Type I interferon gene induction by the interferon regulatory factor family of transcription factors. Immunity. **25:**349-360. doi: 10.1016/j.immuni.2006.08.009.

87. **Tailor, P., T. Tamura, and K. Ozato.** 2006. IRF family proteins and type I interferon induction in dendritic cells. Cell Res. **16:**134-140. doi: 7310018 [pii].

88. **Dixit, E., and J. C. Kagan.** 2013. Intracellular pathogen detection by RIG-I-like receptors. Adv. Immunol. **117:**99-125. doi: 10.1016/B978-0-12-410524-9.00004-9.

89. **Inohara, N., and G. Nunez.** 2003. NODs: intracellular proteins involved in inflammation and apoptosis. Nat. Rev. Immunol. **3:**371-382. doi: 10.1038/nri1086.

90. **Rubino, S. J., T. Selvanantham, S. E. Girardin, and D. J. Philpott.** 2012. Nod-like receptors in the control of intestinal inflammation. Curr. Opin. Immunol. **24:**398-404. doi: 10.1016/j.coi.2012.04.010.

91. **Staehli, F., K. Ludigs, L. X. Heinz, Q. Seguin-Estevez, I. Ferrero, M. Braun, K. Schroder, M. Rebsamen, A. Tardivel, C. Mattmann, H. R. MacDonald, P. Romero, W. Reith, G. Guarda, and J. Tschopp.** 2012. NLRC5 deficiency selectively impairs MHC class I- dependent lymphocyte killing by cytotoxic T cells. J. Immunol. **188:**3820-3828. doi: 10.4049/jimmunol.1102671.

92. **Kanneganti, T. D.** 2010. Central roles of NLRs and inflammasomes in viral infection. Nat. Rev. Immunol. **10:**688-698. doi: 10.1038/nri2851.

93. **Martinon, F., K. Burns, and J. Tschopp.** 2002. The inflammasome: a molecular platform triggering activation of inflammatory caspases and processing of proIL-beta. Mol. Cell. **10:**417-426.

94. **Samuel, C. E.** 2001. Antiviral actions of interferons. Clin. Microbiol. Rev. **14:**778-809. doi: 10.1128/CMR.14.4.778-809.2001.

95. **Sin, W. X., P. Li, J. P. Yeong, and K. C. Chin.** 2012. Activation and regulation of interferon-beta in immune responses. Immunol. Res. **53**:25-40. doi: 10.1007/s12026-012-8293-7.

96. **Diaz-San Segundo, F., M. P. Moraes, T. de Los Santos, C. C. Dias, and M. J. Grubman.** 2010. Interferon-induced protection against foot-and-mouth disease virus infection correlates with enhanced tissue-specific innate immune cell infiltration and interferon-stimulated gene expression. J. Virol. **84:**2063-2077. doi: 10.1128/JVI.01874-09.

97. **Sen, G. C., and S. N. Sarkar.** 2007. The interferon-stimulated genes: targets of direct signaling by interferons, double-stranded RNA, and viruses. Curr. Top. Microbiol. Immunol. **316:**233-250.

98. **Platanias, L. C.** 2005. Mechanisms of type-I- and type-II-interferon-mediated signaling. Nat. Rev. Immunol. **5:**375-386. doi: 10.1038/nri1604.

99. **Fabri, M., S. Stenger, D. M. Shin, J. M. Yuk, P. T. Liu, S. Realegeno, H. M. Lee, S. R. Krutzik, M. Schenk, P. A. Sieling, R. Teles, D. Montoya, S. S. Iyer, H. Bruns, D. M. Lewinsohn, B. W. Hollis, M. Hewison, J. S. Adams, A. Steinmeyer, U. Zugel, G. Cheng, E. K. Jo, B. R. Bloom, and R. L. Modlin.** 2011. Vitamin D is required for IFN-gamma-mediated antimicrobial activity of human macrophages. Sci. Transl. Med. **3:**102-104. doi: 10.1126/scitranslmed.3003045.

100. **Kotenko, S. V., G. Gallagher, V. V. Baurin, A. Lewis-Antes, M. Shen, N. K. Shah, J. A. Langer, F. Sheikh, H. Dickensheets, and R. P. Donnelly.** 2003. IFN-lambdas mediate antiviral protection through a distinct class II cytokine receptor complex. Nat Immunol. **4(1):**69-77.

101. **Sang, Y., R. R. Rowland, and F. Blecha.** 2010. Molecular characterization and antiviral analyses of porcine type III interferons. J. Interferon Cytokine Res. **30:**801-807. doi: 10.1089/jir.2010.0016.

102. **Diaz-San Segundo, F., M. Weiss, E. Perez-Martin, M. J. Koster, J. Zhu, M. J. Grubman, and T. de los Santos.** 2011. Antiviral activity of bovine type III interferon against foot-and-mouth disease virus. Virology. **413:**283-292. doi: 10.1016/j.virol.2011.02.023.

103. **Perez-Martin, E., M. Weiss, F. Diaz-San Segundo, J. M. Pacheco, J. Arzt, M. J. Grubman, and T. de los Santos.** 2012. Bovine type III interferon significantly delays and reduces the severity of foot-and-mouth disease in cattle. J. Virol. **86:**4477-4487. doi: 10.1128/JVI.06683-11.

104. **Schoggins, J. W., S. J. Wilson, M. Panis, M. Y. Murphy, C. T. Jones, P. Bieniasz, and C. M. Rice.** 2011. A diverse range of gene products are effectors of the type I interferon antiviral response. Nature. **472:**481-485. doi: 10.1038/nature09907.

105. **David, M.** 2010. Interferons and microRNAs. J. Interferon Cytokine Res. **30:**825-828. doi: 10.1089/jir.2010.0080.

106. **Yan, N., and Z. J. Chen.** 2012. Intrinsic antiviral immunity. Nat. Immunol. **13:**214-222. doi: 10.1038/ni.2229.

107. **Pavlovic, J., O. Haller, and P. Staeheli.** 1992. Human and mouse Mx proteins inhibit different steps of the influenza virus multiplication cycle. J. Virol. **66:**2564-2569.

108. **Li, X. L., J. A. Blackford, and B. A. Hassel.** 1998. RNase L mediates the antiviral effect of interferon through a selective reduction in viral RNA during encephalomyocarditis virus infection. J. Virol. **72:**2752-2759.

109. **Stawowczyk, M., S. Van Scoy, K. P. Kumar, and N. C. Reich.** 2011. The interferon stimulated gene 54 promotes apoptosis. J. Biol. Chem. **286:**7257-7266. doi: 10.1074/jbc.M110.207068.

110. **Espert, L., G. Degols, C. Gongora, D. Blondel, B. R. Williams, R. H. Silverman, and N. Mechti.** 2003. ISG20, a new interferon-induced RNase specific for single-stranded RNA, defines an alternative antiviral pathway against RNA genomic viruses. J. Biol. Chem. **278:**16151-16158. doi: 10.1074/jbc.M209628200.

111. **Wang, X., E. R. Hinson, and P. Cresswell.** 2007. The interferon-inducible protein viperin inhibits influenza virus release by perturbing lipid rafts. Cell. Host Microbe. **2:**96-105. doi: 10.1016/j.chom.2007.06.009.

112. **Bego, M. G., J. Mercier, and E. A. Cohen.** 2012. Virus-activated interferon regulatory factor 7 upregulates expression of the interferon-regulated BST2 gene independently of interferon signaling. J. Virol. **86:**3513-3527. doi: 10.1128/JVI.06971-11.

113. **Nathan, C.** 1997. Inducible nitric oxide synthase: what difference does it make?. J. Clin. Invest. **100:**2417-2423. doi: 10.1172/JCI119782.

114. **Lenschow, D. J.** 2010. Antiviral properties of ISG15. Viruses. **2:**2154-2168. doi: 10.3390/v2102154.

115. **Haller, O., G. Kochs, and F. Weber.** 2006. The interferon response circuit: induction and suppression by pathogenic viruses. Virology. **344:**119-130. doi: 10.1016/j.virol.2005.09.024.

116. **Lin, R., P. Genin, Y. Mamane, and J. Hiscott.** 2000. Selective DNA binding and association with the CREB binding protein coactivator contribute to differential activation of alpha/beta interferon genes by interferon regulatory factors 3 and 7. Mol. Cell. Biol. **20:**6342-6353.

117. **Ivashkiv, L.,B, and L. T. Donlin.** 2014. Regulation of type I interferon responses. Nat Rev Immunol. **14:**36-49. doi: 10.1038/nri3581.

118. **Nfon, C. K., G. S. Ferman, F. N. Toka, D. A. Gregg, and W. T. Golde.** 2008. Interferon-alpha production by swine dendritic cells is inhibited during acute infection with foot-and-mouth disease virus. Viral Immunol. **21:**68-77. doi: 10.1089/vim.2007.0097.

119. **de Los Santos, T., S. de Avila Botton, R. Weiblen, and M. J. Grubman.** 2006. The leader proteinase of foot-and-mouth disease virus inhibits the induction of beta interferon mRNA and blocks the host innate immune response. J. Virol. **80:**1906-1914. doi: 10.1128/JVI.80.4.1906-1914.2006.

120. **Wang, D., L. Fang, J. Bi, Q. Chen, L. Cao, R. Luo, H. Chen, and S. Xiao.** 2011. Foot-and-mouth disease virus leader proteinase inhibits dsRNA-induced RANTES transcription in PK-15 cells. Virus Genes. **42:**388-393. doi: 10.1007/s11262-011-0590-z.

121. **Wang, D., L. Fang, R. Luo, R. Ye, Y. Fang, L. Xie, H. Chen, and S. Xiao.** 2010. Foot-and-mouth disease virus leader proteinase inhibits dsRNA-induced type I interferon transcription by decreasing interferon regulatory factor 3/7 in protein levels. Biochem. Biophys. Res. Commun. **399:**72-78. doi: 10.1016/j.bbrc.2010.07.044.

122. **Wang, D., L. Fang, P. Li, L. Sun, J. Fan, Q. Zhang, R. Luo, X. Liu, K. Li, H. Chen, Z. Chen, and S. Xiao.** 2011. The leader proteinase of foot-and-mouth disease virus negatively regulates the type I interferon pathway by acting as a viral deubiquitinase. J. Virol. **85:**3758-3766. doi: 10.1128/JVI.02589-10.

123. **Wang, D., L. Fang, K. Li, H. Zhong, J. Fan, C. Ouyang, H. Zhang, E. Duan, R. Luo, Z. Zhang, X. Liu, H. Chen, and S. Xiao.** 2012. Foot-and-mouth disease virus 3C protease cleaves NEMO to impair innate immune signaling. J. Virol. **86:**9311-9322. doi: 10.1128/JVI.00722-12.

124. **Du, Y., J. Bi, J. Liu, X. Liu, X. Wu, P. Jiang, D. Yoo, Y. Zhang, J. Wu, R. Wan, X. Zhao, L. Guo, W. Sun, X. Cong, L. Chen, and J. Wang.** 2014. 3Cpro of FMDV antagonizes IFN signaling pathway by blocking STAT1/STAT2 nuclear translocation. J. Virol. . doi: 10.1128/JVI.03668-13.

125. **Chinsangaram, J., M. E. Piccone, and M. J. Grubman.** 1999. Ability of foot-and-mouth disease virus to form plaques in cell culture is associated with suppression of alpha/beta interferon. J. Virol. **73:**9891-9898.

126. **Chinsangaram, J., M. Koster, and M. J. Grubman.** 2001. Inhibition of L-deleted foot-and-mouth disease virus replication by alpha/beta interferon involves

double-stranded RNA-dependent protein kinase. J. Virol. **75:**5498-5503. doi: 10.1128/JVI.75.12.5498-5503.2001.

127. **Zhu, J., M. Weiss, M. J. Grubman, and T. de los Santos.** 2010. Differential gene expression in bovine cells infected with wild type and leaderless foot-and-mouth disease virus. Virology. **404:**32-40. doi: 10.1016/j.virol.2010.04.021.

128. **Wu, Q., M. C. Brum, L. Caron, M. Koster, and M. J. Grubman.** 2003. Adenovirus-mediated type I interferon expression delays and reduces disease signs in cattle challenged with foot-and-mouth disease virus. J. Interferon Cytokine Res. **23:**359-368. doi: 10.1089/107999003322226014.

129. **Chinsangaram, J., M. P. Moraes, M. Koster, and M. J. Grubman.** 2003. Novel viral disease control strategy: adenovirus expressing alpha interferon rapidly protects swine from foot-and-mouth disease. J. Virol. **77:**1621-1625.

130. **Dias, C. C., M. P. Moraes, F. D. Segundo, T. de los Santos, and M. J. Grubman.** 2011. Porcine type I interferon rapidly protects swine against challenge with multiple serotypes of foot-and-mouth disease virus. J. Interferon Cytokine Res. **31:**227-236. doi: 10.1089/jir.2010.0055.

131. **Masters, P. S., and C. E. Samuel.** 1983. Mechanism of interferon action: inhibition of vesicular stomatitis virus replication in human amnion U cells by cloned human leukocyte interferon. I. Effect on early and late stages of the viral multiplication cycle. J. Biol. Chem. **258:**12019-12025.

132. **Masters, P. S., and C. E. Samuel.** 1983. Mechanism of interferon action: inhibition of vesicular stomatitis virus replication in human amnion U cells by cloned

human leukocyte interferon. II. Effect on viral macromolecular synthesis. J. Biol. Chem. **258:**12026-12033.

133. **Masters, P. S., and C. E. Samuel.** 1984. Mechanism of interferon action. Inhibition of vesicular stomatitis virus in human amnion U cells by cloned human leukocyte interferon. Biochem. Biophys. Res. Commun. **119:**326-334.

134. **Gresser, I., M. G. Tovey, and C. Bourali-Maury.** 1975. Efficacy of exogenous interferon treatment initiated after onset of multiplication of vesicular stomatitis virus in the brains of mice. J. Gen. Virol. **27:**395-398.

135. **Gresser, I., M. G. Tovey, C. Maury, and M. T. Bandu.** 1976. Role of interferon in the pathogenesis of virus diseases in mice as demonstrated by the use of anti-interferon serum. II. Studies with herpes simplex, Moloney sarcoma, vesicular stomatitis, Newcastle disease, and influenza viruses. J. Exp. Med. **144:**1316-1323.

136. **Steinhoff, U., U. Muller, A. Schertler, H. Hengartner, M. Aguet, and R. M. Zinkernagel.** 1995. Antiviral protection by vesicular stomatitis virus-specific antibodies in alpha/beta interferon receptor-deficient mice. J. Virol. **69:**2153-2158.

137. **Trinchieri, G.** 2010. Type I interferon: friend or foe?. J. Exp. Med. **207:**2053-2063. doi: 10.1084/jem.20101664.

138. **Honda, K., H. Yanai, H. Negishi, M. Asagiri, M. Sato, T. Mizutani, N. Shimada, Y. Ohba, A. Takaoka, N. Yoshida, and T. Taniguchi.** 2005. IRF-7 is the master regulator of type-I interferon-dependent immune responses. Nature. **434:**772-777. doi: 10.1038/nature03464.

139. **Sato, M., H. Suemori, N. Hata, M. Asagiri, K. Ogasawara, K. Nakao, T. Nakaya, M. Katsuki, S. Noguchi, N. Tanaka, and T. Taniguchi.** 2000. Distinct and essential roles of transcription factors IRF-3 and IRF-7 in response to viruses for IFN-alpha/beta gene induction. Immunity. **13:**539-548.

140. **Sato, M., N. Hata, M. Asagiri, T. Nakaya, T. Taniguchi, and N. Tanaka.** 1998. Positive feedback regulation of type I IFN genes by the IFN-inducible transcription factor IRF-7. FEBS Lett. **441:**106–110.

141. **Liang, Q., H. Deng, C. W. Sun, T. M. Townes, and F. Zhu.** 2011. Negative regulation of IRF7 activation by activating transcription factor 4 suggests a cross-regulation between the IFN responses and the cellular integrated stress responses. J Immunol. **186:**1001-1010. doi: 10.4049/jimmunol.1002240.

142. **Thiel, V., E. Y. Chiang, R. J. Johnston, and J. L. Grogan.** 2013. EBI2 Is a negative regulator of type I interferons in plasmacytoid and myeloid dendritic cells. Plos One. **8:**e83457. doi: 10.1371/journal.pone.0083457.

143. **Ning, S., J. S. Pagano, and G. N. Barber.** 2011. IRF7: activation, regulation, modification and function. Genes Immun. **12:**399-414. doi: 10.1038/gene.2011.21.

144. **Colina, R., M. Costa-Mattioli, R. J. Dowling, M. Jaramillo, L. H. Tai, C. J. Breitbach, Y. Martineau, O. Larsson, L. Rong, Y. V. Svitkin, A. P. Makrigiannis, J. C. Bell, and N. Sonenberg.** 2008. Translational control of the innate immune response through IRF-7. Nature. **452:**323-328. doi: 10.1038/nature06730.

145. **Lee, M. S., B. Kim, G. T. Oh, and Y. J. Kim.** 2013. OASL1 inhibits translation of the type I interferon–regulating transcription factor IRF7. Nat. Immunol. **14:**346-355. doi: 10.1038/ni.2535.

146. **Pause, A., G. J. Belsham, A. C. Gingras, O. Donze, T. A. Lin, J. C. Lawrence Jr, and N. Sonenberg.** 1994. Insulin-dependent stimulation of protein synthesis by phosphorylation of a regulator of 5'-cap function. Nature. **371:**762-767. doi: 10.1038/371762a0.

147. **Poulin, F., A. C. Gingras, H. Olsen, S. Chevalier, and N. Sonenberg.** 1998. 4E-BP3, a new member of the eukaryotic initiation factor 4E-binding protein family. J. Biol. Chem. **273:**14002-14007.

148. **Teleman, A. A., Y. W. Chen, and S. M. Cohen.** 2005. 4E-BP functions as a metabolic brake used under stress conditions but not during normal growth. Genes Dev. **19:**1844-1848. doi: 10.1101/gad.341505.

149. **Rong, L., M. Livingstone, R. Sukarieh, E. Petroulakis, A. C. Gingras, K. Crosby, B. Smith, R. D. Polakiewicz, J. Pelletier, M. A. Ferraiuolo, and N. Sonenberg.** 2008. Control of eIF4E cellular localization by eIF4E-binding proteins, 4E-BPs. Rna. **14:**1318-1327. doi: 10.1261/rna.950608.

150. **Kaur, S., L. Lal, A. Sassano, B. Majchrzak-Kita, M. Srikanth, D. P. Baker, E. Petroulakis, N. Hay, N. Sonenberg, E. N. Fish, and L. C. Platanias.** 2007. Regulatory effects of mammalian target of rapamycin-activated pathways in type I and II interferon signaling. J. Biol. Chem. **282:**1757-1768. doi: 10.1074/jbc.M607365200.

151. **Kaur, S., A. Sassano, A. M. Joseph, B. Majchrzak-Kita, E. A. Eklund, A. Verma, S. M. Brachmann, E. N. Fish, and L. C. Platanias.** 2008. Dual regulatory roles of phosphatidylinositol 3-kinase in IFN signaling. J. Immunol. **181:**7316-7323.

152. **Carrera, A. C.** 2004. TOR signaling in mammals. J. Cell. Sci. **117:**4615-4616. doi: 10.1242/jcs.01311.

153. **Kim, D. H., D. D. Sarbassov, S. M. Ali, J. E. King, R. R. Latek, H. Erdjument-Bromage, P. Tempst, and D. M. Sabatini.** 2002. mTOR interacts with raptor to form a nutrient-sensitive complex that signals to the cell growth machinery. Cell. **110:**163-175.

154. **Sarbassov, D. D., S. M. Ali, D. H. Kim, D. A. Guertin, R. R. Latek, H. Erdjument-Bromage, P. Tempst, and D. M. Sabatini.** 2004. Rictor, a novel binding partner of mTOR, defines a rapamycin-insensitive and raptor-independent pathway that regulates the cytoskeleton. Curr. Biol. **14:**1296-1302. doi: 10.1016/j.cub.2004.06.054.

155. **Gingras, A. C., B. Raught, and N. Sonenberg.** 2004. mTOR signaling to translation Curr. Top. Microbiol. Immunol. **279:**169-197.

156. **Rousseau, D., A. C. Gingras, A. Pause, and N. Sonenberg.** 1996. The eIF4E-binding proteins 1 and 2 are negative regulators of cell growth. Oncogene. **13:**2415-2420.

157. **Burke, J. D., N. Sonenberg, L. C. Platanias, and E. N. Fish.** 2011. Antiviral effects of interferon-beta are enhanced in the absence of the translational suppressor 4E-BP1 in myocarditis induced by Coxsackievirus B3. Antivir Ther. **16:**577-584. doi: 10.3851/IMP1752.

158. **Erickson, A. K., and M. Gale.** 2008. Regulation of interferon production and innate antiviral immunity through translational control of IRF-7. Cell Res. **18:**433-435. doi: 10.1038/cr.2008.46.

159. **Horvath, P., and R. Barrangou.** 2010. CRISPR/Cas, the Immune System of Bacteria and Archaea. Science. **327:**167-170. doi: 10.1126/science.1179555.

160. **Deltcheva, E., K. Chylinski, C. M. Sharma, K. Gonzales, Y. Chao, Z. A. Pirzada, M. R. Eckert, J. Vogel, and E. Charpentier.** 2011. CRISPR RNA maturation by trans-encoded small RNA and host factor RNase III. Nature. **471:**602- 607. doi: 10.1038/nature09886.

161. **Makarova, K. S., D. H. Haft, R. Barrangou, S. J. J. Brouns, E. Charpentier, P. Horvath, S. Moineau, F. J. M. Mojica, Y. I. Wolf, A. F. Yakunin, J. van der Oost, and E. V. Koonin.** 2011. Evolution and classification of the CRISPR–Cas systems. Nature Reviews Microbiology. **9:**467-477. doi: 10.1038/nrmicro2577.

162. **Haft, D. H., J. Selengut, E. F. Mongodin, and K. E. Nelson.** 2005. A guild of 45 CRISPR-associated (Cas) protein families and multiple CRISPR/Cas subtypes exist in prokaryotic genomes. PLoS Comput. Biol. **1:**e60. doi: 10.1371/journal.pcbi.0010060.

163. **Barrangou, R., C. Fremaux, H. Deveau, M. Richards, P. Boyaval, S. Moineau, D. A. Romero, and P. Horvath.** 2007. CRISPR provides acquired resistance against viruses in prokaryotes. Science. **315:**1709-1712. doi: 10.1126/science.1138140.

164. **Bikard, D., and L. A. Marraffini.** 2013. Control of gene expression by CRISPR-Cas systems. F1000Prime Rep. **5:**47. eCollection 2013. doi: 10.12703/P5-47; 10.12703/P5-47.

165. **Jinek, M., K. Chylinski, I. Fonfara, M. Hauer, J. A. Doudna, and E. Charpentier.** 2012. A programmable dual-RNA-guided DNA endonuclease in adaptive bacterial immunity. Science. **337:**816-821. doi: 10.1126/science.1225829.

166. **Cong, L., F. A. Ran, D. Cox, S. Lin, R. Barretto, N. Habib, P. D. Hsu, X. Wu, W. Jiang, L. A. Marraffini, and F. Zhang.** 2013. Multiplex genome engineering using CRISPR/Cas systems. Science. **339:**819-823. doi: 10.1126/science.1231143.

167. **Hwang, W. Y., Y. Fu, D. Reyon, M. L. Maeder, S. Q. Tsai, J. D. Sander, R. T. Peterson, J. J. Yeh, and J. K. Joung.** 2013. Efficient genome editing in zebrafish using a CRISPR-Cas system. Nat. Biotechnol. **31:**227 - 229. doi: 10.1038/nbt.2501.

168. **Thompson, J. D., D. G. Higgins, and T. J. Gibson.** 1994. CLUSTAL W: improving the sensitivity of progressive multiple sequence alignment through sequence weighting, position-specific gap penalties and weight matrix choice. Nucleic Acids Res. **22:**4673-4680.

169. **Gruber, A. R., R. Lorenz, S. H. Bernhart, R. Neubock, and I. L. Hofacker.** 2008. The Vienna RNA websuite. Nucleic Acids Res. **36:**70-74. doi: 10.1093/nar/gkn188.

170. **Freshney, R.** 1987. Culture of animal cells: a manual of basic technique, p. 117. Wiley-Liss, NY, USA.

171. **Condit, R. C.** 2007. Principles of Virology, p. 2108. *In* Howley, D. Griffin Knipe P. (ed.), Fields' Virology, 5th ed., vol. I. Lippincott Williamms & Wilkins, PA, USA.

172. **Rieder, E., T. Bunch, F. Brown, and P. W. Mason.** 1993. Genetically engineered foot-and-mouth disease viruses with poly(C) tracts of two nucleotides are virulent in mice. J. Virol. **67:**5139-5145.

173. **Grubman, M. J., B. Baxt, and H. L. Bachrach.** 1979. Foot-and-mouth disease virion RNA: studies on the relation between the length of its 3'-poly(A) segment and infectivity Virology. **97:**22-31.

174. **Beretta, L., A. C. Gingras, Y. V. Svitkin, M. N. Hall, and N. Sonenberg.** 1996. Rapamycin blocks the phosphorylation of 4E-BP1 and inhibits cap-dependent initiation of translation. Embo j. **15:**658-664.

175. **Bustin, S. A., V. Benes, J. A. Garson, J. Hellemans, J. Huggett, M. Kubista, R. Mueller, T. Nolan, M. W. Pfaffl, G. L. Shipley, J. Vandesompele, and C. T. Wittwer.** 2009. The MIQE guidelines: minimum information for publication of quantitative real-time PCR experiments. Clin. Chem. **55:**611-622. doi: 10.1373/clinchem.2008.112797.

176. **Livak, K. J., and T. D. Schmittgen.** 2001. Analysis of relative gene expression data using real-time quantitative PCR and the 2(-Delta Delta C(T)) method. Methods. **25:**402-408. doi: 10.1006/meth.2001.1262.

177. **Chen, C. C., J. C. Lee, and M. C. Chang.** 2012. 4E-BP3 regulates eIF4E-mediated nuclear mRNA export and interacts with replication protein A2. FEBS Lett. **586:**2260-2266. doi: 10.1016/j.febslet.2012.05.059.

178. **Kleijn, M., G. C. Scheper, M. L. Wilson, A. R. Tee, and C. G. Proud.** 2002. Localisation and regulation of the eIF4E-binding protein 4E-BP3. FEBS Lett. **532:**319-323.

179. **Gingras, A. C., B. Raught, S. P. Gygi, A. Niedzwiecka, M. Miron, S. K. Burley, R. D. Polakiewicz, A. Wyslouch-Cieszynska, R. Aebersold, and N. Sonenberg.** 2001. Hierarchical phosphorylation of the translation inhibitor 4E-BP1. Genes Dev. **15:**2852-2864. doi: 10.1101/gad.912401.

180. **van der Velden, A. W., and A. A. Thomas.** 1999. The role of the 5' untranslated region of an mRNA in translation regulation during development. Int. J. Biochem. Cell Biol. **31:**87-106. doi: S1357-2725(98)00134-4 [pii].

181. **Choo, A. Y., S. O. Yoon, S. G. Kim, P. P. Roux, and J. Blenis.** 2008. Rapamycin differentially inhibits S6Ks and 4E-BP1 to mediate cell-type-specific repression of mRNA translation. Proc. Natl. Acad. Sci. U. S. A. **105:**17414-17419. doi: 10.1073/pnas.0809136105.

182. **Nawroth, R., F. Stellwagen, W. A. Schulz, R. Stoehr, A. Hartmann, B. J. Krause, J. E. Gschwend, and M. Retz.** 2011. S6K1 and 4E-BP1 are independent regulated and control cellular growth in bladder cancer. PLoS One. **6:**e27509. doi: 10.1371/journal.pone.0027509.

183. **Roberts, W. K., A. Hovanessian, R. E. Brown, M. J. Clemens, and I. M. Kerr.** 1976. Interferon-mediated protein kinase and low-molecular-weight inhibitor of protein synthesis. Nature. **264:**477-480.

184. **Justesen, J., R. Hartmann, and N. O. Kjeldgaard.** 2000. Gene structure and function of the 2'-5'-oligoadenylate synthetase family. Cell Mol. Life Sci. **57:**1593-1612.

185. **Kakuta, S., S. Shibata, and Y. Iwakura.** 2002. Genomic structure of the mouse 2',5'-oligoadenylate synthetase gene family. J. Interferon Cytokine Res. **22:**981-993. doi: 10.1089/10799900260286696.

186. **Eskildsen, S., J. Justesen, M. H. Schierup, and R. Hartmann.** 2003. Characterization of the 2'-5'-oligoadenylate synthetase ubiquitin-like family. Nucleic Acids Res. **31:**3166-3173.

187. **Hartmann, R., J. Justesen, S. N. Sarkar, G. C. Sen, and V. C. Yee.** 2003. Crystal structure of the 2'-specific and double-dtranded RNA-activated interferon-induced antiviral protein 2'-5'-oligoadenylate synthetase. Mol. Cell. **12:**1173-1185. doi: 10.1016/S1097-2765(03)00433-7.

188. **Kristiansen, H., H. H. Gad, S. Eskildsen-Larsen, P. Despres, and R. Hartmann.** 2011. The oligoadenylate synthetase family: an ancient protein family with multiple antiviral activities. J Interferon Cytokine Res. **31:**41-47.

189. **Ghosh, A., S. N. Sarkar, T. M. Rowe, and G. C. Sen.** 2001. A specific isozyme of 2'-5' oligoadenylate synthetase is a dual function proapoptotic protein of the Bcl-2 family. J. Biol. Chem. **276:**25447-25455. doi: 10.1074/jbc.M100496200.

190. **Perelygin, A. A., A. A. Zharkikh, S. V. Scherbik, and M. A. Brinton.** 2006. The mammalian 2'-5' oligoadenylate synthetase gene family: evidence for concerted evolution of paralogous Oas1 genes in Rodentia and Artiodactyla. J. Mol. Evol. **63:**562-576. doi: 10.1007/s00239-006-0073-3.

191. **Hovnanian, A., D. Rebouillat, M. G. Mattei, E. R. Levy, I. Marie, A. P. Monaco, and A. G. Hovanessian.** 1998. The human 2',5'-oligoadenylate synthetase locus is composed of three distinct genes clustered on chromosome 12q24.2 encoding the 100-, 69-, and 40-kDa forms. Genomics. **52:**267-277. doi: 10.1006/geno.1998.5443.

192. **Marques, J., J. Anwar, S. Eskildsen-Larsen, D. Rebouillat, S. R. Paludan, G. Sen, B. R. G. Williams, and R. Hartmann.** 2008. The p59 oligoadenylate synthetase-like protein possesses antiviral activity that requires the C-terminal ubiquitin-like domain. J. Gen. Virol. **89:**2767-2772. doi: 10.1099/vir.0.2008/003558-0.

193. **Guo, X., X. Li, Y. Xu, T. Sun, G. Yang, Z. Wu, and E. Li.** 2012. Identification of OASL d, a splice variant of human OASL, with antiviral activity. Int. J. Biochem. Cell Biol. **44:**1133 -1138. doi: 10.1016/j.biocel.2012.04.001.

194. **Melchjorsen, J., H. Kristiansen, R. Christiansen, J. Rintahaka, S. Matikainen, S. R. Paludan, and R. Hartmann.** 2009. Differential Regulation of the OASL and OAS1 Genes in Response to Viral Infections.. J. Virol. **29:** 199- 208. doi: 10.1089/jir.2008.0050.

195. **Lee, M. S., C. H. Park, Y. H. Jeong, Y. J. Kim, and S. J. Ha.** 2013. Negative regulation of type I IFN expression by OASL1 permits chronic viral infection

and CD8(+) T-cell exhaustion. PLoS Pathog. **9:**e1003478. doi: 10.1371/journal.ppat.1003478.

196. **Floyd-Smith, G., Q. Wang, and G. C. Sen.** 1999. Transcriptional induction of the p69 isoform of 2',5'-oligoadenylate synthetase by interferon-beta and interferon-gamma involves three regulatory elements and interferon-stimulated gene factor 3 Exp. Cell Res. **246:**138-147. doi: S0014-4827(98)94296-3 [pii].

197. **Edgar, R. C.** 2004. MUSCLE: multiple sequence alignment with high accuracy and high throughput. Nucleic Acids Res. **32:**1792-1797. doi: 10.1093/nar/gkh340.

198. **Tamura, K., G. Stecher, D. Peterson, A. Filipski, and S. Kumar.** 2013. MEGA6: Molecular evolutionary genetics analysis version 6.0. Mol. Biol. Evol. **30:**2725-2729. doi: 10.1093/molbev/mst197.

199. **Baxevanis, A. D., and F. F. Ouellette.** 2005. Bioinformatics: a practical guide to the analysis of genes and proteins.p 215-230. John Wiley & Sons, NY, USA.

200. **Tamura, T., H. Yanai, D. Savitsky, and T. Taniguchi.** 2008. The IRF family transcription factors in immunity and oncogenesis. Annu Rev Immunol. **26:**535-84. doi: 10.1146/annurev.immunol.26.021607.090400.

201. **Tanaka, N., and T. Taniguchi.** 2000. The interferon regulatory factors and oncogenesis. Semin. Cancer Biol. **10:**73-81. doi: 10.1006/scbi.2000.0310.

202. **Lazear, H. M., A. Lancaster, C. Wilkins, M. S. Suthar, A. Huang, S. C. Vick, L. Clepper, L. Thackray, M. M. Brassil, H. W. Virgin, J. Nikolich-Zugich, A. V. Moses, M. Gale Jr, K. Fruh, and M. S. Diamond.** 2013. IRF-3, IRF-5, and IRF-7

coordinately regulate the type I IFN response in myeloid dendritic cells downstream of MAVS Signaling. PLoS Pathog. **9:**e1003118. doi: 10.1371/journal.ppat.1003118.

203. **Matsuyama, T., T. Kimura, M. Kitagawa, K. Pfeffer, T. Kawakami, N. Watanabe, T. M. Kundig, R. Amakawa, K. Kishihara, and A. Wakeham.** 1993. Targeted disruption of IRF-1 or IRF-2 results in abnormal type I IFN gene induction and aberrant lymphocyte development. Cell. **75:**83-97.

204. **De Ioannes, P., C. R. Escalante, and A. K. Aggarwal.** 2011. Structures of apo IRF-3 and IRF-7 DNA binding domains: effect of loop L1 on DNA binding. Nucleic Acids Res. **39:**7300-7307. doi: 10.1093/nar/gkr325.

205. **Au, W. C., P. A. Moore, W. Lowther, Y. T. Juang, and P. M. Pitha.** 1995. Identification of a member of the interferon regulatory factor family that binds to the interferon-stimulated response element and activates expression of interferon-induced genes. Proc. Natl. Acad. Sci. USA. **92:**11657-11661.

206. **Lin, R., C. Heylbroeck, P. M. Pitha, and J. Hiscott.** 1998. Virus-dependent phosphorylation of the IRF-3 transcription factor regulates nuclear translocation, transactivation potential, and proteasome-mediated degradation. Mol. Cell. Biol. **18:**2986-2996.

207. **Lin, R., C. Heylbroeck, P. Genin, P. M. Pitha, and J. Hiscott.** 1999. Essential role of interferon regulatory factor 3 in direct activation of RANTES chemokine transcription. Mol. Cell. Biol. **19:**959-966.

208. **Lin, R., Y. Mamane, and J. Hiscott.** 1999. Structural and functional analysis of interferon regulatory factor 3: localization of the transactivation and autoinhibitory domains. Mol. Cell. Biol. **19:**2465-2474.

209. **Higgs, R., and C. A. Jefferies.** 2008. Targeting IRFs by ubiquitination: regulating antiviral responses. Biochem. Soc. Trans. **36:**453-458. doi: 10.1042/BST0360453.

210. **Kim, H., and B. Seed.** 2010. The transcription factor MafB antagonizes antiviral responses by blocking recruitment of coactivators to the transcription factor IRF3. Nat. Immunol. **11:**743-750. doi: 10.1038/ni.1897.

211. **Chattopadhyay, S., J. T. Marques, M. Yamashita, K. L. Peters, K. Smith, A. Desai, B. R. Williams, and G. C. Sen.** 2010. Viral apoptosis is induced by IRF-3-mediated activation of Bax. Embo j. **29:**1762-1773. doi: 10.1038/emboj.2010.50.

212. **Au, W. C., P. A. Moore, D. W. LaFleur, B. Tombal, and P. M. Pitha.** 1998. Characterization of the interferon regulatory factor-7 and its potential role in the transcription activation of interferon A genes. J. Biol. Chem. **273:**29210-29217.

213. **Lu, R., P. A. Moore, and P. M. Pitha.** 2002. Stimulation of IRF-7 gene expression by tumor necrosis factor alpha: requirement for NFkappa B transcription factor and gene accessibility. J. Biol. Chem. **277:**16592-16598. doi: 10.1074/jbc.M111440200.

214. **Hemmi, H., O. Takeuchi, S. Sato, M. Yamamoto, T. Kaisho, H. Sanjo, T. Kawai, K. Hoshino, K. Takeda, and S. Akira.** 2004. The roles of two IkappaB

kinase-related kinases in lipopolysaccharide and double stranded RNA signaling and viral infection. J. Exp. Med. **199:**1641-1650. doi: 10.1084/jem.20040520.

215. **Kawai, T., S. Sato, K. J. Ishii, C. Coban, H. Hemmi, M. Yamamoto, K. Terai, M. Matsuda, J. Inoue, S. Uematsu, O. Takeuchi, and S. Akira.** 2004. Interferon-alpha induction through Toll-like receptors involves a direct interaction of IRF7 with MyD88 and TRAF6. Nat. Immunol. **5:**1061-1068. doi: 10.1038/ni1118.

216. **Yu, Y., and G. S. Hayward.** 2010. The ubiquitin E3 ligase RAUL negatively regulates type I interferon through ubiquitination of the transcription factors IRF7 and IRF3. Immunity. **33:**863-877. doi: 10.1016/j.immuni.2010.11.027.

217. **Kubota, T., M. Matsuoka, T. H. Chang, P. Tailor, T. Sasaki, M. Tashiro, A. Kato, and K. Ozato.** 2008. Virus infection triggers SUMOylation of IRF3 and IRF7, leading to the negative regulation of type I interferon gene expression. J. Biol. Chem. **283:**25660-25670. doi: 10.1074/jbc.M804479200.

218. **Caillaud, A., A. Prakash, E. Smith, A. Masumi, A. G. Hovanessian, D. E. Levy, and I. Marie.** 2002. Acetylation of interferon regulatory factor-7 by p300/CREB-binding protein (CBP)-associated factor (PCAF) impairs its DNA binding. J. Biol. Chem. **277:**49417-49421. doi: 10.1074/jbc.M207484200.

219. **Lu, R., W. C. Au, W. S. Yeow, N. Hageman, and P. M. Pitha.** 2000. Regulation of the promoter activity of interferon regulatory factor-7 gene. Activation by interferon snd silencing by hypermethylation. J. Biol. Chem. **275:**31805-31812. doi: 10.1074/jbc.M005288200.

220. **Qing, J., C. Liu, L. Choy, R. Y. Wu, J. S. Pagano, and R. Derynck.** 2004. Transforming growth factor beta/Smad3 signaling regulates IRF-7 function and transcriptional activation of the beta interferon promoter Mol. Cell. Biol. **24:**1411-1425.

221. **Prakash, A., and D. E. Levy.** 2006. Regulation of IRF7 through cell type-specific protein stability. Biochem. Biophys. Res. Commun. **342:**50-56. doi: 10.1016/j.bbrc.2006.01.122.

222. **Zhang, L., J. Zhang, Q. Lambert, C. J. Der, L. Del Valle, J. Miklossy, K. Khalili, Y. Zhou, and J. S. Pagano.** 2004. Interferon regulatory factor 7 is associated with Epstein-Barr virus-transformed central nervous system lymphoma and has oncogenic properties. J. Virol. **78:**12987-12995. doi: 10.1128/JVI.78.23.12987-12995.2004.

223. **Romieu-Mourez, R., M. Solis, A. Nardin, D. Goubau, V. Baron-Bodo, R. Lin, B. Massie, M. Salcedo, and J. Hiscott.** 2006. Distinct roles for IFN regulatory factor (IRF)-3 and IRF-7 in the activation of antitumor properties of human macrophages. Cancer Res. **66:**10576-10585. doi: 10.1158/0008-5472.CAN-06-1279.

224. **Genin, P., R. Lin, J. Hiscott, and A. Civas.** 2009. Differential regulation of human interferon A gene expression by interferon regulatory factors 3 and 7. Mol. Cell. Biol. **29:**3435-3450. doi: 10.1128/MCB.01805-08.

225. **Rudd, P. A., J. Wilson, J. Gardner, T. Larcher, C. Babarit, T. T. Le, I. Anraku, Y. Kumagai, Y. M. Loo, M. Gale, S. Akira, A. A. Khromykh, and A. Suhrbier.** 2012. Interferon response factors 3 and 7 protect against Chikungunya virus hemorrhagic fever and shock. J. Virol. **86:**9888-98. doi: 10.1128/JVI.00956-12.

226. **Taylor, K. E., and K. L. Mossman.** 2013. Recent advances in understanding viral evasion of type I interferon. Immunology. **138:**190-197. doi: 10.1111/imm.12038; 10.1111/imm.12038.

227. **Bramson, J. L., K. Dayball, J. R. Hall, J. B. Millar, M. Miller, Y. H. Wan, R. Lin, and J. Hiscott.** 2003. Super-activated interferon-regulatory factors can enhance plasmid immunization. Vaccine. **21:**1363-1370.

228. **Graham, F. L., and L. Prevec.** 1991. Manipulation of adenovirus vectors. Methods Mol. Biol. **7:**109-128. doi: 10.1385/0-89603-178-0:109.

229. **Moraes, M. P., G. A. Mayr, and M. J. Grubman.** 2001. pAd5-Blue: direct ligation system for engineering recombinant adenovirus constructs. Biotechniques. **31:**1050, 1052, 1054-6.

230. **Moraes, M. P., T. de Los Santos, M. Koster, T. Turecek, H. Wang, V. G. Andreyev, and M. J. Grubman.** 2007. Enhanced antiviral activity against foot-and-mouth disease virus by a combination of type I and II porcine interferons. J. Virol. **81:**7124-7135. doi: 10.1128/JVI.02775-06.

231. **Cheng, G., W. Chen, Z. Li, W. Yan, X. Zhao, J. Xie, M. Liu, H. Zhang, Y. Zhong, and Z. Zheng.** 2006. Characterization of the porcine alpha interferon multigene family. Gene. **382:**28-38. doi: 10.1016/j.gene.2006.06.013.

232. **Cheng G, Zhao X, Chen W, Yan W, Liu M, Chen J, and Zheng Z.** 2007. Detection of differential expression of porcine IFN-alpha subtypes by reverse transcription polymerase chain reaction. J Interferon Cytokine Res. **27:**7:579-87.

233. **Sang, Y., R. R. Rowland, R. A. Hesse, and F. Blecha.** 2010. Differential expression and activity of the porcine type I interferon family. Physiol. Genomics. **42:**248-258. doi: 10.1152/physiolgenomics.00198.2009.

234. **Diaz-San Segundo, F., C. C. Dias, M. P. Moraes, M. Weiss, E. Perez-Martin, G. Owens, M. Custer, K. Kamrud, T. de Los Santos, and M. J. Grubman.** 2013. Venezuelan equine encephalitis replicon particles can induce rapid protection against foot-and-mouth disease virus. J. Virol. **87:**5447-5460. doi: 10.1128/JVI.03462-12.

235. **Salguero, F. J., M. A. Sánchez-Martín, F. Díaz-San Segundo, A. deAvila, and N. Sevilla.** 2005. Foot-and-mouth disease virus (FMDV) causes an acute disease that can be lethal for adult laboratory mice. Virology. **332(1):**384-96.

236. **Dias, C. C., M. P. Moraes , M. Weiss, F. Diaz-San Segundo, E. Perez-Martin, A. Salazar, T. de los Santos, and M. Grubman.** 2012. Novel antiviral therapeutics to control foot-and-mouth disease. J Interferon Cytokine Res. **32:**462-73. doi: 10.1089/jir.2012.0012.

237. **Golde, W. T., J. M. Pacheco, H. Duque, T. Doel, B. Penfold, G. S. Ferman, D. R. Gregg, and L. L. Rodriguez.** 2005. Vaccination against foot-and-mouth disease virus confers complete clinical protection in 7 days and partial protection in 4 days: Use in emergency outbreak response. Vaccine. **23:**5775-5782. doi: 10.1016/j.vaccine.2005.07.043.

238. **Pacheco, J. M., M. C. Brum, M. P. Moraes, W. T. Golde, and M. J. Grubman.** 2005. Rapid protection of cattle from direct challenge with foot-and-mouth

disease virus (FMDV) by a single inoculation with an adenovirus-vectored FMDV subunit vaccine. Virology. **337:**205-209. doi: 10.1016/j.virol.2005.04.014.

239. **Mayr, G. A., J. Chinsangaram, and M. J. Grubman.** 1999. Development of replication-defective adenovirus serotype 5 containing the capsid and 3C protease coding regions of foot-and-mouth disease virus as a vaccine candidate. Virology. **263:**496-506. doi: 10.1006/viro.1999.9940.

240. **Mayr, G. A., V. O'Donnell, J. Chinsangaram, P. W. Mason, and M. J. Grubman.** 2001. Immune responses and protection against foot-and-mouth disease virus (FMDV) challenge in swine vaccinated with adenovirus-FMDV constructs. Vaccine. **19:**2152-2162.

241. **Heylbroeck, C., S. Balachandran, M. J. Servant, C. DeLuca, G. N. Barber, R. Lin, and J. Hiscott.** 2000. The IRF-3 transcription factor mediates Sendai virus-induced apoptosis. J. Virol. **74:**3781-3792.

242. **Grandvaux, N., M. J. Servant, B. tenOever, G. C. Sen, S. Balachandran, G. N. Barber, R. Lin, and J. Hiscott.** 2002. Transcriptional profiling of interferon regulatory factor 3 target genes: direct involvement in the regulation of interferon-stimulated genes. J. Virol. **76:**5532-5539.

243. **Colamonici, O. R., P. Domanski, S. M. Sweitzer, A. Larner, and R. M. Buller.** 1995. Vaccinia virus B18R gene encodes a type I interferon-binding protein that blocks interferon alpha transmembrane signaling. J. Biol. Chem. **270:**15974-15978.

244. **Symons, J. A., A. Alcami, and G. L. Smith.** 1995. Vaccinia virus encodes a soluble type I interferon receptor of novel structure and broad species specificity. Cell. **81:**551-560.

245. **Barnes, B. J., J. Richards, M. Mancl, S. Hanash, L. Beretta, and P. M. Pitha.** 2004. Global and distinct targets of IRF-5 and IRF-7 during innate response to viral infection. J. Biol. Chem. **279:**45194-45207. doi: 10.1074/jbc.M400726200.

246. **Asensio, V. C., J. Maier, R. Milner, K. Boztug, C. Kincaid, M. Moulard, C. Phillipson, K. Lindsley, T. Krucker, H. S. Fox, and I. L. Campbell.** 2001. Interferon-independent, human immunodeficiency virus type 1 gp120-mediated induction of CXCL10/IP-10 gene expression by astrocytes *in vivo* and *in vitro.* J. Virol. **75:**7067-7077. doi: 10.1128/JVI.75.15.7067-7077.2001.

247. **Marié, I., J. E. Durbin, and D. E. Levy.** 1998. Differential viral induction of distinct interferon-alpha genes by positive feedback through interferon regulatory factor-7. Embo j. **17:**6660-9.

248. **Weidner, J. M., D. Jiang, X. B. Pan, J. Chang, T. M. Block, and J. T. Guo.** 2010. Interferon-induced cell membrane proteins, IFITM3 and tetherin, inhibit vesicular stomatitis virus infection via distinct mechanisms. J. Virol. **84:**12646-57. doi: doi: 10.1128/JVI.01328-10.

249. **Clarke, J. B., and R. E. Spier.** 1983. An investigation into causes of resistance of a cloned line of BHK cells to a strain of foot-and-mouth disease virus. Vet. Microbiol. **8:**259-270.

250. **Moutailler, S., B. Roche, J. M. Thiberge, V. Caro, F. Rougeon, and A. B. Failloux.** 2011. Host alternation is necessary to maintain the genome stability of rift valley fever virus. PLoS Negl Trop. Dis. **5:**e1156. doi: 10.1371/journal.pntd.0001156.

251. **Amadori, M., G. Volpe, P. Defilippi, and C. Berneri.** 1997. Phenotypic features of BHK-21 cells used for production of foot-and-mouth disease vaccine. Biologicals. **25:**65-73. doi: 10.1006/biol.1996.0061.

252. **Osterlund, P. I., T. E. Pietila, V. Veckman, S. V. Kotenko, and I. Julkunen.** 2007. IFN regulatory factor family members differentially regulate the expression of type III IFN (IFN-lambda) genes. J. Immunol. **179:**3434-3442.

253. **Iversen, M. B., and S. R. Paludan.** 2010. Mechanisms of type III interferon expression. J Interferon Cytokine Res. **30:**573-8. doi: 10.1089/jir.2010.0063.

254. **Siegel, R., J. Eskdale, and G. Gallagher.** 2011. Regulation of IFN-lambda1 promoter activity (IFN-lambda1/IL-29) in human airway epithelial cells. J. Immunol. **187:**5636-5644. doi: 10.4049/jimmunol.1003988.

255. **van Pesch, V., H. Lanaya, J. C. Renauld, and T. Michiels.** 2004. Characterization of the murine alpha interferon gene family. J. Virol. **78:**8219-8228. doi: 10.1128/JVI.78.15.8219-8228.2004.

256. **Lefevre, F., M. Guillomot, S. D'Andrea, S. Battegay, and C. La Bonnardiere.** 1998. Interferon-delta: the first member of a novel type I interferon family. Biochimie. **80:**779-788.

257. **Tan, W., D. F. Carlson, C. A. Lancto, J. R. Garbe, D. A. Webster, P. B. Hackett, and S. C. Fahrenkrug.** 2013. Efficient nonmeiotic allele introgression in

livestock using custom endonucleases. Proc. Natl. Acad. Sci. USA. doi: 10.1073/pnas.1310478110.

258. **Fingar, D. C., S. Salama, C. Tsou, E. Harlow, and J. Blenis.** 2002. Mammalian cell size is controlled by mTOR and its downstream targets S6K1 and 4EBP1/eIF4E. Genes Dev. **16:**1472-1487. doi: 10.1101/gad.995802.